IST-2000-30148 I-METRA

D4

Performance Evaluation

Contractual Date of Delivery to the CEC:	**30 June, 2003**
Actual Date of Delivery to the CEC:	**30 September, 2003**
Author(s):	**Markku J. Heikkilä, Kari Majonen, Javier Fonollosa, Alba Pagès, Juha Ylitalo, Esa Tiirola, Adam Pollard**
Participant(s):	**NMP, NET, UPC, VOD, AAU**
Workpackage:	**WP4: Performance Evaluation**
Est. person months:	**36**
Security:	**Public**
Nature:	**Report**
Version:	**1.1**
Total number of pages:	**82**

Abstract:

This document considers the performance of multiantenna transmit/receive techniques in high-speed downlink and uplink packet access. The evaluation is done using both link and system level simulations by taking into account link adaptation and packet retransmissions. The document is based on the initial studies carried out in deliverables D3.1 and D3.2.

Keyword list: Adaptive Antennas, MIMO Systems, Space-Time Coding, Adaptive Modulation and Coding, HSDPA, HSUPA, Turbo Coding, Equalization, Scheduling.

0 EXECUTIVE SUMMARY

This document considers the performance of multiantenna transmit and receive techniques in high-speed downlink packet access (HSDPA) and high-speed uplink packet access (HSUPA). The evaluation is done using both link and system level simulations. The document is based on the techniques reviewed in I-METRA project deliverables D3.1 [1] and D3.2 [2].

Link-level HSDPA simulations showed that channel equalization is required in multipath channels in order to utilize higher-order modulation (16-QAM) applied in HSDPA. Chip-level equalization may increase peak data rates significantly. This is true also with dual-antenna receivers.

The performance of different transmit diversity and layered transmission techniques was also studied in HSDPA. With uncorrelated antennas a comprehensive evaluation was done between different transmit diversity schemes showing that the benefit against single-antenna transmission is not very significant. In fact, transmit diversity makes effective channel equalization difficult. A short evaluation between layered and diversity HSDPA techniques was carried out and the results were compared to a case where an advanced receiver is used in connection to single-antenna transmission. The conclusion is that in Pedestrian A channel the gain is mainly due to additional receive antenna, while in Vehicular A channel the use of layered MIMO schemes or equalization with single-antenna transmission can be equally beneficial. However, layered schemes as significantly more complex.

Performance of layered MIMO HSDPA techniques is seriously affected by antenna correlation. It was shown that in most cases even STTD with two receive antennas can outperform the layered schemes, and additional gain over STTD can be achieved by using dual-antenna equalization. In the most difficult cases where high level of interference becomes a limiting factor for both layered schemes and STTD, only the equalizer was able to achieve adequate performance.

HSUPA performance in WCDMA uplink was studied with SIMO and MIMO approaches using different antenna constellations. Both uplink coverage and capacity results indicate that doubling the number of receive antennas from two to four brings significant improvement. However, the MIMO approach does not perform better than the SIMO scheme. Moreover, simple advanced receiver techniques such as interference rejection (optimum) combining and 1-stage partial PIC do not give significant gains compared to the RAKE receiver performance. HSUPA studies with ARQ and hybrid-ARQ (HARQ) showed that the HARQ scheme has the potential to bring significant performance improvement in cell and system throughput.

At system level, multiantenna receivers improve HSDPA capacity significantly. However, transmit diversity does not seem to have any positive impact on the system. Layered MIMO schemes are not very promising either when the terminal receiver is limited to have only two receive antennas.

DISCLAIMER

The work associated with this report has been carried out in accordance with the highest technical standards and the I-METRA partners have endeavoured to achieve the degree of accuracy and reliability appropriate to the work in question. However since the partners have no control over the use to which the information contained within the report is to be put by any other party, any other such party shall be deemed to have satisfied itself as to the suitability and reliability of the information in relation to any particular use, purpose or application.

Under no circumstances will any of the partners, their servants, employees or agents accept any liability whatsoever arising out of any error or inaccuracy contained in this report (or any further consolidation, summary, publication or dissemination of the information contained within this report) and/or the connected work and disclaim all liability for any loss, damage, expenses, claims or infringement of third party rights.

1 INTRODUCTION

The objective of WP4 of I-METRA project is to perform performance evaluation of the multiantenna algorithms studied in WP3. This document collects the results which were obtained both at the link and the system level.

High Speed Downlink Packet Access (HSDPA) and High Speed Uplink Packet Access (HSUPA) are currently being developed to offer high data rate services for WCDMA systems. HSDPA is currently included in WCDMA release 5. These packet access techniques are planned to incorporate forms of reconfigurability such as adaptive modulation and coding schemes. An essential part of the future systems may be utilization of multiple transmit and receive antennas. The so-called multiple-input multiple-output (MIMO) channels have been shown to increase the channel capacity. It is a target of this document to find out ways to utilize this theoretical capacity increase.

The document is divided into three main parts: HSDPA link results, HSUPA link results, and HSDPA system-level simulation results. While link-level simulations may indicate differences in the performance of different MIMO transmission schemes and receiver algorithms, they do not determine the practical system performance gain. This is why, the main conclusions should be drawn based on system simulation results.

2 LINK-LEVEL PERFORMANCE OF MIMO HSDPA

2.1 Link Simulation Approach

Figure 2.1 illustrates the used HSDPA link simulator implemented in CoCentric System Studio®. It includes most of the important functionality of actual HSDPA systems excluding adaptive modulation and coding (AMC), that is, the used channel coding rate and modulation order cannot be changed dynamically.

The simulator records data about average packet error rate and link throughput as function of geometry (G) factor defined as

$$G = \frac{I_{or}}{I_{oc}},$$

where I_{or} denotes the average base station transmit power and I_{oc} the average interference power from other cells. Link throughput is defined as the total bit payload of successfully received packets divided by the time spent assuming that adaptive modulation and coding is not used.

G factor is related to user's position within the cell; G is high when the terminal is near the serving base station and vice versa. Intercell interference is assumed to be additive white Gaussian noise. This may affect the performance gain of some advanced receivers. For example, linear minimum mean-square error receivers are able to utilize the structure of interference in mitigation of its effects. Thus, the obtained results are pessimistic in cases where there is only a single dominating source of interference in addition to the serving base station. Maximum likelihood receivers, on the other hand, may assume white noise and interference which is may not be the case in practical situations. The obtained results may thus be slightly optimistic because the made assumption ideally matches with the simulation environment.

The link simulator is also able to record performance data as a function packet E_b/N_0 which can be used for HSDPA systems simulations. It is important to note that only system level simulations reveal the true benefit from using different MIMO schemes. This is mainly due to scheduling and link adaptation not fully included in link level studies.

When hybrid-ARQ is applied in the link simulator, the maximum number of packet retransmissions can be adjusted. As illustrated in Figure 2.1, the channel decoder signals the index of the erroneous packet to the transmitter after a selected delay. This feedback is assumed to be always unerroneous. The retransmitted packet is combined to the earlier copy of the packet using Chase combining (i.e. maximal-ratio combining).

If not stated otherwise, channel estimation is performed using the transmitted common pilot channel which typically is allocated 10% of the total base station transmit power. In case of multiple transmit antennas, orthogonal pilot symbol

sequences are applied in different antennas and the pilot power is divided between the antennas. A moving average filter is applied to filter the despread pilot symbols to generate a channel estimate.

Part of the performance evaluation is done using Matlab® which is convenient way of simulating complex receiver algorithms.

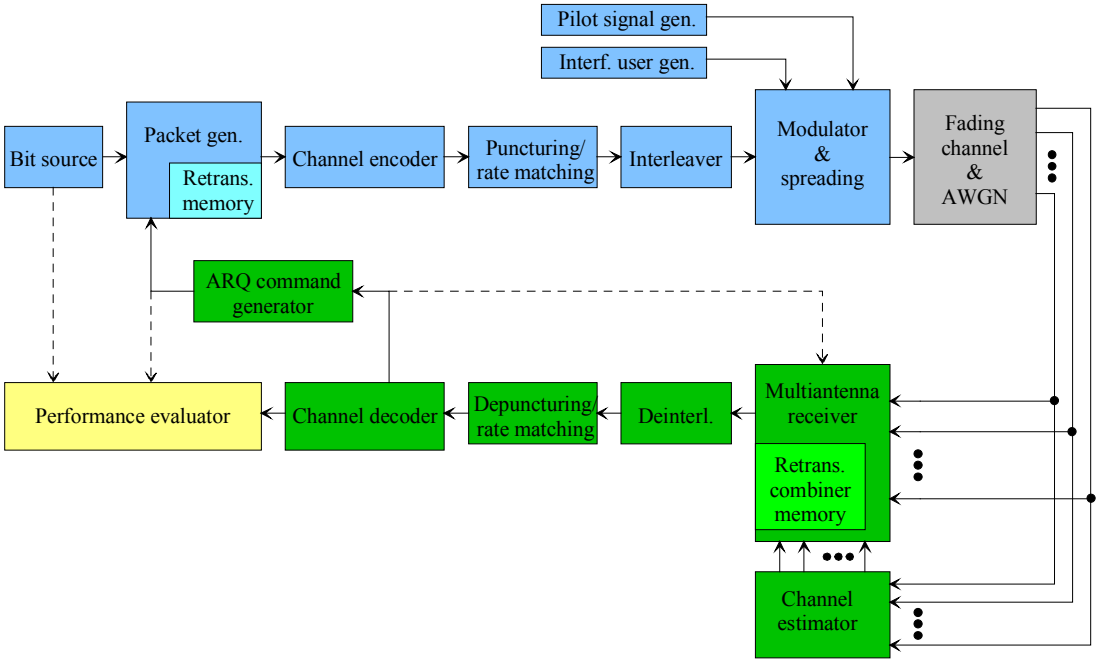

Figure 2.1. HSDPA link simulator supporting MIMO communication, channel estimation and hybrid-ARQ with Chase-combining.

2.2 HSDPA Performance with Advanced Receivers Applying Channel Equalization

One of the most straightforward ways of improving the downlink performance is to replace conventional RAKE receiver by an advanced receiver capable of equalizing the channel. Although it has long been considered that CDMA based communication does not require use of channel equalization due to interference suppression properties of the applied spreading codes, this is not the case in practice when the number of active code channels may be large to improve the spectral efficiency and when high-order modulation is used for achieving high data rates.

An important aspect of WCDMA channel equalization is the fact that a linear equalizer does not work properly if applied to a symbol-level narrow band WCDMA signal. This is due the long scrambling code used in the downlink. The code randomizes the short spreading codes making the intersymbol and multiple access interference non-stationary. In other words, the interference due to multipath propagation loses its structure after despreading operation and is very difficult to be suppressed without knowledge of all the active spreading codes and their powers in the received signal. This leads to the annoying fact that equalization should be carried

out using wideband chip-level signal. Due to the high chip rate of 3.84 MHz, chip-equalization is computationally very heavy operation as was shown in I-METRA deliverable D5.1 [3]. However, in channels with a reasonably short delay spread, chip-equalization is implementable.

We have studied the performance of single and dual-antenna RAKE and linear minimum mean-square error (LMMSE) equalizer in different channels and with different modulation and coding schemes (MCS) in HSDPA applying a single transmit antenna in the base station. More discussion about equazation can be found in [2]. We have selected five different MCSs:

- QPSK, rate 1/3 channel code (peak data rate 0.8 Mbit/s)
- QPSK, rate 1/2 channel code (peak data rate 1.2 Mbit/s)
- QPSK, rate 3/4 channel code (peak data rate 1.8 Mbit/s)
- 16-QAM, rate 1/2 channel code (peak data rate 2.4 Mbit/s)
- 16-QAM, rate 3/4 channel code (peak data rate 3.6 Mbit/s)

It should be noted that the used link simulator does not apply adaptive modulation and coding (AMC). Instead, the selected MCS is fixed during the simulation while actual packet retransmission is implemented assuming hybrid-ARQ (H-ARQ) and Chase-combining. Actual AMC is simulated in system simulator.

Maximum of three packet retransmissions are allowed per packet. HSDPA has 5 active code channels which are allocated 80% of the total transmit power. A common pilot channel with 10% power allocation is used for channel estimation at the receiver. In addition, there are a number of interfering dedicated channels (e.g. speech users) with 10% power allocation. We assume that the receive antennas are uncorrelated.

Figure 2.2 shows the throughput performance (kbit/s) of single-antenna RAKE in ITU Vehicular A channel (50 km/h) with each MCS. The ITU channel model is modified so that channel paths are chip-spaced. Link throughput is presented as a function of average G factor (defined in Section 2.1). The set of curves shows how the throughput with each MCS increases with G until no packet errors occur anymore and the peak data rate of the MCS in question is reached. A higher data rate can be achieved by using a more bandwidth efficient MCS. Figure 2.2 however indicates that RAKE can not support 16-QAM modulation in Vehicular A channel. With a high G values the irreducible interference due to multipath propagation dominates and causes an error floor to the packet error rate.

Figure 2.3 shows the performance of single-antenna LMMSE chip equalizer in Vehicular A. Now, all MCSs are performing well and even 3.6 Mbit/s service is usable if G > 13 dB. Unfortunately, such a high geometry value occurs only rarely in macro cells where the geometry factor has commonly values from 0 to 3 dB [1]. It is the geometry factor which states the operation SNR of the equalizer and thus the expected gain compared to RAKE. The fact that LMMSE receiver is equivalent with RAKE with low G values will limit the system level gain of channel equalizers in

macro cell environment. However, significant system level performance improvement can be expected in micro cells.

Performance of dual-antenna RAKE is depicted in Figure 2.4. When comparing to the throughput of single-antenna RAKE, SNR gain due to two receiver chains is clear. Now, also 16-QAM modulation seems to be usable but only with rate ½ channel code. In addition, the operation region of different MCS is at lower G values.

Figure 2.5 illustrates the link throughput of dual-antenna chip-equalizer. Equalization is performance using a joint LMMSE equalization over the receive antennas. In spite of the significant multipath interference, 16-QAM modulation becomes applicable already with geometry factor G = 2 dB. The gain compared to 2-antenna RAKE is small at low G region as expected. Thus, in macro cell environment, most of the system performance gain compared to single antenna receivers can be expected to be due to the additional receiver chain, not due the advance receiver algorithm. A much larger gain can be expected in micro cells.

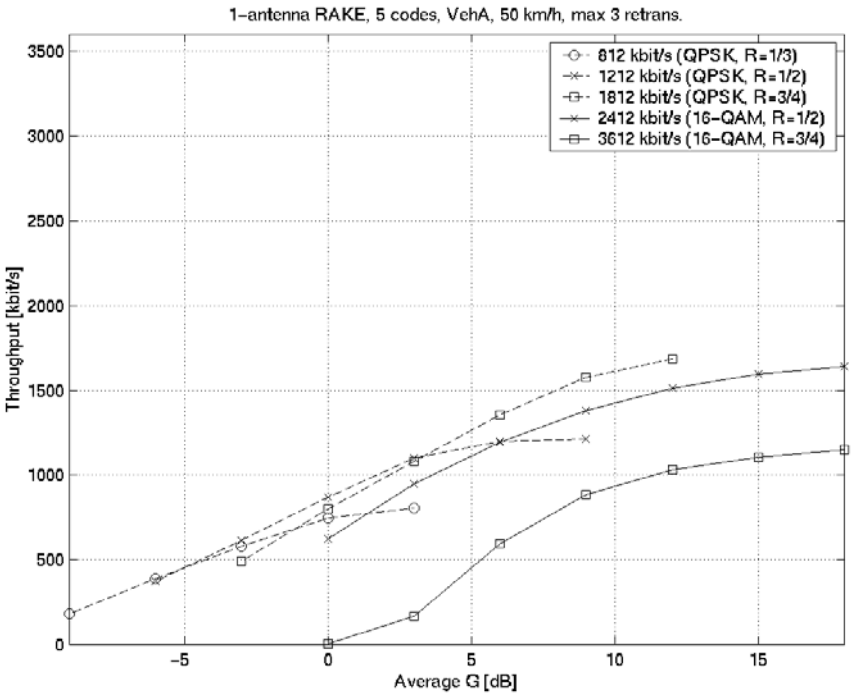

Figure 2.2. Performance of single-antenna RAKE in Vehicular A channel (HSDPA with 5 code channels and 80% power allocation).

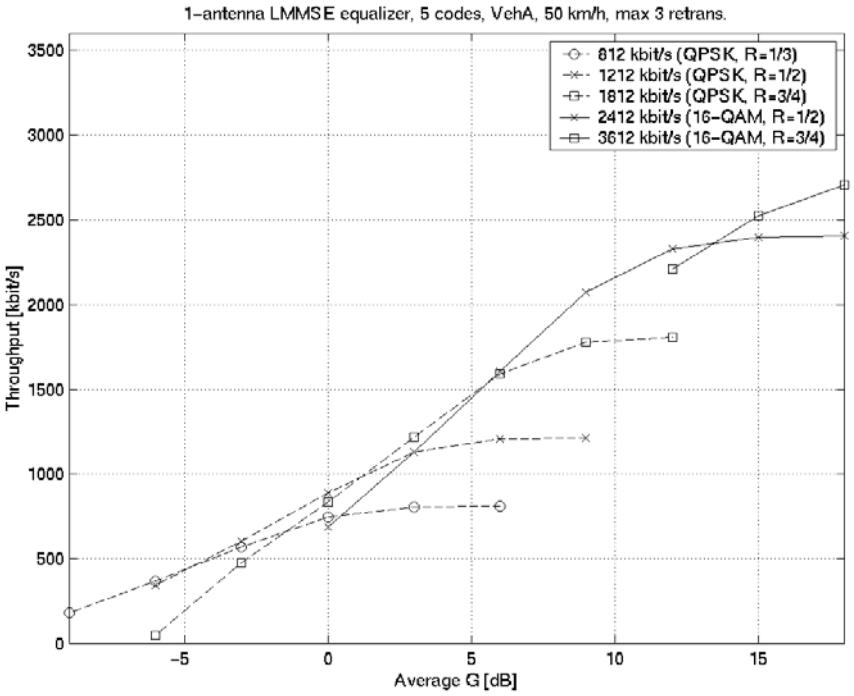

Figure 2.3. Performance of single-antenna LMMSE equalizer in Vehicular A channel (HSDPA with 5 code channels and 80% power allocation).

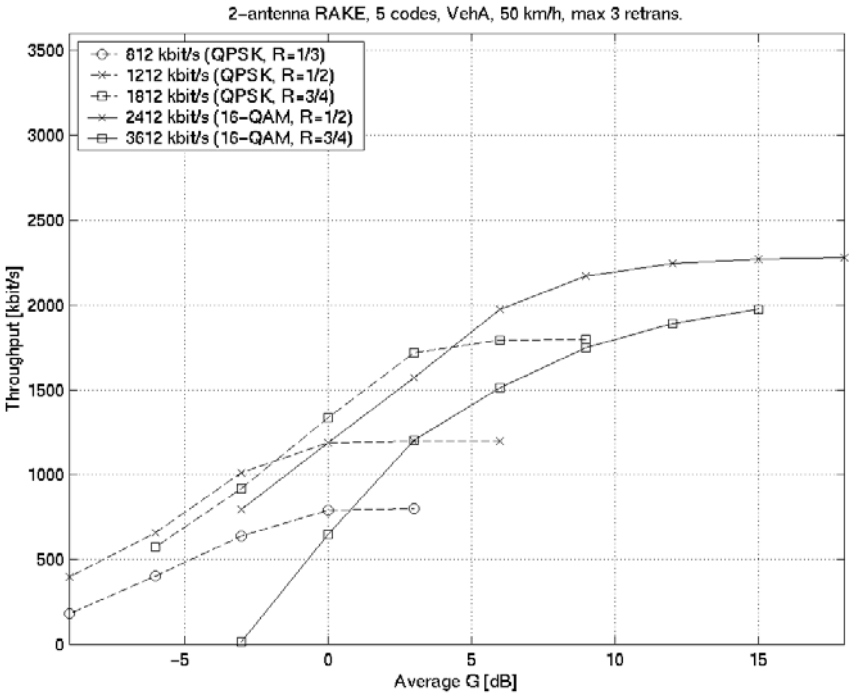

Figure 2.4. Performance of dual-antenna RAKE in Vehicular A channel (HSDPA with 5 code channels and 80% power allocation).

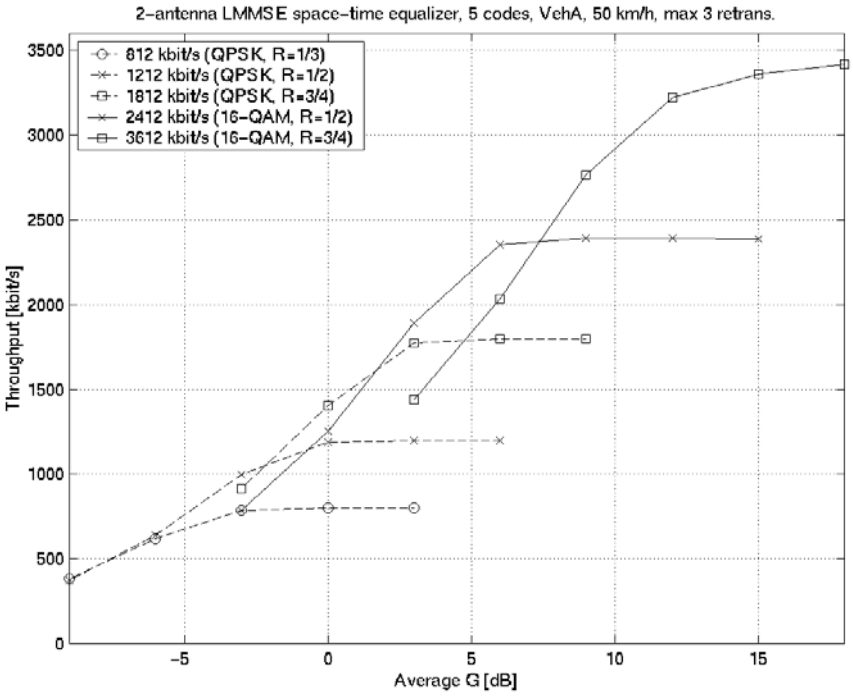

Figure 2.5. Performance of dual-antenna LMMSE equalizer in Vehicular A channel (HSDPA with 5 code channels and 80% power allocation).

The effect of the increased diversity order due to multiple transmit or receive antennas is expected to be rather small in HSDPA. In vehicular channels, the receiver is most probably supplied with sufficient multipath diversity order. In addition, it is a property of HSDPA system that especially with QPSK modulation the SNR operation region is very low reducing the effect of diversity. Since the effect of a higher diversity order becomes visible only at high SNR region where steeper slope of error rate curves have a clearer impact, only higher-order modulation benefits from diversity. When a data packet transmission fails it a task of H-ARQ procedure to increase the packet SNR until the packet is decoded correctly and the role of diversity is smaller.

Equalization is not required in near-flat fading channels, such as in ITU Pedestrian A. In addition, QPSK modulation seem not to require equalization at the receiver because of the low SNR operation region as discussed above. However, when intercell interference is dominated by a single source and/or the interference is otherwise strongly directional, joint multiantenna LMMSE equalization is an efficient way to suppress the interference even in flat channels and with robust modulation methods like QPSK.

2.3 Comparison of Diversity and Layered HSDPA Transmission Methods

In the context of HSDPA the specification of transmit diversity is still ongoing with one open loop and one closed loop transmit diversity technique already defined and several layered MIMO techniques under discussion. Here we compare the link-level performance of some of the possible candidate techniques such as STTD, CSTD,

Trombi, D-STTD and V-BLAST, that were introduced in [2]. The simulation models and parameters have also been described in detail in [2].

In order to select suitable diversity and layered HSDPA transmission techniques for system level performance evaluation, a preliminary performance comparison between different transmit diversity techniques was performed on link level. The performance evaluation was done using throughput of single antenna transmission with one and two receive antennas as a reference for the presented transmit diversity schemes. For single antenna transmission and different transmit diversity schemes a set of simulations was done for two different modulation schemes, QPSK and 16-QAM, as well as for different coding rates (1/3, 1/2 and 3/4). From those simulations the combination of modulation and coding was chosen so that the achieved throughput for certain geometry parameter G was maximized. The performance evaluation was done in a Rayleigh fading multipath environment. The chosen channel configurations were Pedestrian A channel with two chip-spaced multipath components and 3 km/h mobile velocity, and Vehicular A channel with five chip-spaced multipath components and 50 km/h mobile velocity. Table 2.1 illustrates the temporal properties of the channel models and Table 2.2 presents the main parameters used in simulation for this chapter.

Table 2.1. Simulation channel models

Channel model	Relative path powers [dB]	UE velocity [km/h]
Mod. ITU Pedestrian A (2-paths)	0 -12.7	3
Mod. ITU Vehicular A (5-paths)	0 -1.9 -7.3 -10.4 -10.9	50

Table 2.2. Simulation parameters

Number of HSDPA code channels	5, 10
Carrier frequency	2.15 GHz
Chip rate	3.84 MHz
Spreading factor for the desired user	16
HSDPA power	80%
CPICH power	10%
Maximum number of retransmissions	4
Other (speech) users	10
Spreading factor for the other users	128
Retransmission delay	7 slots

An example of how the performance evaluation was carried out is presented in Figure 2.6 for single antenna transmission and reception in 3 km/h Pedestrian A channel. For each transmission scheme a set of simulations with different coding rates and modulations was performed. From the obtained set of throughput results an envelope curve was produced so that for each G value the combination of coding and modulation providing the largest throughput was selected. In Figure 2.6 the envelope curve is illustrated with a heavier dotted line.

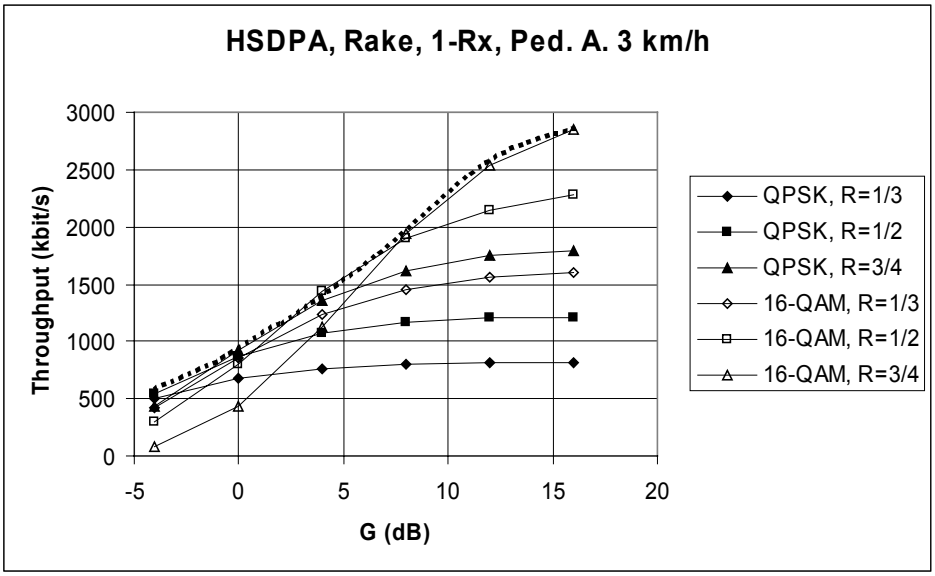

Figure 2.6. Evaluation example for 1-Tx 1-Rx in Pedestrian A channel.

The simulations were performed with one and two receive antennas. As can be expected, transmit diversity schemes give some gain in throughput over single antenna transmission in Pedestrian A channel presented in Figure 2.7. However, the throughput gains from transmit diversity are quite small when compared to gains usually seen for required transmission powers to achieve certain bit error rates. In HSDPA kind of packet-based system, even though the pedestrian channel is almost flat fading, H-ARQ provides diversity even for single antenna transmission. For transmit diversity techniques the signals transmitted from different antennas interfere with each other because the orthogonality between the spreading codes is destroyed by the multipath channel. In addition, the 16-QAM modulation is highly sensitive to channel estimation errors, which becomes more of an issue for the transmit diversity schemes since the pilot power per antenna gets smaller when the number of antennas is increased. As expected, when additional receive antenna is employed, much more significant increase in achievable throughput can be noticed when compared to single receive antenna case. This is due to the fact that 16-QAM modulation and weaker coding through increased puncturing can be used compared to single antenna receiver, while the difference between different transmission schemes using equivalent number of receive antennas is again quite small.

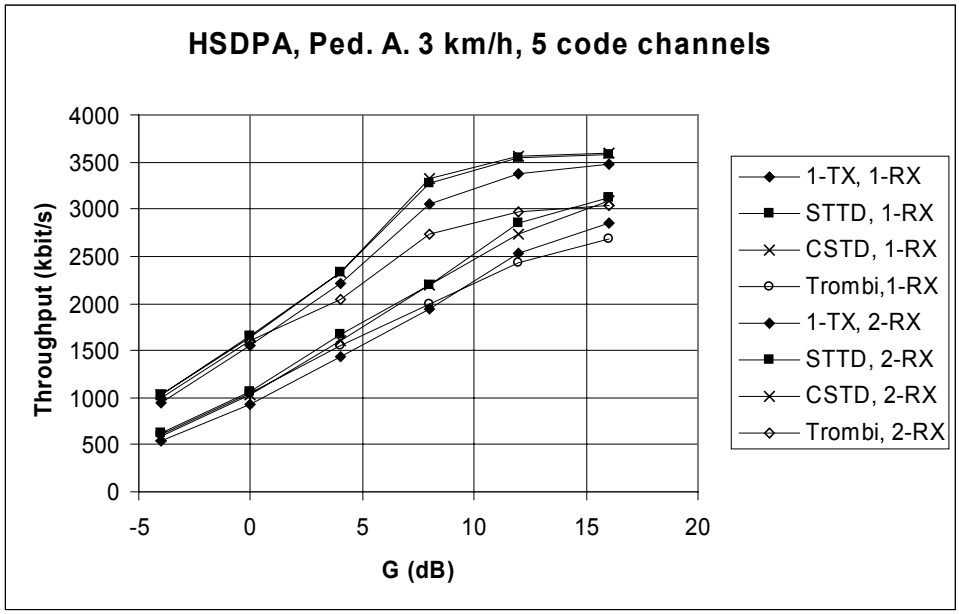

Figure 2.7. Transmit diversity results with one and two receive antennas in Pedestrian A channel.

In vehicular channel, presented in Figure 2.8, the situation is almost similar to the pedestrian case. With single receive antenna the achieved throughputs are very low since only QPSK modulation can be supported since using 16-QAM provides lower throughputs. This is because with rake receiver the interference level in this kind of multipath scenario becomes too severe, and the need for some kind of advanced receiver, such as equalizer or interference canceller, becomes obvious. Again, the additional receive antenna provides some improvement, but the difference between different transmit diversity techniques is almost unnoticeable.

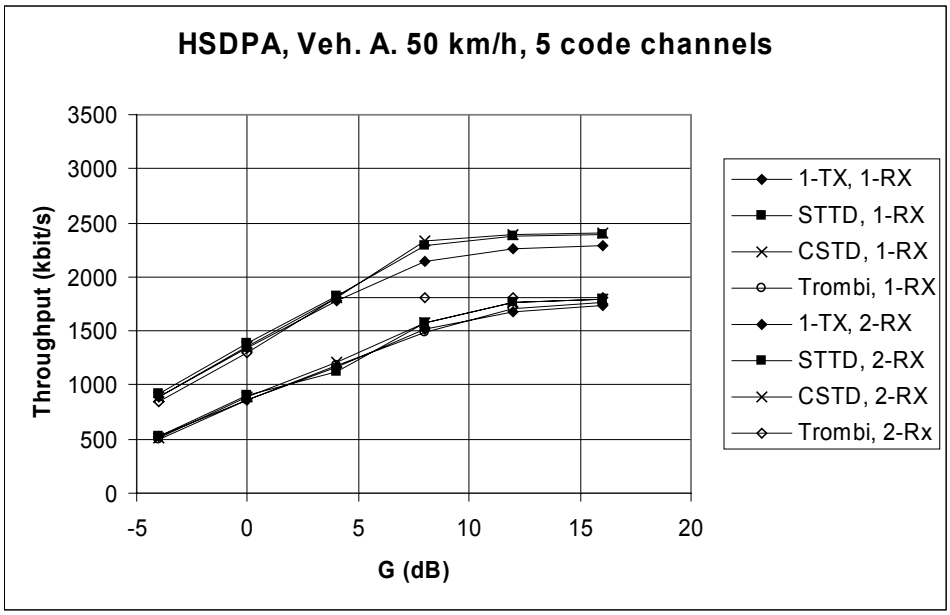

Figure 2.8. Transmit diversity results with one and two receive antennas in Vehicular A channel.

An important note of the simulation results presented above is that for actual HSDPA the link adaptation functions on packet level while for these results the modulation and coding were fixed for each curve in Figure 2.6. This implies that even though in Figure 2.8 for single receive antenna 16-QAM is always worse than QPSK and thus not used, in practise it is likely that in some cases the channel quality can be such that also 16-QAM can be employed, thus improving the overall system throughput.

In addition to transmit diversity evaluation a comparison between different transmit diversity schemes and layered schemes was performed and is presented in Figure 2.9 and Figure 2.10 for Pedestrian A and Vehicular A channel, respectively. In the evaluation a fixed coding rate R=0.62 was used and evaluated techniques had equivalent maximum throughput, which was achieved by using 16-QAM modulation with single stream techniques and QPSK with multi stream techniques. In addition to Rake based receivers also the performance of the chip equalizer is presented for single antenna transmission. Again, from Figure 2.9 it can be clearly seen that most of the gain in Pedestrian A channel comes from the employment of the second receive antenna, while the performance for different techniques with the same number of receive antennas is almost the same. However, in Vehicular A channel in Figure 2.10 the benefit form using equalization becomes obvious. Dual antenna equalizer achieves the same performance as the layered schemes and even the single antenna equalizer does the same in high G region. For transmit diversity techniques using a Rake-type receiver the combination of 16-QAM modulation and frequency selective fading becomes too challenging, even though the second receive antenna alleviates the situation.

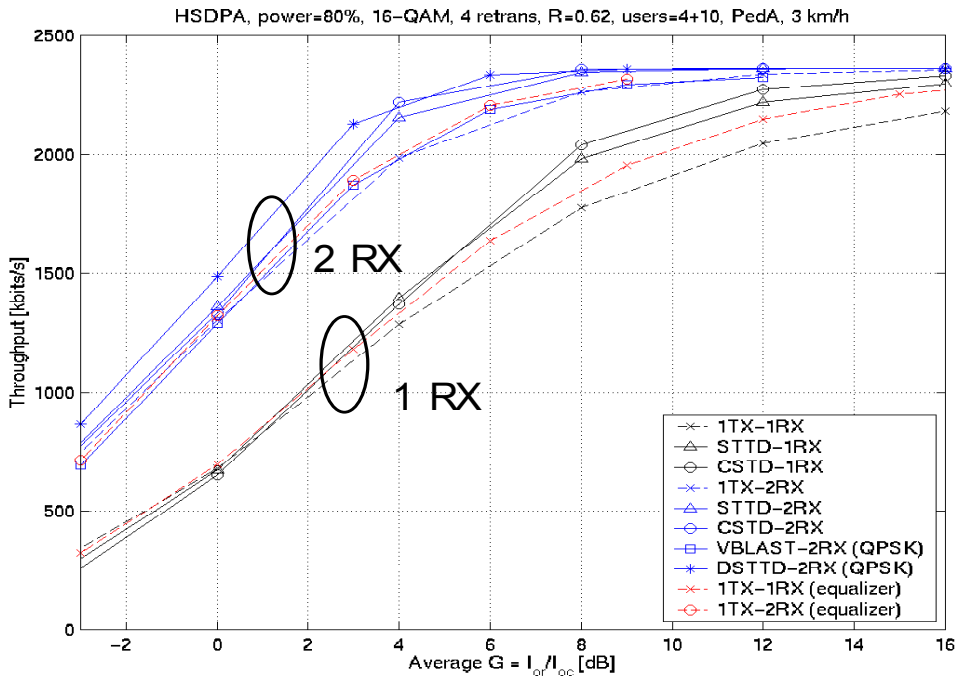

Figure 2.9. Throughput performance of layered and transmit diversity techniques in uncorrelated Pedestrian A channel.

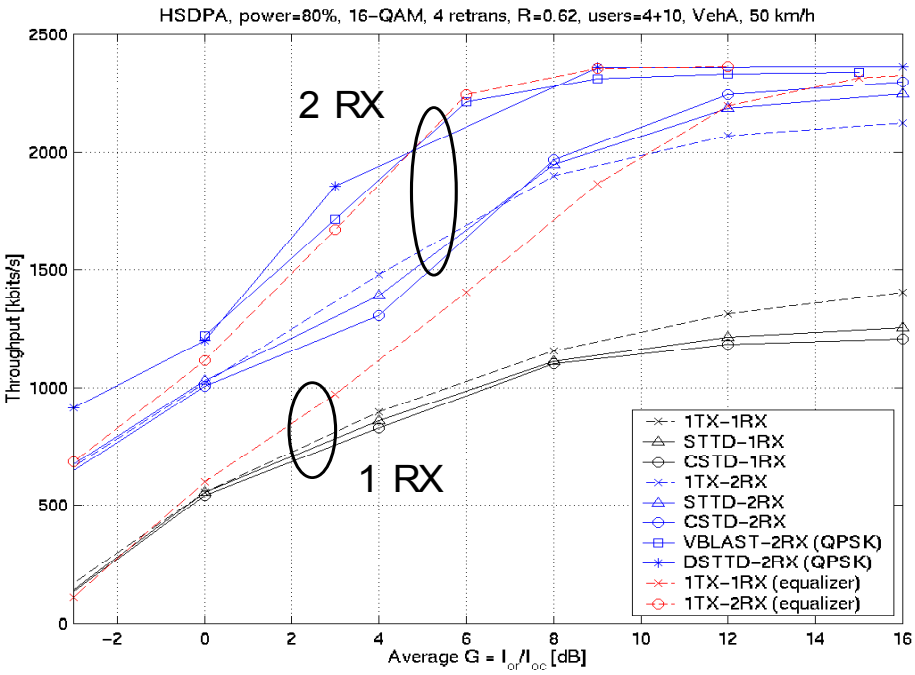

Figure 2.10. Throughput performance of layered and transmit diversity techniques in uncorrelated Vehicular A channel.

Based on the above results we selected STTD as a transmit diversity scheme to be evaluated also in system level with layered V-BLAST and D-STTD schemes (including also single antenna transmission as a reference). Figure 2.11 presents the results of throughput comparison between STTD with two receive antennas and 2-by-2 V-BLAST with OSIC receiver and 4-by-2 D-STTD with ML receiver in uncorrelated Pedestrian A channel. In order to have equal maximum throughput, STTD was again used with 16-QAM modulation and V-BLAST as well as D-STTD with QPSK modulation since they transmit two parallel data streams. It can be noticed that there are no large differences in throughput with the evaluated schemes.

In Figure 2.12 the same situation is presented in Vehicular A channel. It can be noticed that STTD cannot support the lowest coding rate since the rate R=1/2 provides higher throughput. With V-BLAST both data rates are usable and have the best throughput throughout the tested region. Since the ML receiver used with D-STTD does not take inter symbol interference arising from the frequency selective channel into account, clear performance loss can be noticed compared to V-BLAST and the performance is actually quite close to that achieved with much simpler STTD scheme.

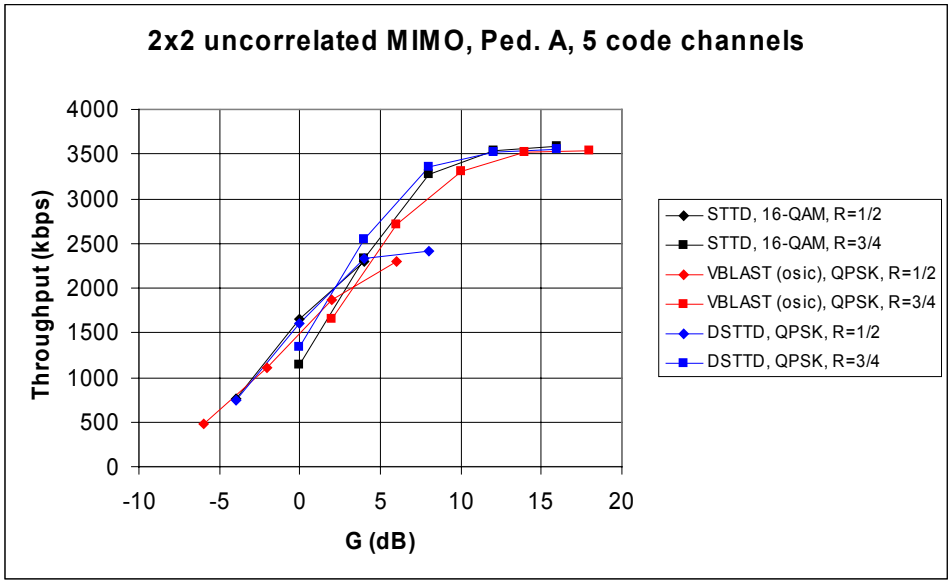

Figure 2.11. Throughput in uncorrelated Pedestrian A channel with five code channels for STTD, D-STTD and V-BLAST.

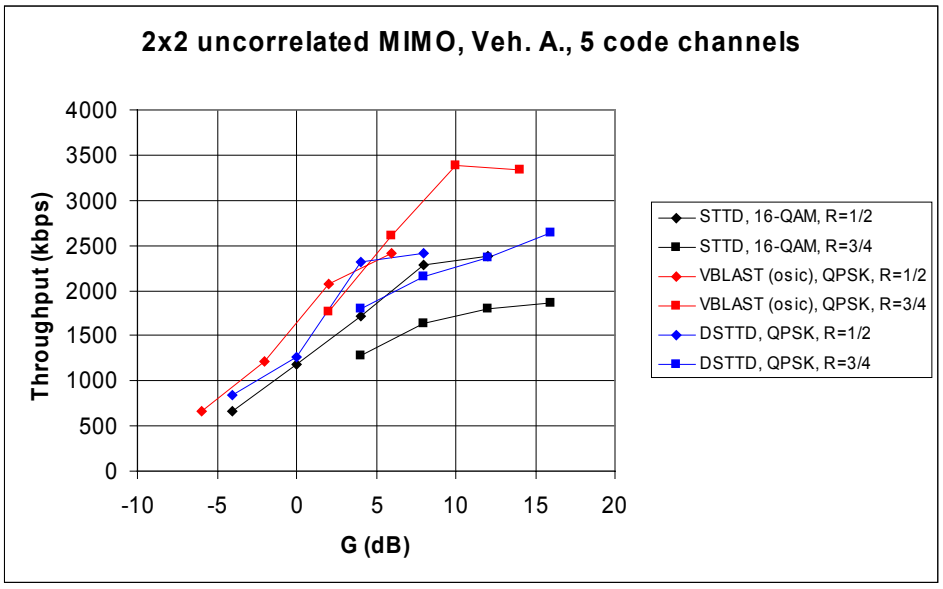

Figure 2.12. Throughput in uncorrelated Vehicular A channel with five code channels for STTD, D-STTD and V-BLAST.

2.3.1 Effect of Antenna Correlation

Considering the performance with uncorrelated fading presented in Figure 2.11 and Figure 2.12 as a starting point, we evaluate also the link-level performance in case of correlated transmit and receive antennas. The evaluation is limited to single antenna transmission using a dual-antenna equalizer at the receiver, STTD with dual-antenna RAKE, and layered V-BLAST and D-STTD schemes. With V-BLAST two different receiver structures, OSIC and ML, are considered while with D-STTD only ML receiver is used.

The correlations between different transmit and receive antennas are defined with complex valued correlation matrices, from which the fading correlations are generated. The UE correlation matrix equals

$$C_{Rx} = \begin{bmatrix} 1 & -0.6906 - 0.3419j \\ -0.6906 + 0.3419j & 1 \end{bmatrix}$$

and the Node B (base station) matrix equals

$$C_{Tx} = \begin{bmatrix} 1 & 0.4640 - 0.8499j & -0.4802 - 0.7421j & -0.7688 + 0.0625j \\ 0.4640 + 0.8499j & 1 & 0.4640 - 0.8499j & -0.4802 - 0.7421j \\ -0.4802 + 0.7421j & 0.4640 + 0.8499j & 1 & 0.4640 - 0.8499j \\ -0.7688 - 0.0625j & -0.4802 + 0.7421j & 0.4640 + 0.8499j & 1 \end{bmatrix}.$$

The 2-by-2 scenario can be defined by taking a fragment along the diagonal of the matrices above.

In Figure 2.13 the performance in Pedestrian A channel with 5 code channels is presented. It is clear from the figure that the performance of multi streaming MIMO schemes is degraded much more by the channel correlation than the performance of single antenna transmission and transmit diversity. In case of D-STTD the performance degradation due to correlated fading is not as significant as with V-BLAST but it is still inferior to 2-by-2 STTD especially with low G values. With similar type of ML receiver D-STTD is always better than V-BLAST with more than 500 kbps when G is larger than 5 dB. In Pedestrian A type almost flat fading channel where the inter-symbol interference is not very significant V-BLAST with ML receiver clearly outperforms OSIC type receiver. This is quite understandable since with correlating antennas there can sometimes be serious problems with OSIC to separate the data layers properly.

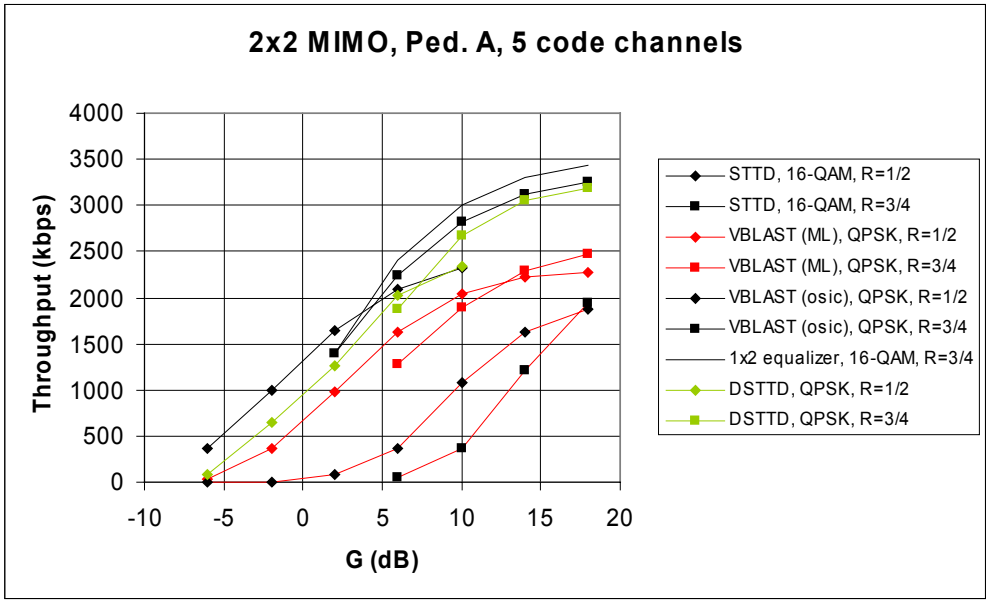

Figure 2.13. Throughput in correlated Pedestrian A channel with five code channels for dual-antenna equalizer, STTD, D-STTD and V-BLAST.

In Figure 2.14 the same situation is shown in case of 10 HSDPA code channels. Now both V-BLAST receivers are unable to support the use of rate R=3/4 channel coding, while with STTD it is still usable with sufficiently large G values. With D-STTD the performance is again between STTD and V-BLAST. Also the gain from equalization becomes more visible with larger number of code channels with G values larger than 5 dB.

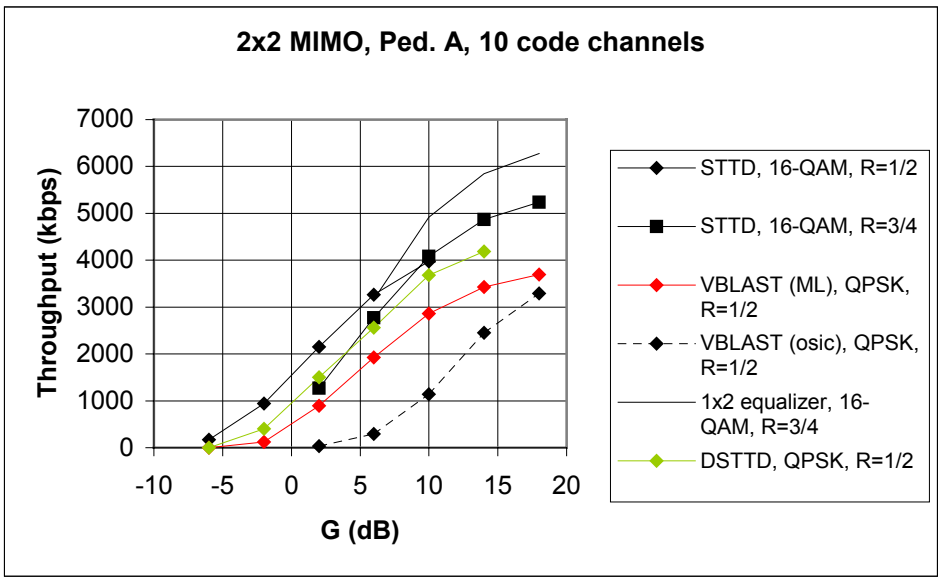

Figure 2.14. Throughput in correlated Pedestrian A channel with 10 code channels for dual-antenna equalizer, STTD, D-STTD and V-BLAST.

In Vehicular A channel, presented in Figure 2.15, the effect of increased multipath interference can be clearly seen in the inadequate performance of the V-BLAST scheme. Also with transmit diversity the throughput performance saturates well below the level achieved using single antenna transmission with dual-antenna equalizer. In contrast to Pedestrian A channel, in Vehicular A channel D-STTD is able to outperform STTD transmission while it is still inferior to single antenna transmission with dual antenna equalizer. The same situation can be also seen with 10 code channels in Figure 2.16. Here only dual antenna equalizer achieves even close the theoretical maximum throughput, while with transmit diversity and multi streaming MIMO the performance is limited by the high interference level.

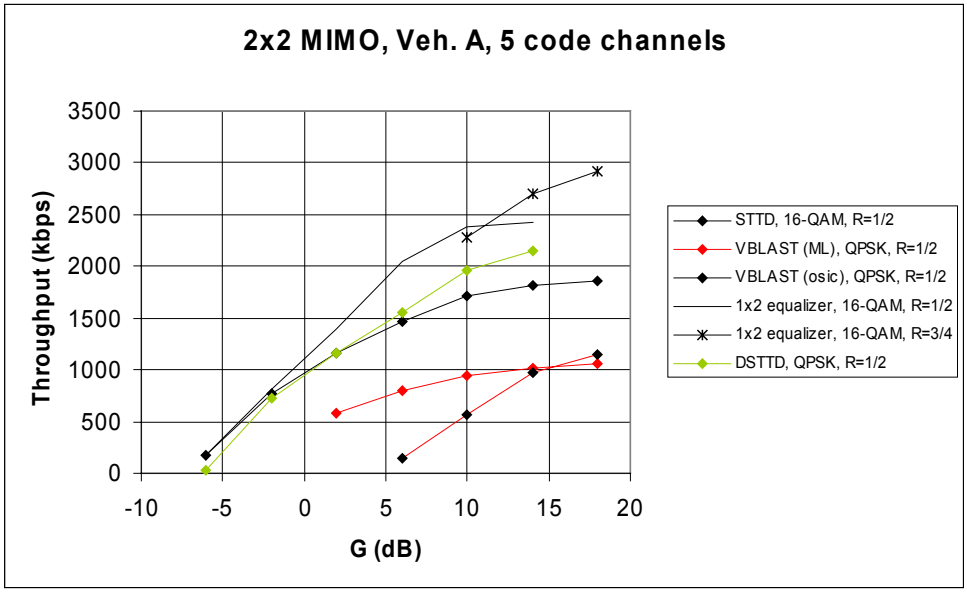

Figure 2.15. Throughput in correlated Vehicular A channel with five code channels for dual-antenna equalizer, STTD, D-STTD and V-BLAST.

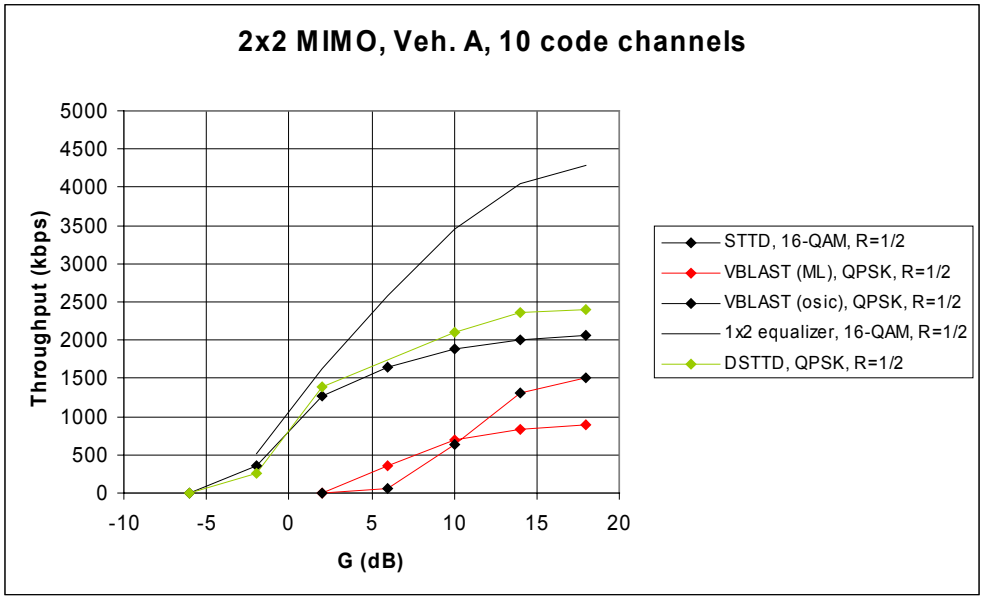

Figure 2.16. Throughput in correlated Vehicular A channel with 10 code channels for dual-antenna equalizer, STTD, D-STTD and V-BLAST.

2.4 Comparison of Advanced Receivers for Layered Transmission

In the sequel, we assume that the layered transmission is implemented using V-BLAST applying code re-use, i.e., the same spreading codes are used in all of the transmit antennas [2]. The parallel data streams (layers) interfere strongly with each other but they can be separated when the transmit and receive antennas do not correlate with each other too much.

It is further assumed that the data in the parallel streams form a single code word. This means that it is not possible to decode a single layers and then apply the decoded and thus more reliable data to cancel the interference experienced by the other layers. Such a post-decoding interference cancellation (IC) would require buffering, re-encoding, re-modulation and re-spreading of the data bits and filtering by a channel filter prior to cancellation. Since each layer also requires its own space-time equalizer (similarly to OSIC described in the next section), the total complexity would be overwhelming. For this reason, post-decoding IC is not considered as an option in this section.

2.4.1 Summary of the Applied Algorithms

The basic V-BLAST receiver is a spatial domain zero-forcing (ZF) or LMMSE antenna combiner matched to the response of the desired transmit antenna. Each transmit antenna (layer) requires its own spatial domain receiver. However, space-time processing is preferred, because practical channels are typically multipath channels. This complicates the detection of MIMO signals significantly [3] when also noting that space-time processing is most efficient when it applies chip-level signal.

Since the performance of data layer experiencing the most severe channel conditions dominates the performance the basic space-time receiver, it is beneficial to order the layers according to their relative powers (or post-detection signal-to-noise ratios). So called Ordered Successive Interference Canceller (OSIC) detects first the strongest layer using layer-specific LMMSE space-time equalizer and cancels it from the input signal. Other layers are detected similarly in a successive manner. The structure of OSIC receiver for the detection of two layers is illustrated in Figure 2.17 [2].

If symbol-level, despread signal is applied in the detection, maximum likelihood (ML) detector can be used to detect the interfering symbols [2]. For simplicity, symbol-by-symbol ("one-shot") detection is applied instead of sequence estimation. In multipath channels, each delayed version of the signal is despread separately like in conventional RAKE. The strong interference due to code re-use is optimally taken into account by simple ML search over all symbol combinations using the vector of spread multipath as an input signal. It should be noted that the interference due to multipath is not taken into account. This is contrary to the OSIC receiver which applies channel equalization.

A novel receiver for BLAST referred to as SPRI detector is also included in the performance comparison (its structure is not included in this document). The receiver is designed to efficiently mitigate effects of both multipath propagation and antenna correlation.

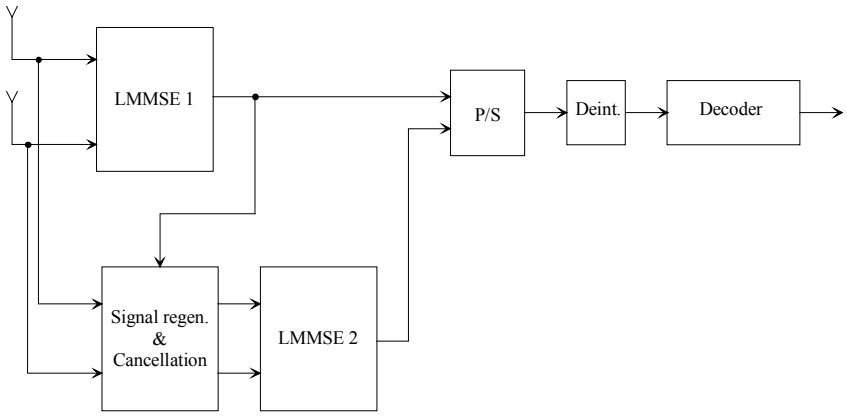

Figure 2.17. Structure of dual-antenna OSIC receiver for V-BLAST detection.

2.4.2 Performance Comparison

First, block error rate (BLER) performance of ML, OSIC and SPRI techniques is compared in ITU Vehicular A channel. V-BLAST HSDPA transmission with 5 code channels, rate 1/3 turbo code, 16-QAM modulation and 80% power allocation in (2, 2) MIMO channel with uncorrelated antennas has been assumed. H-ARQ with maximum of three retransmissions has been applied.

Figure 2.18 shows the performance of the receivers as a function of geometry factor G. The performance of ML detector suffers from multipath propagation which it is not

taken into account in the detection process to avoid sequence estimation. OSIC achieves BLER lower than 10% which is sufficient for effective HSDPA communication. However, even with such a high HSDPA power allocation its BLER saturates rather early which indicates possible problems with lower SNR levels or with high antenna correlation. SPRI detector achieves lower than 1% BLER which indicates high interference mitigation capability. However, it performs worse than OSIC at low G region.

Figure 2.19 illustrates link throughput when 5 or 10 HSDPA code channels are active in (2, 2) MIMO with V-BLAST transmission. Again, 16-QAM with rate 1/3 turbo coding has been used. It is interesting to note that, in spite of the very low block error rate achieved by SPRI, it does not improve link throughput significantly when 5 codes are used. This is because BLER of OSIC is low enough for H-ARQ operation. When 10 HSDPA code channels are used (with the same 80% power allocation), OSIC detector suffers from imperfect interference suppression between layers. SPRI detector is able to improve the data rate about 40% at maximum. It should be noted that code rates higher than the applied 1/3 do not work properly in the selected Vehicular A channel.

Finally, Figure 2.20 shows the performance of OSIC and SPRI in ITU Pedestrian A channel. Ten HSDPA code channels with 16-QAM and turbo code rates 1/3, 1/2 and 3/4 have been used to achieve different peak data rates. Since the pedestrian channel is almost flat channel, both receivers perform very well and nearly achieve the peak data rates of the selected MCSs. SPRI offers a steady performance improvement over the tested G region. It is expected that the improvement would be larger with correlating transmit and receive antennas since data layer separation becomes more non-ideal. Comparing to Figure 2.19 reveals the difficulty of MIMO communication in multipath channels.

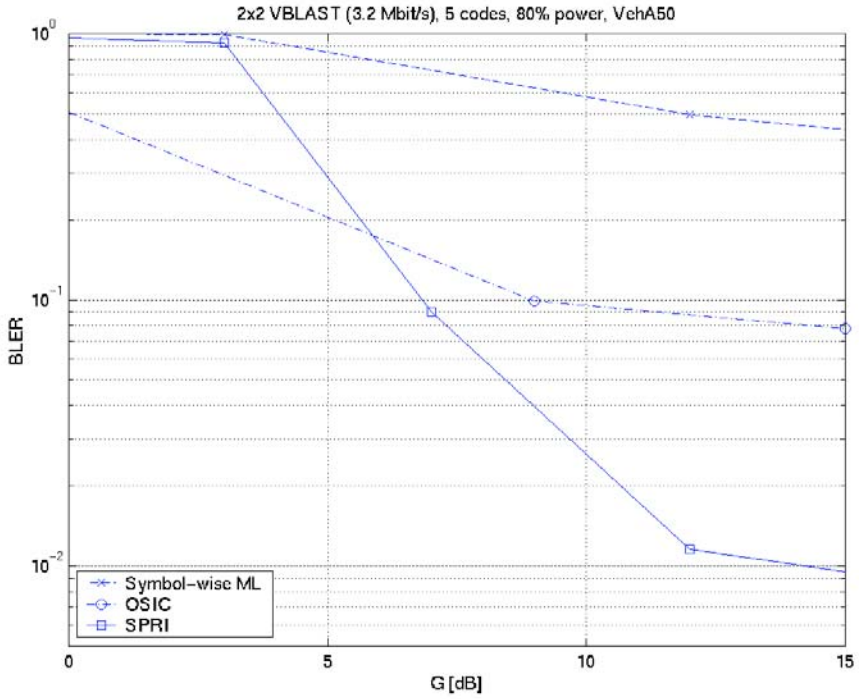

Figure 2.18. Block error rate for ML, OSIC and SPRI detectors for (2, 2) MIMO (16-QAM V-BLAST transmission in Vehicular A channel assumed).

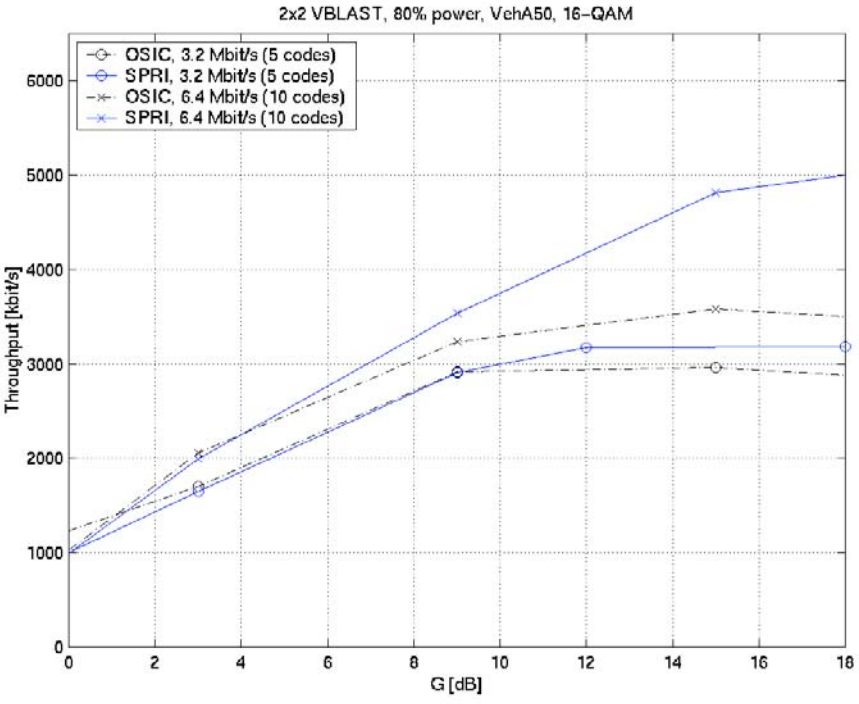

Figure 2.19. Link throughput of OSIC and SPRI detectors in Vehicular A channel. (2, 2) MIMO with V-BLAST transmission assumed.

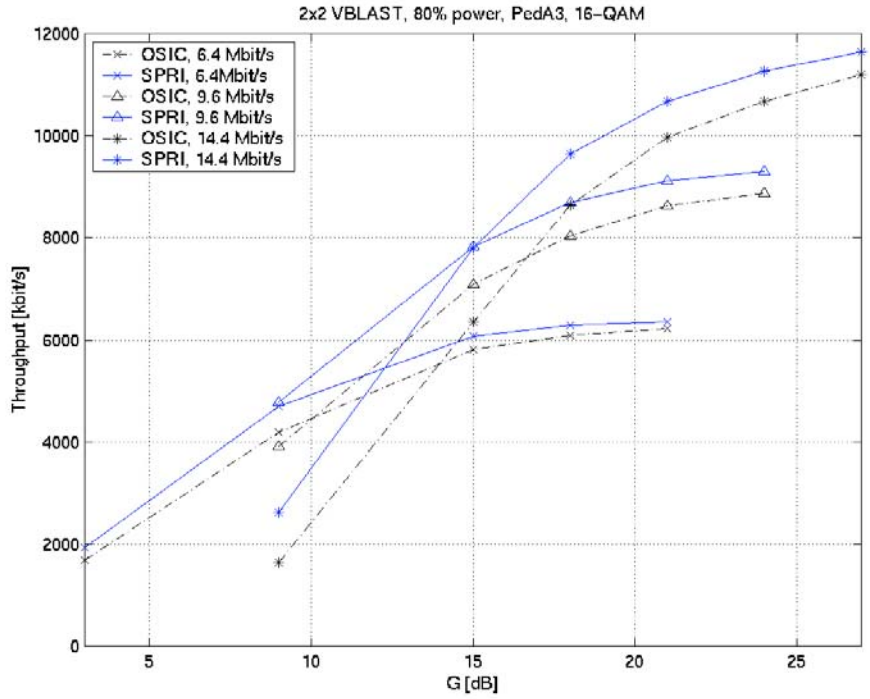

Figure 2.20. Link throughput of OSIC and SPRI detectors in Pedestrian A channel. (2, 2) MIMO with V-BLAST transmission and three different coding schemes assumed.

2.5 Scheme Combining Linear Dispersion Codes with Turbo Space Time Decoding

This section focuses on a different transmitter-receiver scheme that combines a Linear Dispersion Code (LDC) at the transmitter side with a receiver based on the turbo concept. The platform selected to implement this scheme has been MATLAB© and that is why a link-level simulator different from the one included in Section 2.1 is presented before showing the link-level results of the proposed scheme.

2.5.1 Transmitter and Receiver Structure

The transmitter is based on a combination of a turbo encoder with linear dispersion space time codes and multicode spreading [2]. First, a coding block of raw data bits is encoded using a standard Turbo Code with rate R. The coded bits are interleaved, and modulated using Q bits per symbol. These symbols are then multiplexed into the P parallel space-time encoders. After that, the signal is spread with the corresponding spreading code and conveniently scrambled as shown in Figure 2.21. The receiver structure can be also found in [2].

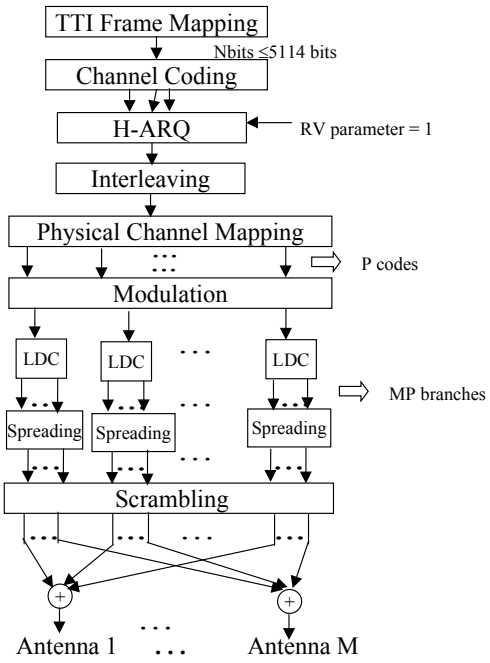

Figure 2.21. Transmitter structure.

Three different space-time coding alternatives are going to be checked:

- **STTD scheme or Alamouti scheme** with 2 antennas at the transmitter and 1 at the receiver [6].
- A linear dispersion code (**LDC scheme**) for 3 transmitter antennas and 2 receiver antennas provided in [5].
- **V-BLAST scheme** for 4 antennas at both the transmitter and receiver.

2.5.2 Metric Definition and Intra-cell Interference Modeling

The channel metric for this system has been defined as the EbNo with:

- Eb the mean value (averaged over a coding block equal to 5114 bits) of the received Eb per antenna.
- No/2 the noise power spectral density. The noise takes into account the effect of the thermal noise and both intra and inter-cell interferences.

It is important to point out that both the intra-cell and the inter-cell interferences are modelled as an additive zero mean white Gaussian noise at the receiver side. Thus, the temporal correlation of the intra-cell interference at the receiver is not taken into account. Nevertheless, the robustness of the proposed transmitter-receiver structure to the proposed interference modelling has been successfully checked. Figure 2.22 shows the TTI Error Rate versus EbNo in a Vehicular A channel for an Alamouti scheme with 4.8 Mbps when the intra-cell interference is generated at the transmitter

side and when it is modelled as a zero mean white Gaussian noise. Figure 2.23 shows the same curve for a V-BLAST configuration with 9.6 Mbps.

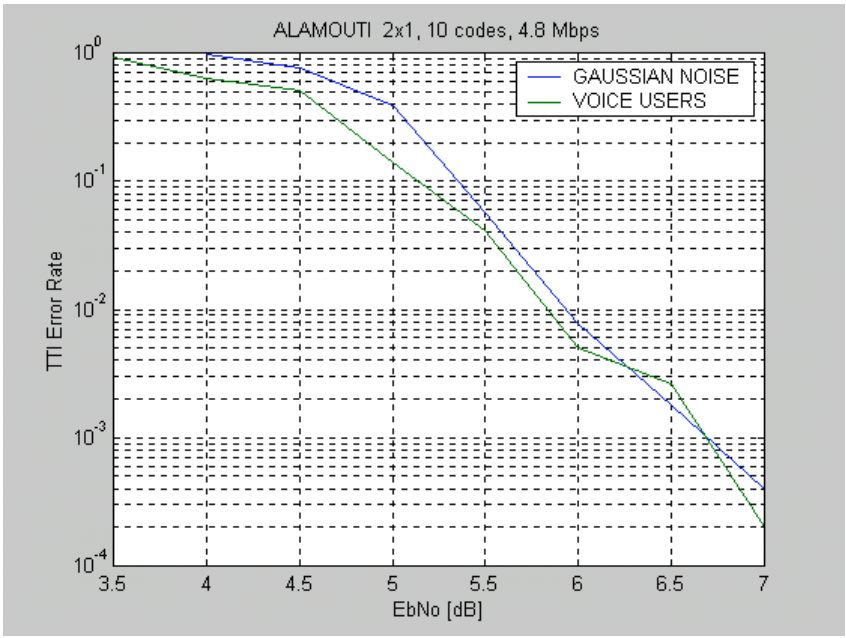

Figure 2.22. Comparison of TTI Error Rate for structured intra-cell interference modelling and a zero mean white Gaussian noise intra-cell interference modelling in a Vehicular A channel (120 km/h) for an Alamouti scheme with 4.8 Mbps.

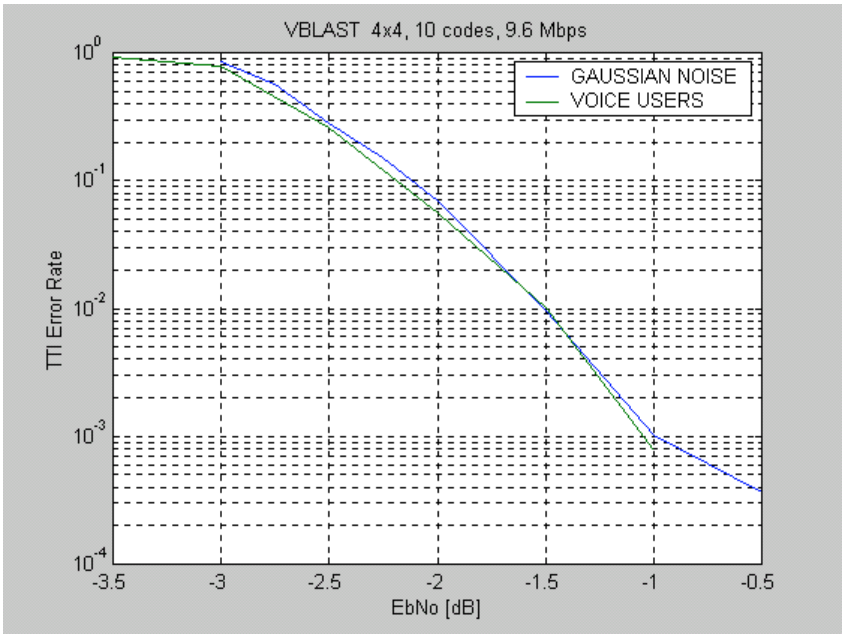

Figure 2.23. Comparison of TTI Error Rate for structured intra-cell interference modelling and a zero mean white Gaussian noise intra-cell interference modelling modelling in a Vehicular A channel (120 km/h) for and V-BLAST scheme with 9.6 Mbps.

As it can be seen, both modeling alternatives provide approximately the same performance. In consequence, the proposed receiver scheme allows us to model the intra-cell interference as an additive zero mean Gaussian noise at the receiver side.

2.5.3 Selection of configurations

The selected configurations are the following ones:

- MIMO configurations {M,N}=({2,1}, {4,4}, {3,2}), with M the number of transmitter antennas and N the number of receiver antennas.
- Number of codes = 1 HSDPA user with (1,5,10) codes and 2 HSDPA users with 5 codes each one (we refer to this last case as #codes=(5,5)).
- Modulation ={QPSK,16QAM}
- Channel Coding Rate = {0.75, 0.5}
- Channels {Pedestrian A with 3Kmh,Vehicular A with 50kmh, Vehicular A with 20kmh,Flat Rayleigh 3kmh, PedestrianB 3kmh}.

Notice that the percentage of Node B transmitted power used for the HSDPA user is not specified because the proposed metric, the EbNo, includes the intra-cell interference power. Thus, the same Frame or TTI Error Rate (FER) vs. EbNo look-up table is useful for different percentages of the HSDPA user power because a change of this percentage reflects in a different EbNo.

The previous combinations would end up with 50 simulations for each channel scenario but some of them will be skipped due to the reasons detailed below:

- **Simulations for 2 HSDPA users with 5 codes each one - #codes = (5,5).** Only the low bit rates are kept, that is, configurations with rate higher than 4.8Mbps are skipped.

- **Simulations for QPSK with coding rate 0.75 and 16QAM with coding rate 0.5**. It has been observed that the minimum EbNo needed for the QPSK with coding rate 0.75 is almost the same than the one needed for the 16QAM with coding rate 0.5. We'll skip all the simulations with QPSK and coding rate of 0.75.

- **Simulations with 16QAM and coding rate 0.75**. We'll skip these configurations because the EbNo needed for the maximum throughput can not be attained due to the intra-cell interference (even if 80% of the power is assigned to the HSDPA user).

- **Simulations with QPSK and 10 codes and with 16QAM and 5 codes, both with the same coding rate**. This pair of simulations achieve the same rate. We'll skip the simulations with 16QAM because we have observed they need more EbNo to achieve the same maximum throuthput.

Thus, the final set of simulations to be run for each channel and each MIMO configuration are listed in Table 2.3, Table 2.4 and Table 2.5. In these tables, P denotes the number of codes for the HSDPA user, K is equal to the number of bits per symbol and R is the coding rate of the Turbo channel encoder.

Table 2.3. Configurations for the Alamouti scheme with M=2 and N=1 and for each channel.

case	LDC	LDC R	P	Mod	K	R	Rate
1	Alamouti {2,1}	1	1	QPSK	2	0,5	0,24
2	Alamouti {2,1}	1	1	16-QAM	4	0,5	0,48
4	Alamouti {2,1}	1	5	QPSK	2	0,5	1,2
5	Alamouti {2,1}	1	5	16-QAM	2	0,5	2,4
7	Alamouti {2,1}	1	5,5	QPSK	2	0,5	1,2
8	Alamouti {2,1}	1	5,5	16-QAM	4	0,5	2,4
10	Alamouti {2,1}	1	10	QPSK	2	0,5	2,4
11	Alamouti {2,1}	1	10	16-QAM	4	0,5	4,8

Table 2.4. Configurations for the Linear Dispersion Code (LDC) scheme with M=3 and N=2 and for each channel.

case	LDC	LDC R	P	Mod	K	R	Rate
14	Bell-LDC {3,2}	2	1	QPSK	2	0,5	0,48
15	Bell-LDC {3,2}	2	1	16-QAM	4	0,5	0,96
17	Bell-LDC {3,2}	2	5	QPSK	2	0,5	2,4
18	Bell-LDC {3,2}	2	5	16-QAM	2	0,5	4,8
20	Bell-LDC {3,2}	2	5,5	QPSK	2	0,5	2,4
22	Bell-LDC {3,2}	2	10	QPSK	2	0,5	4,8
23	Bell-LDC {3,2}	2	10	16-QAM	4	0,5	9,6

Table 2.5. Configurations for the V-BLAST scheme with M=4 and N=4 and for each channel.

case	LDC	LDC R	P	Mod	K	R	Rate
26	V-BLAST {4,4}	4	1	QPSK	2	0,5	0,96
27	V-BLAST {4,4}	4	1	16-QAM	4	0,5	1,92
29	V-BLAST {4,4}	4	5	QPSK	2	0,5	4,8
30	V-BLAST {4,4}	4	5	16-QAM	2	0,5	9,6
32	V-BLAST {4,4}	4	5,5	QPSK	2	0,5	4,8
33	V-BLAST {4,4}	4	10	QPSK	2	0,5	9,6
34	V-BLAST {4,4}	4	10	16-QAM	4	0,5	19,2

2.5.4 Simulation Results for Alamouti 2x1[1].

The following figures show the TTI Error Rate versus the EbNo for the Alamouti 2x1 MIMO system and for 3 different channels: Pedestrian A with 3Km/h, Vehicular A with 50 Km/h and Vehicular A with 120 Km/h. Figure 2.24, Figure 2.25, Figure 2.26 and Figure 2.27 include these results for 1, 5, (5,5) and 10 codes, respectively.

[1] See Appendix A for tabulated values

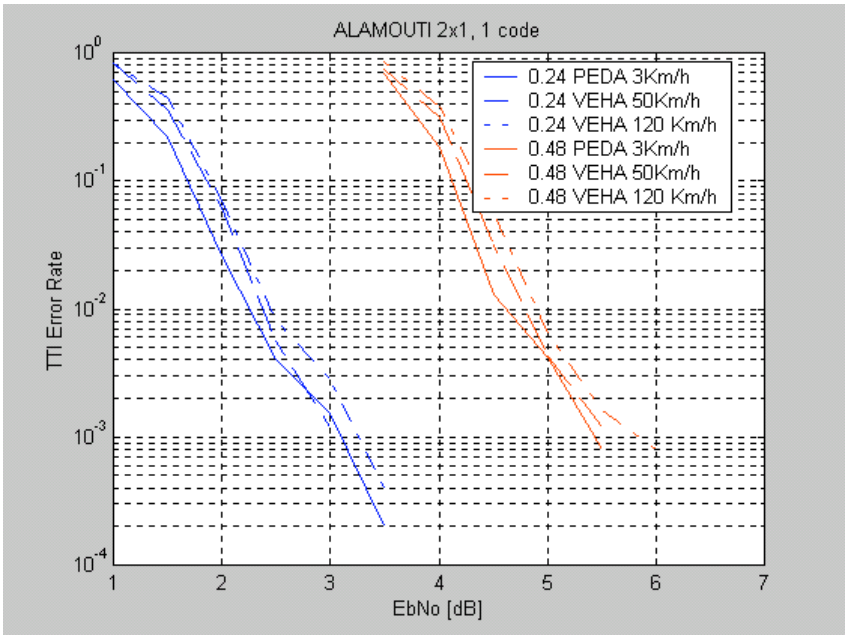

Figure 2.24. TTI Error Rate versus EbNo for Alamouti 2x1 with 1 code (cases 1 and 2 of Table 2.3) and for 3 different channels, Pedestrian A with 3Km/h, Vehicular A with 50 Km/h and Vehicular A with 120 Km/h.

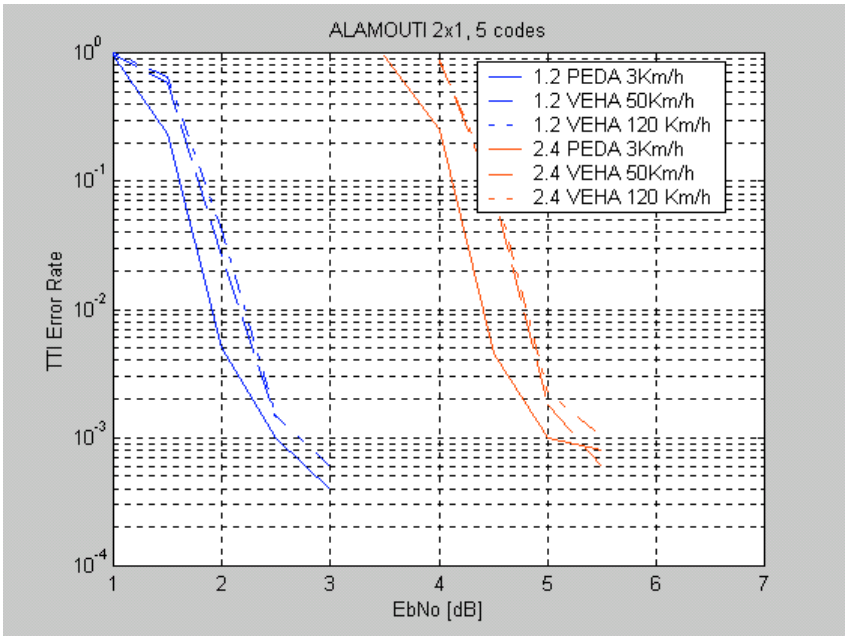

Figure 2.25. TTI Error Rate versus EbNo for Alamouti 2x1 with 5 code (cases 4 and 5 of Table 2.3) and for 3 different channels, Pedestrian A with 3Km/h, Vehicular A with 50 Km/h and Vehicular A with 120 Km/h.

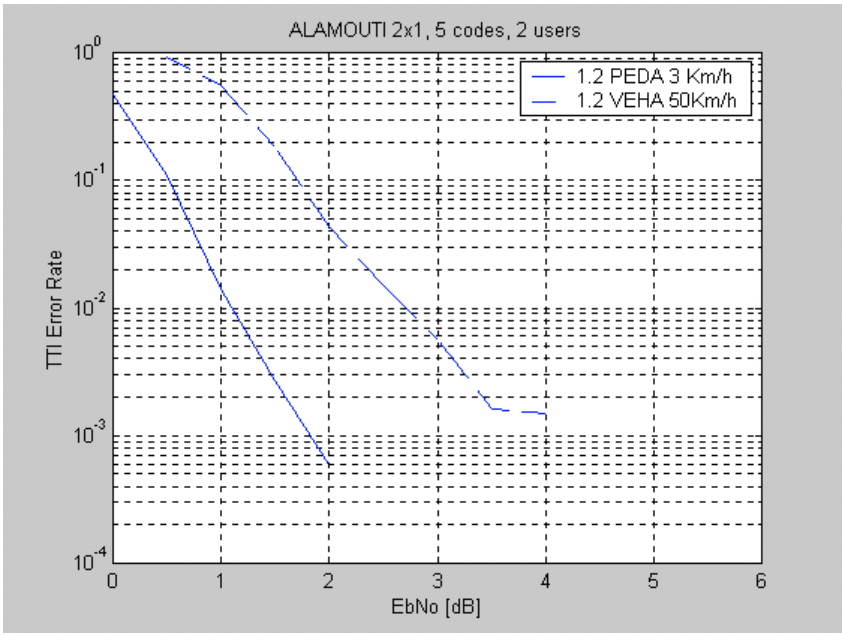

Figure 2.26. TTI Error Rate versus EbNo for Alamouti 2x1 with 5 code and 2 HSDPA users (cases 7 and 8 of Table 2.3) for 2 different channels, Pedestrian A with 3Km/h and Vehicular A with 50 Km/h.

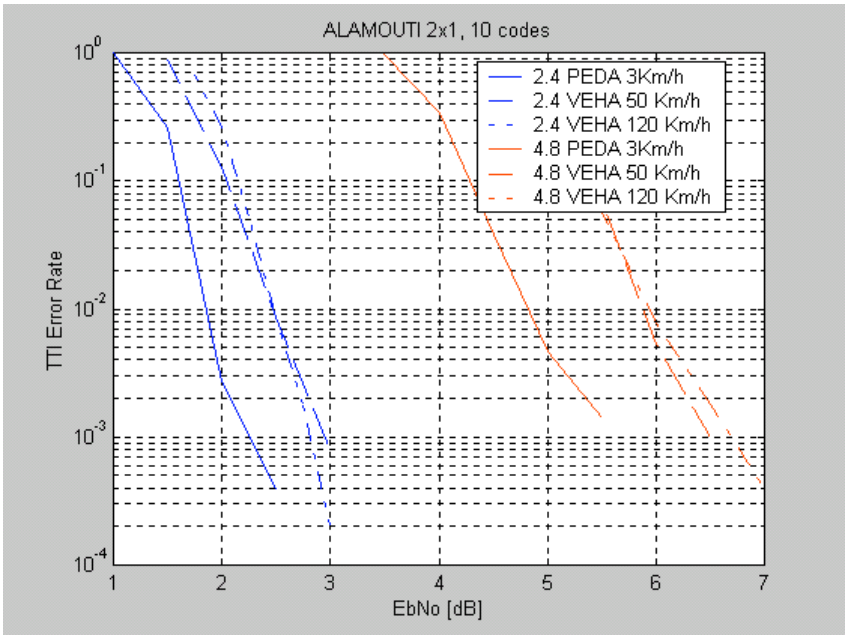

Figure 2.27. TTI Error Rate versus EbNo for Alamouti 2x1 with 10 code (cases 10 and 11 of Table 2.3) and for 3 different channels, Pedestrian A with 3Km/h, Vehicular A with 50 Km/h and Vehicular A with 120 Km/h.

Figure 2.28, Figure 2.29 and Figure 2.30 show the previous results gathered by channel type. Thus, the behavior of the transmit-receive structure for different number of codes can be checked.

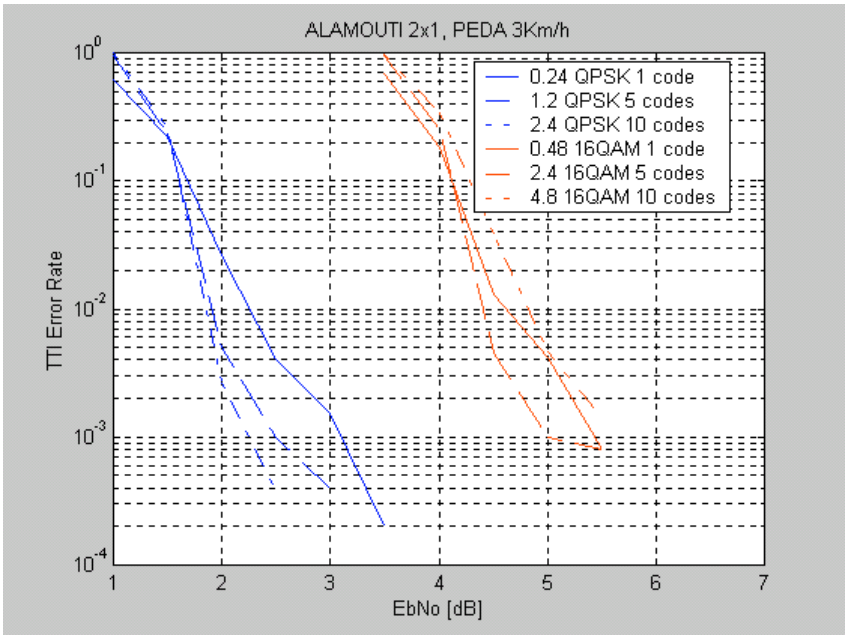

Figure 2.28. TTI Error Rate versus EbNo for Alamouti 2x1 and Pedestrian A with 3Km/h for 1, 5 and 10 codes and for QPSK and 16QAM modulations.

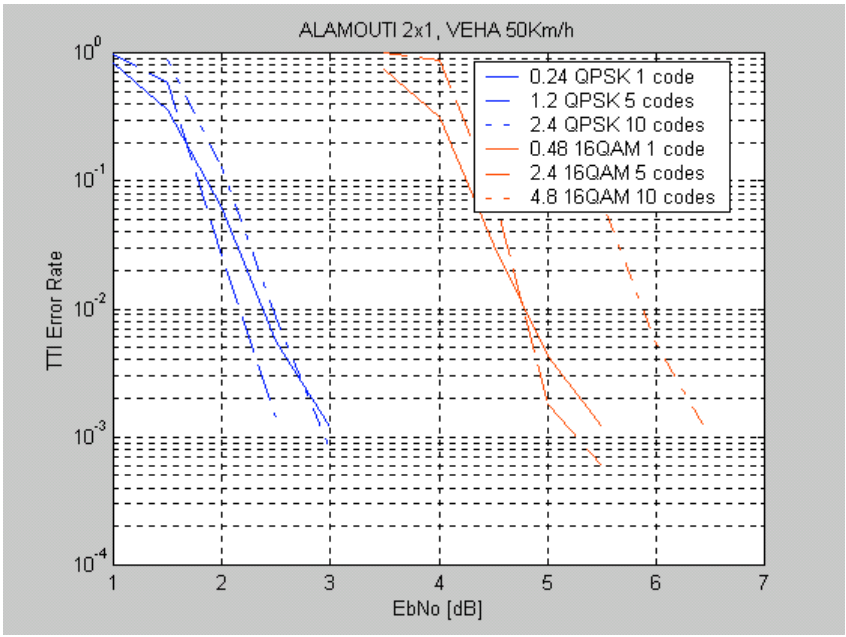

Figure 2.29. TTI Error Rate versus EbNo for Alamouti 2x1 and Vehicular A with 50 Km/h for 1, 5 and 10 codes and for QPSK and 16QAM modulations.

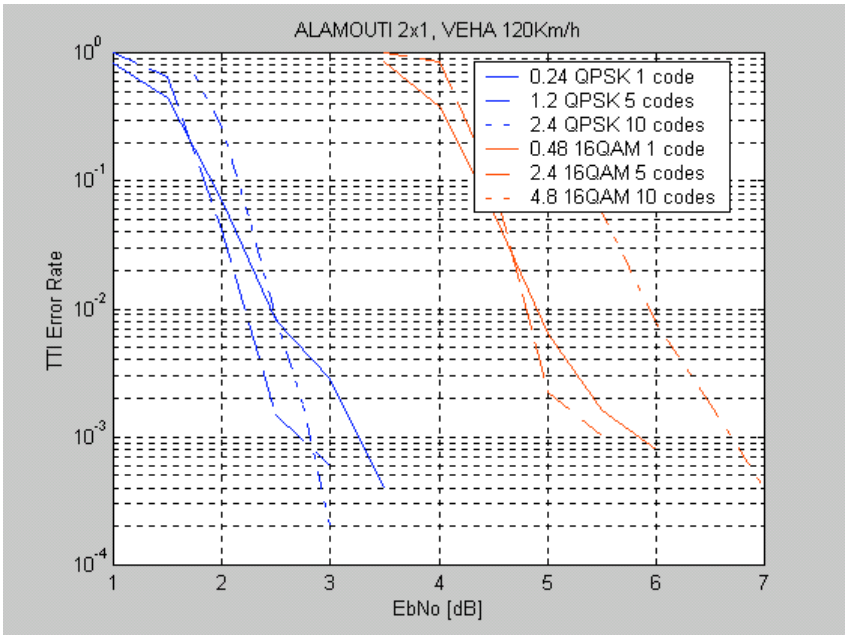

Figure 2.30. TTI Error Rate versus EbNo for Alamouti 2x1 and Vehicular A with 120 Km/h for 1, 5 and 10 codes and for QPSK and 16QAM modulations.

Several aspects are worth pointing out. Firstly, note that the configurations of QPSK with 10 codes and 16QAM with 5 codes achieve the same 2.4 Mbps data rate whenever both have the same channel coding rate. However, the QPSK configuration needs 2dB less of EbNo to achieve the TTI Error Rate (see Figure 2.28, Figure 2.29 and Figure 2.30). Thus, only the QPSK with 10 codes configuration will be simulated for the other two MIMO schemes of LDC 3x2 and V-BLAST 4x4.

Another important aspect to remark is the fact that, except for the Vehicular A channel, the proposed transmit-receive systems performs almost the same independently of the number of parallel code (see, Figure 2.28, Figure 2.29 and Figure 2.30).

2.5.5 Simulation Results for LDC 3x2[2].

This section includes the TTI Error Rate results for the named LDC with 3 transmitter antennas and 2 receiver antennas (see [2]). Figure 2.31 shows the results for one HSDPA user with 1 code using different modulation and coding rates and for a Veh. A (50km/h) and Ped.A (3km/h). Additionally, Figure 2.35 and Figure 2.36 include the same results but for one HSDPA user with 5 and 10 codes, respectively.

[2] See Appendix A for tabulated values

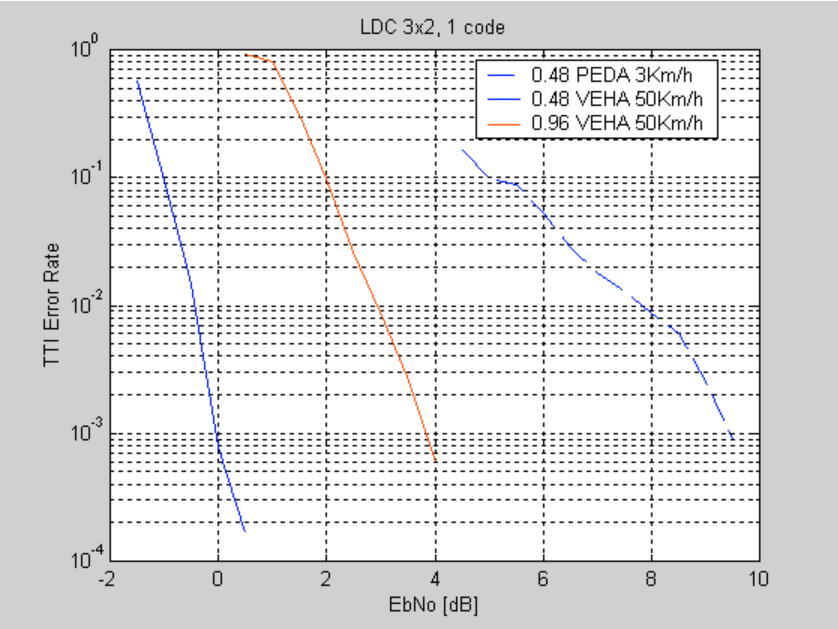

Figure 2.31. TTI Error Rate versus EbNo for LDC 3x2 with 1 code (cases 14 and 15 of Table 2.4 in blue and red, respectively) and for Pedestrian A with 3 Km/h (dashed line) and Vehicular A Channel with 50 Km/h (solid line).

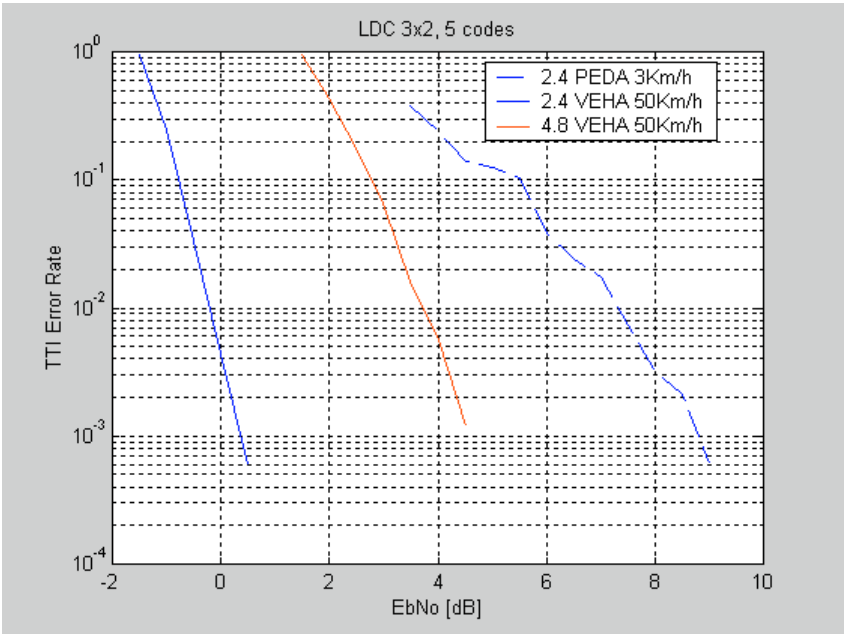

Figure 2.32. TTI Error Rate versus EbNo for LDC 3x2 with 5 codes (cases 17 and 18 of Table 2.4 in blue and red, respectively) and for Pedestrian A with 3 Km/h (dashed line) and Vehicular A Channel with 50 Km/h (solid line).

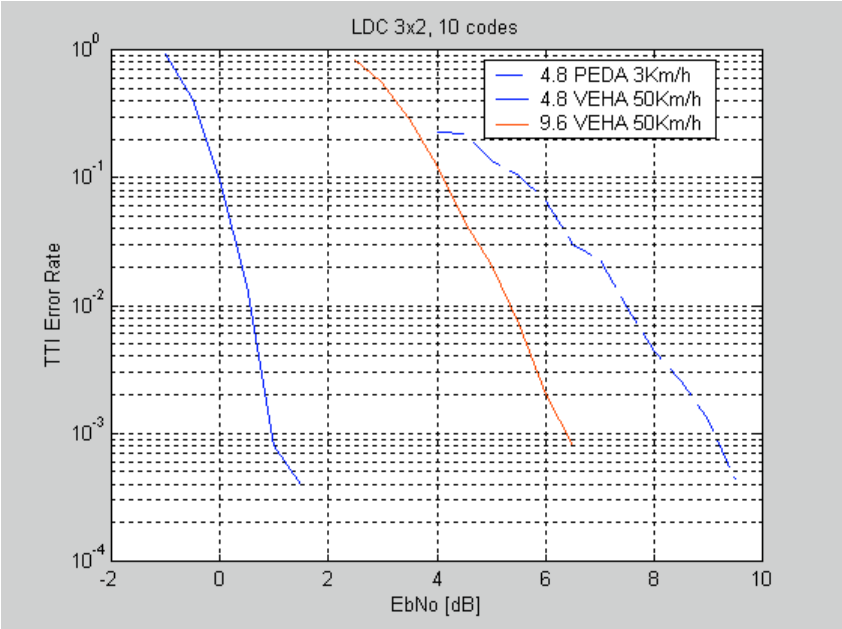

Figure 2.33. TTI Error Rate versus EbNo for LDC 3x2 with 10 codes (cases 22 and 23 of Table 2.4 in blue and red, respectively) and for Pedestrian A with 3 Km/h (dashed line) and Vehicular A Channel with 50 Km/h (solid line).

Concerning the Pedestrian A with 3 km/h channel and 16-QAM modulation, it has been checked that the TTI Error Rate obtained for the maximum achievable EbNo (that is, the EbNo obtained with 80% of the power assigned to the HSDPA user) is larger than 10^{-1}. Therefore, we conclude that it is not worth simulating the 3x2 LDC configuration for this scenario.

2.5.6 Simulation Results for V-BLAST 4x4[3].

This section is devoted to present the results obtained for the V-BLAST system with 4 transmitter antennas and 4 receiver antennas (see [2]). First, Figure 2.34 and Figure 2.35 show the results for one HSDPA user with 1 code using different modulation and coding rates and for a Veh. A (50km/h) and Ped.A (3km/h). As it can be seen the performance of this layered transmitter system in a slow fading channel is really poor.

[3] See Appendix A for tabulated values

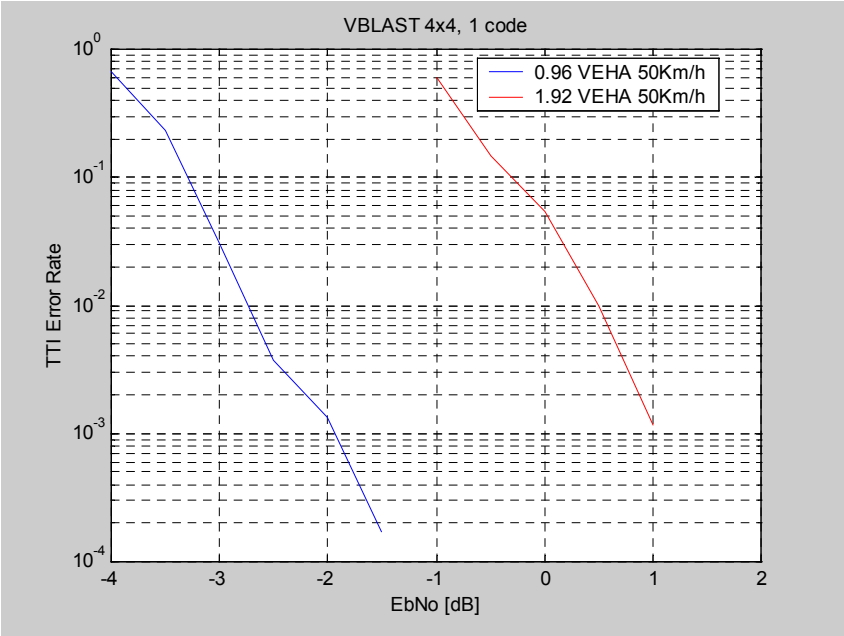

Figure 2.34. TTI Error Rate versus EbNo for V-BLAST 4x4 with 1 code (cases 26 and 27 of Table 2.5) and for Vehicular A Channel with 50 Km/h.

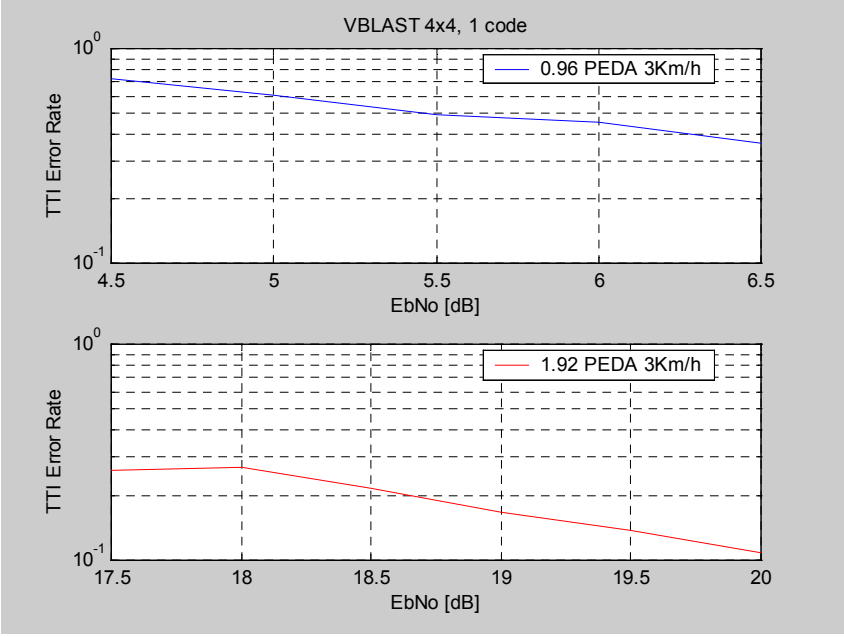

Figure 2.35. TTI Error Rate versus EbNo for V-BLAST 4x4 with 1 code (cases 26 and 27 of Table 2.5) and for Pedestrian A Channel with 3 Km/h.

Figure 2.36 and Figure 2.37 show the results for a Veh. A channel with 50km/h for different modulation and coding schemes and for 5 and 10 codes, respectively.

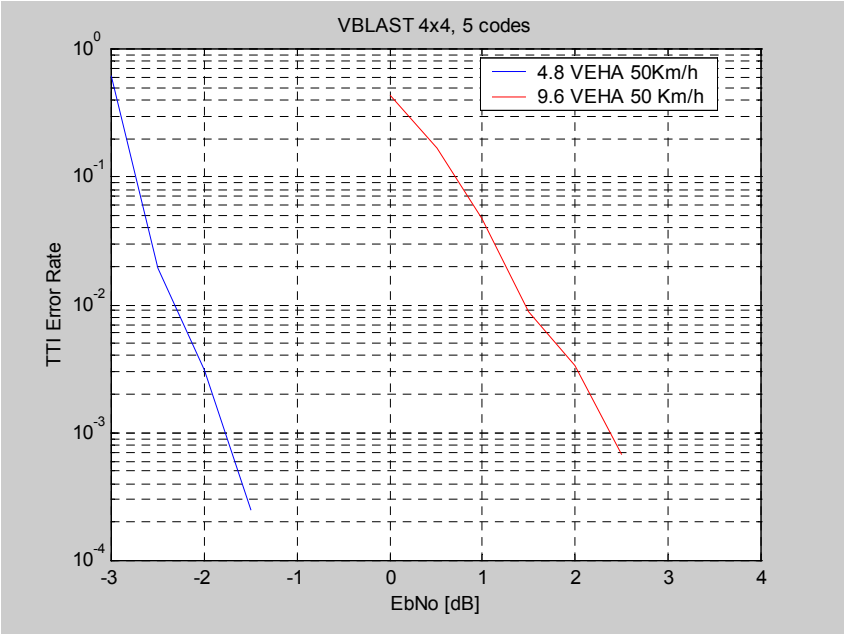

Figure 2.36. TTI Error Rate versus EbNo for V-BLAST 4x4 with 5 codes (cases 29 and 30 of Table 2.5) and for Vehicular A Channel with 50 Km/h.

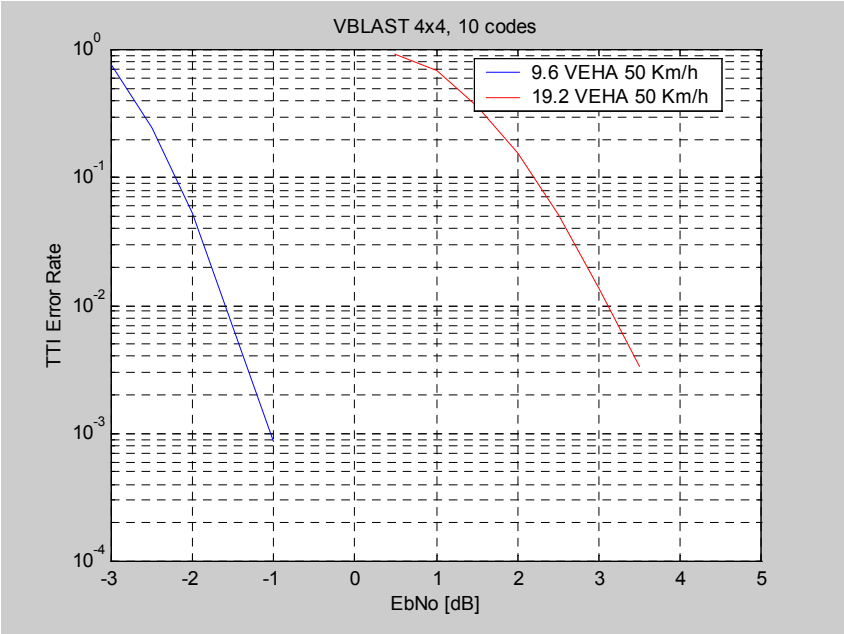

Figure 2.37. TTI Error Rate versus EbNo for V-BLAST 4x4 with 10 codes (cases 33 and 34 of Table 2.5) and for Vehicular A Channel with 50 Km/h.

Concerning the Pedestrian A channel, it has been checked that the TTI Error Rate obtained for the maximum achievable EbNo (that is, the EbNo obtained with 80% of the power assigned to the HSDPA user) is larger than 10^{-1}. Therefore, we conclude that it is not worth simulating the 4x4 V-BLAST configuration for this scenario.

2.6 Link to System Simulator

HSDPA system simulations should be used to draw the final conclusions about the actual performance differences of the tested MIMO techniques. System simulations require input data from link simulator since actual transmission and reception techniques cannot be simulated in the system simulator. The data is in the form of frame error rate (FER) tables. It should be noted that FER, block error rate (BLER) and packet error rate (PER) may be used interchangeably in the sequel.

A system simulator does not simulate practical signals but maps the instantaneous channel conditions to FER which is then applied for emulating random packet errors. In many cases, simple FER(E_b/N_0) tables are sufficient. Signal-to-noise ratio per bit, E_b/N_0, is computed in a different way for each antenna configuration. For example, for SISO case it can be computed as

$$\frac{E_b}{N_0} = \frac{SF}{N_c N_{b/s} R} \sum_{l=1}^{L} \frac{E_c |h_l|^2}{\sigma_1^2 + I_{or} \sum_{l' \neq l} |h_{l'}|^2}$$

where the symbols are defined as

E_c	HSDPA power for desired user (including all code channels)
I_{or}	total BS transmission power
N_c	number of HSDPA code channels for desired user (total power = E_c)
SF	spreading factor (=16)
$\lvert h_l \rvert^2$	average power of channel path l (averaged over one TTI)
$\lvert h_{l,n,m} \rvert^2$	average power of channel path l for TX antenna n to RX antenna m (averaged over one TTI)
σ_m^2	received intercell interference wideband power (variance) at RX antenna m
R	code rate (<1)
$N_{b/s}$	number of bits per symbol
L	number of channel paths.

With STTD transmission and two RX antennas a definitions of packet E_b/N_0 can be approximated as

$$\frac{E_b}{N_0} = \frac{SF}{N_c N_{b/s} R} \sum_{m=1}^{2} \sum_{l=1}^{L} \left(\frac{\frac{E_c}{2} \left(|h_{l,1,m}|^2 + |h_{l,2,m}|^2 \right)}{\sigma_m^2 + \frac{I_{or}}{2} \sum_{l' \neq l} \left(|h_{l',1,m}|^2 + |h_{l',2,m}|^2 \right)} \right).$$

In case the Turbo Space-Time Receiver presented is used, E_b/N_0 should be calculated using

$$E_b = \%HSDPA\_User\_Power \cdot \left(\frac{1}{N} \sum_{n=1}^{N} \sum_{m=1}^{M} \sum_{l=1}^{L} \frac{E_c}{M} \left| h_{n,m}(l) \right|^2 \cdot \frac{SF \cdot T}{N_c \cdot Q \cdot N_{b/s} \cdot R} \right)$$

and

$$N_0 = \sigma_n^2 + (1 - \%Power\_HSDPA\_user) \cdot \hat{I}_{or} + I_{oc}$$

with σ_n^2 due to the thermal noise and

E_c	average transmit energy per PN chip, equal to $P_T \cdot Tc$, with P_T the total transmit power and T_c the chip period
E_c/M	average transmit energy per PN chip per transmitter antenna.
$\hat{I}_{or}$	received power spectral density of the downlink as measured at the UE antenna connector
I_{oc}	power spectral density of a band limited white noise source (simulating interference from other cells) as measured at the UE antenna connector
M	number of transmit antennas
N	number of receive antennas
$N_{b/s}$	number of bits per symbol
R	turbo encoder rate
SF	spreading factor
N_c	number of used codes
Q	number of symbols per LDC block
B	number of LDC block per frame
T	number of time slots used to transmit each LDC block
H(l)	$\in C^{NxM}$ for $l=\{1,2,\ldots L\}$ where is L number of taps; each component is denoted by $h_{n,m}(l)$.

Assuming only one antenna is used to transmit the voice users signal, let us say antenna $m = 1$, then the $\hat{I}_{or}$ corresponds to

$$\hat{I}_{or} = \left(1 - \%HSDPA\_User\_Power\right) \cdot \frac{E_c}{N} \sum_{n=1}^{N} \sum_{l=1}^{L} \left| h_{n,1}(l) \right|^2 .$$

According to the metric used to generate the look-up tables with the Turbo Space-Time Receiver, this E_b/N_0 should be averaged over a coding block. The length in terms of chip channel uses of a coding block depends on the selected configuration, i.e., the modulation and coding scheme, the number of transmit antennas and number of codes.

When certain advanced algorithms, such as linear equalizers are used, E_b/N_0 alone may not be sufficient to obtain accurate, one-to-one mapping to FER. In other words, different channel conditions may result in a same E_b/N_0 but the actual FERs can differ substantially. In this case, two dimensional FER tables can be used. A simple way is to use FER(E_b/N_0, G) tables, where both parameters are "instantaneous" in the sense that they are averaged over one packet interval. Since in the current link simulator

intercell interference is modelled as white Gaussian noise, packet G is a rough function of the whiteness of the signal. Signal whiteness, in turn, affects the performance of channel equalizers when compared to conventional RAKE.

Link simulations are used to generate either one or two dimensional FER tables which are then used by the system simulator. Packet retransmissions are naturally not allowed during the table generation since H-ARQ is emulated in the system level.

2.7 Conclusions from HSDPA Link Performance Evaluation

Link simulations indicate that channel equalization is required in multipath channels in order to utilize higher-order modulation (16-QAM). Chip-level equalization increases peak data rates significantly. In macro cell environment, the increase is only moderate due to high intercell interference power. Dual-antenna RAKE increases the received signal-to-noise ratio and diversity order but this is not sufficient to support the MCS that offers the highest data rate. Dual-antenna space-time receiver is superior to other SIMO receivers.

We also evaluated the performance of different transmit diversity and layered techniques in HSDPA downlink. With uncorrelated fading a comprehensive evaluation was done between different transmit diversity schemes showing that the benefit against single antenna transmission is not very significant. Also the difference between the evaluated transmit diversity schemes was almost unnoticeable. A short evaluation between layered and diversity techniques, including also advanced receiver for single antenna transmission, was done showing that in Pedestrian A channel the main gain is due to additional receive antenna, while in Vehicular A channel the use of layered schemes and equalization can be significantly and equally beneficial.

However, with correlated fading the analysis showed that the performance of multi streaming MIMO is seriously affected by the channel correlation. It was shown that in most cases even STTD with two receive antennas can outperform the layered schemes, and additional gain over STTD can be achieved by using dual antenna equalization. In the most difficult cases where high level of interference becomes a limiting factor for both layered schemes and STTD, only equalizer was able to achieve adequate performance.

Layered MIMO transmission (e.g. BLAST) requires an advanced receiver. The developed SPRI detector outperforms OSIC with high data rates although it increases the receiver complexity. It is has been shown that OSIC may have problems with practical antenna correlations which may make linear separation of data layers inefficient. However, both ML and SPRI detectors are more insensitive to antenna correlation. ML based detector does not perform properly in multipath channels while in flat channels it is a good option.

3 LINK-LEVEL PERFORMANCE OF MIMO HSUPA

The 3GPP specification for UMTS (Universal Mobile Telecommunication System), known also as wideband CDMA, or WCDMA, supports different modes of smart antenna techniques. However, multi-antenna transmission from an UE to a Node B has not been considered yet in specification work. This chapter reports the performance of different multi-antenna modes in order to evaluate the feasibility of a MIMO approach for the WCDMA uplink. The uplink MIMO performance is compared to a reference case in which the UE transmits with a single antenna. Different Node B receiver algorithms are also compared including Maximal Ratio Combining (MRC), Interference Rejection Combining (IRC), and 1-stage partial Parallel Interference Canceller (PIC). In addition, effect of ARQ and HARQ is studied in uplink packet transmission. Both single-user link-level results and multi-user cell-level results are provided.

The simulation approach, models, and parameters have been described in detail in deliverable D3.2.

3.1 Selected Uplink Scenarios

In the MIMO scheme under study the UE transmits the same data stream via two antennas. In order to separate the two chip streams at the Node B both antennas use different channelisation codes. Thus, the considered MIMO scheme doubles the utilization of the UL channelisation codes when compared it against single antenna transmission of STTD (Space Time Transmit Diversity) (used in 3GPP downlink) but without the need for STTD encoder/decoder. The performance of the considered MIMO scheme is the same as with the UL STTD since both schemes represent two-way transmit diversity. The base station receiver performs MRC (Maximal Ratio Combining) over signal paths, antennas, and Tx-diversity branches (standard Rake receiver).

Four different antenna configurations are considered in the link simulations: 1x2 (one transmit antenna, 2 receive antennas), 2x2, 1x4 and 2x4, respectively. In all the cases both transmit and receive antennas were assumed to be uncorrelated. Table 3.1 illustrates the temporal properties of the considered radio channel models.

Table 3.1. Channel models of simulation

Channel model	Relative path powers [dB]	UE velocity [km/h]
Rayleigh, 1-path	0	3, 50
Mod. ITU Pedestrian A (2-paths)	0 -12.7	3
Mod. ITU Vehicular A (6-paths)	0 -1.9 -7.3 -10.4 -10.9 -17.3	50

The link performance of different antenna configurations is compared by means of Monte-Carlo simulations. In simulations the measure for comparison of different transmission schemes is the receive/transmit (Rx/Tx) E_b/N_0 (bit energy / total noise

power density) that is required to obtain the desired Quality of Service (QoS) (10% BLER). E_b/N_0 values are based on multi-user simulations in which there are multiple simultaneous intracell users in the cell of interest and each of them meets the QoS requirement. Average Rx E_b/N_0 per receiving antenna corresponds to the amount of intracell interference that the other users experience from the given UE. Thus it is a measure of uplink capacity, i.e. the maximum number of users that can be supported by one base station cell. Required Tx E_b/N_0 corresponds to the transmit power of the UE and describes the amount of inter-cell interference that the given UE generates. Tx E_b/N_0 is also used when the UL coverage of different schemes is compared.

Full 3GPP link level modelling was used with inner and outer loop power control and realistic cannel and interference estimation algorithms. 64 kb/s data service specified in 3GPP conformance tests [2] was used in the link simulations (spreading factor of 16, 1/3 Turbo coding, 10 ms interleaving, power ratio of DPCCH/DPDCH=-5.46 dB).

When studying the UL performance of different transmission schemes, an important parameter is UL load factor, denoted as h. The UL load factor is calculated as [3]

$$\eta = (1+i)\cdot\sum_{j=1}^{J}\frac{1}{1+\dfrac{1}{(E_c/N_0)_j}}, \qquad (1)$$

where i is the ratio of other cell to own cell interference, J is the number of users and Ec/No is the chip energy per total noise power density. Ec/No is calculated from the simulated Rx E_b/N_0 as

$$(E_c/N_0)_j = \frac{\text{user bit rate}}{\text{chip rate}}\cdot\left(Rx\ E_b/N_0\right). \qquad (2)$$

Setting $i = 0$ in Equation (1) gives us the load factor in an isolated cell in which the amount of other cell interference is zero. Noise raise is used as a final performance criterion for different transmission schemes. It is calculated from the UL load factor as

$$\text{Noise\_raise} = 10*\log 10\left(\frac{1}{1-\eta}\right). \qquad (3)$$

Equations (3) and (4) can be used to calculate the noise based on the simulated single user Rx E_b/N_0 values. In the performance evaluation we use another approach. As mentioned, we are doing multi-user simulations, which give us Rx E_b/N_0 results in case of multiple users. We calculate the noise raise in case of j users as

$$\text{Noise\_raise}\,(j) = Rx\ E_b/N_0\ \ (j) - Rx\ E_b/N_0\ \ (1) + \text{Noise\_raise}\,(1) \qquad (4),$$

where Rx E_b/N_0 (j) is the simulated average Rx E_b/N_0 obtained from the multi-user simulation having j simultaneous users and Noise_raise (1) corresponds the noise raise of single user case calculated using Equations (3) and (4).

Figure 3.1 shows a reference comparison of an analytical and multiuser simulation result. In this case 1-path Rayleigh channel was applied. Simulated curve is based on actual multiuser E_b/N_0 requirement while the theoretical curve is calculated from (1)-(4) using E_b/N_0 that is required for a single user. Simulated and theoretical curves match very well and both give 21 64 kbps users for noise rise of 3 dB. Figure 3.2 plots the corresponding curves for E_b/N_0 requirement per receiver antenna. It is noted that the power controlled WCDMA uplink operates at a low E_b/N_0 level. Main reason for this is that the pilot power of the 64 kbps service is relatively large which is beneficial from the channel estimation point of view.

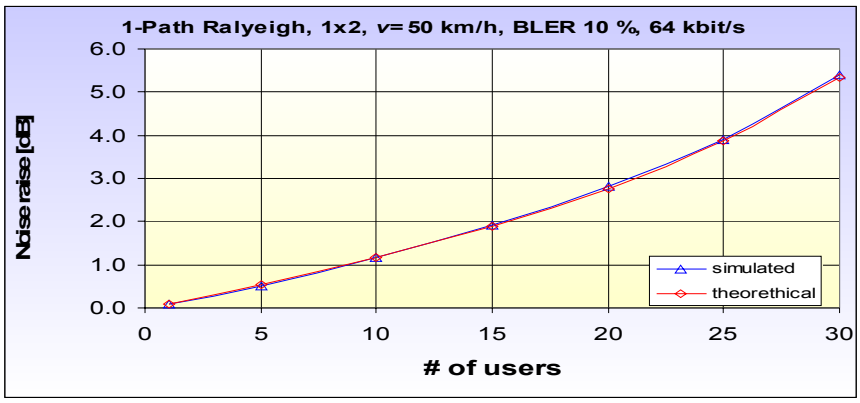

Figure 3.1. Simulated and theoretical noise rise for multiuser WCDMA uplink in 1-path Rayleigh channel, 64 kbps.

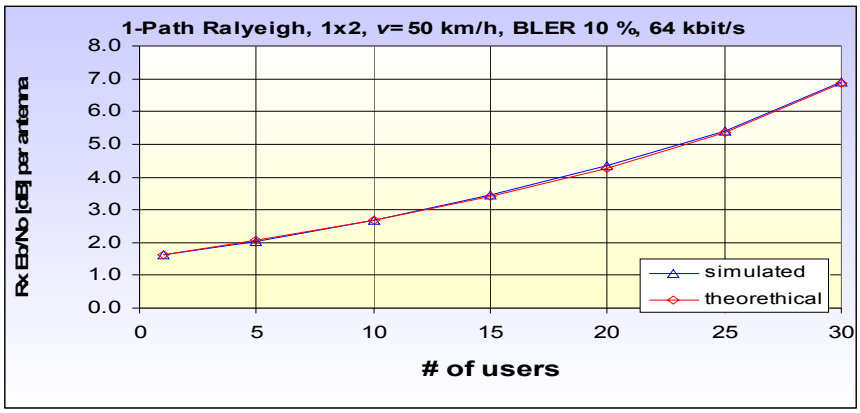

Figure 3.2. Required E_b/N_0 per antenna for multiuser WCDMA uplink in 1-path Rayleigh channel, 64 kbps.

3.2 Uplink Capacity

Figure 3.3 presents the simulated noise raise curves for the considered SIMO (Single-Input-Multiple-Output) and MIMO transmission schemes. We can notice from the

plot that the usage of the 2nd transmit antenna does not increase the isolated cell capacity in a one path Rayleigh channel (v=3 km/h). This can be explained by the fact that in uplink power controlled (PC) system the additional diversity gain provided by the MIMO transmission is visible only at the transmit (UE) side. For that reason the Rx E_b/N_0 requirement is not improved using MIMO and thereby the isolated cell capacity is about the same as in the SIMO case. Doubling the number of receiving antennas will double the isolated cell capacity in both SIMO and MIMO cases.

Figure 3.4 illustrates again one-path Rayleigh channel, but now the speed of mobile is 50 km/h. This is the only simulated case in which the usage of the 2nd transmit antenna provides some capacity gain in isolated cell (about 10% with 2 receive antennas). The reason for that is the non-ideal behavior of power control. UE speed of 50 km/h is relatively high velocity from the PC point of view and it cannot fully compensate the fast fading. Since the MIMO has smaller variance in the received power than SIMO (due to the higher number of diversity branches) the "slowness" of the PC loop does not impact as much in the MIMO case.

Table 3.2 shows the corresponding improvement in cell throughput at 3 dB noise rise (50% loading).

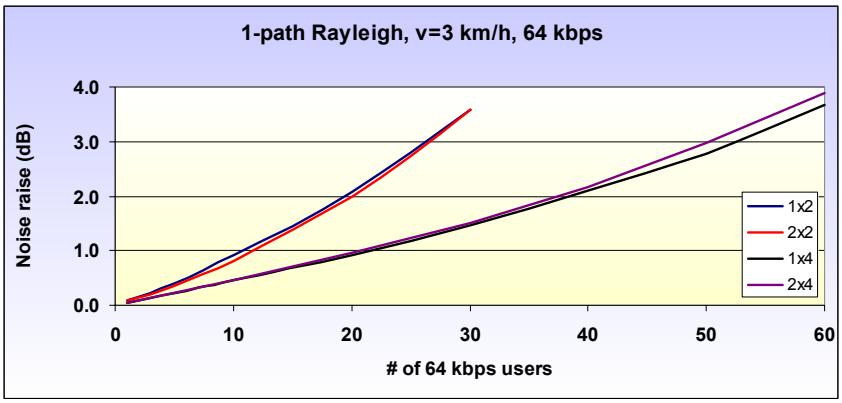

Figure 3.3. WCDMA uplink noise rise as a function of isolated cell throughput in 1-path Rayleigh channel: 64 kbps, UE velocity 3 km/h.

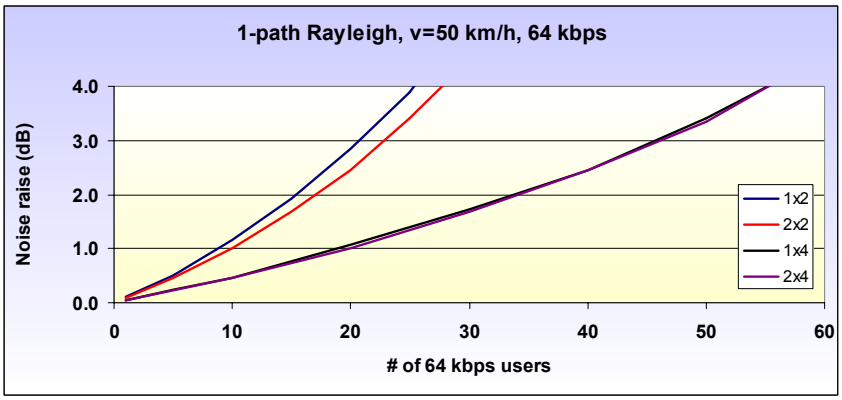

Figure 3.4. WCDMA uplink noise rise as a function of isolated cell throughput in 1-path Rayleigh channel: 64 kbps, UE velocity 50 km/h.

Table 3.2. Isolated cell capacity in 1-path Rayleigh channel for 64 kbps users at 50% loading. Left: 3 km/h, right: 50 km/h

antenna configuration	# of 64kbps users	capacity increase (vs. 1x2)%
1x2	26	0.00%
2x2	26	0.00%
1x4	52	100.00%
2x4	50	92.31%

antenna configuration	# of 64kbps users	capacity increase (vs. 1x2)%
1x2	21	0.00%
2x2	23	9.52%
1x4	46	119.05%
2x4	46	119.05%

Figure 3.5 represents the simulated noise raise in modified ITU Pedestrian A channels (v=3 km/h) for 64 kbps users. We can notice that the usage of the 2nd transmit antenna will actually degrade the isolated cell capacity especially in case of 4 receiving antennas. The reason for that is that the estimation errors (combining loss) are larger in MIMO case since the dedicated pilot must be transmitted via both antennas (pilot power per antenna is 3 dB smaller than in SIMO case). Performance degradation caused by the 2nd transmit antenna increases as the number of multipath components in the radio channel increases. The reason for that is the fact that the SNR (signal-to-noise ratio) per Rake finger decreases as the number of multipath components increases. The considered service has also an impact on the estimation errors: when the data rate is higher (than 64 kb/s) then the power of dedicated pilot channel can be increased and the estimation errors will be decreased (and vice versa).This effect is clearly seen in Figure 3.6 which plots the corresponding noise rise curves for 384 kbps service. In this case the pilot power level is 4 dB larger than with 64 kbps service and therefore the estimation errors are smaller. Consequently, the performance of MIMO is practically the same as that of SIMO. Estimation errors increase also as the number of Tx/Rx antennas and the speed of mobile increase.

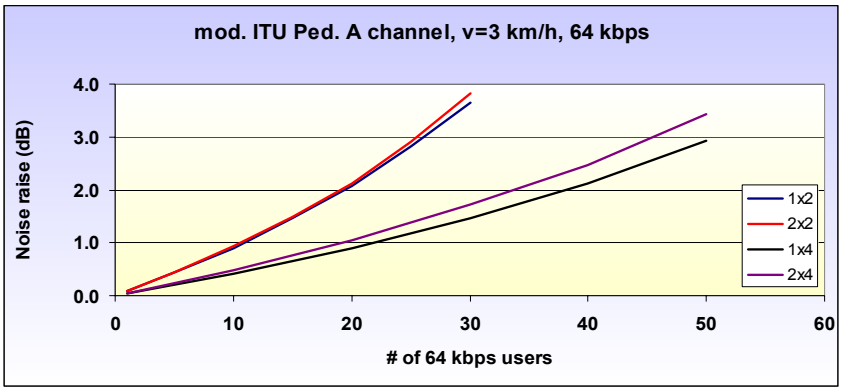

Figure 3.5. WCDMA uplink noise rise as a function of isolated cell throughput in Pedestrian A channel: 64 kbps, UE velocity 3 km/h.

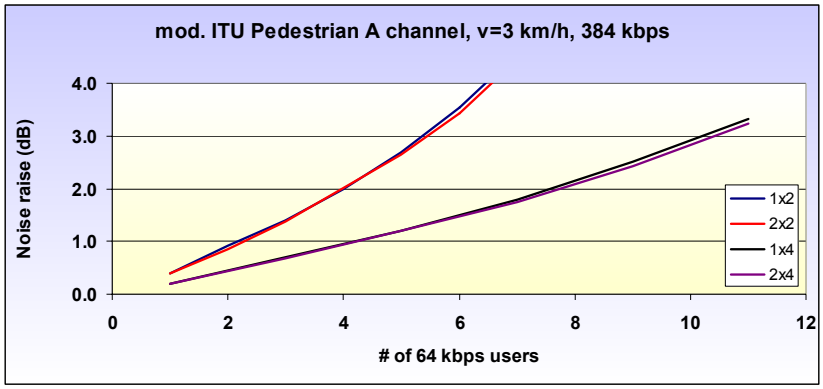

Figure 3.6. WCDMA uplink noise rise as a function of isolated cell throughput in Pedestrian A channel: 384 kbps, UE velocity 3 km/h.

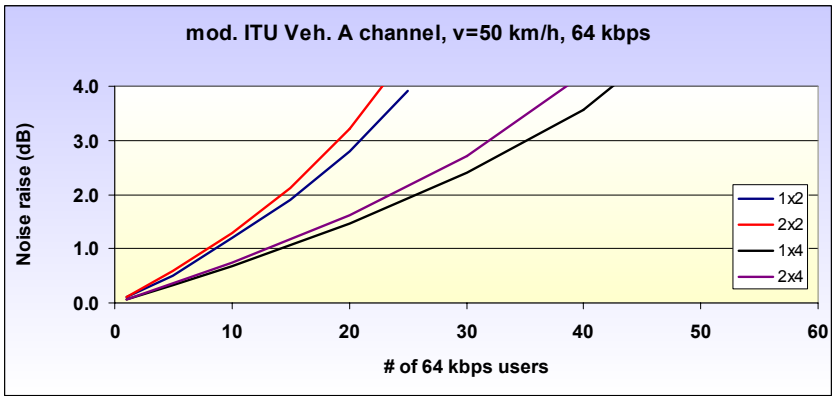

Figure 3.7. WCDMA uplink noise rise as a function of isolated cell throughput in Vehicular A channel: 64 kbps, UE velocity 50 km/h.

Figure 3.7 presents noise raise curves for modified Vehicular A channel (v=50 km/h) and 64 kbps service. We can notice that the isolated cell capacity of the SIMO case is almost 10% better than that of the MIMO case. In this multitap channel the capacity improvement is smaller than in previous cases. Except the above mentioned estimation error also one reason for reduced throughput is the fact that only 8 Rake fingers were applied in both the 2-antenna and 4-antenna reception. Accordingly, a portion of signal energy (0.67 dB) is lost in 4-antenna receiver.

Table 3.3 summarises the improvement in cell throughput at 3 dB noise rise (50% loading) for Pedestrian A and Vehicular A channels.

Table 3.3. Isolated cell capacity for 64 kbps users at 50% loading. Left: Pedestrian A, 3 km/h, right: Vehicular A, 50 km/h

antenna configuration	# of 64kbps users	capacity increase (vs. 1x2)%
1x2	26	0.00%
2x2	25	-3.85%
1x4	51	96.15%
2x4	45	73.08%

antenna configuration	# of 64kbps users	capacity increase (vs. 1x2)%
1x2	21	0.00%
2x2	19	-9.52%
1x4	35	66.67%
2x4	32	52.38%

As a summary from the isolated cell capacity studies, it can be said that the doubling the number of receiving antennas will almost double the isolated cell capacity, whereas the increase of the number of transmit antennas will mostly have negative impact on the cell isolated cell capacity.

3.3 Uplink Coverage

Coverage improvement in a power controlled uplink is based on the average transmitted E_b/N_0 (dB) values. Figure 3.8 presents the relative coverage gain of three different antenna configurations 2x2, 1x4 and 2x4 compared to the 1x2 reference case in a single user scenario. The benefit of the 2nd transmit antenna is seen at the transmitter side (due to the power control). We can notice that the 2x2 MIMO case can support up to 2 dB higher path loss than SIMO with 2 receiving antennas. The coverage gain of the MIMO approach decreases as the amount of time, multipath, or Rx-antenna diversity in the radio channel increases. It can be also on the negative side (mod. ITU Vehicular. A channel, v=50 km/h) when the additional estimation errors are larger than the additional diversity gain provided by the 2nd transmit antenna. One finding is also the fact that for the same degree of diversity the 1x4 antenna constellation is 3 dB better than the 2x2 constellation. In addition to the uplink coverage it is obvious that the required transmitted E_b/N_0 has also a positive impact on fast fading margin, interference to the other cells, and the UE power consumption.

Figure 3.9 and Figure 3.10 illustrate coverage evaluation in a multi-user modified Pedestrian A channel with UE speed of 3 km/h. Figure 3.9 compares 2x2 configuration against 1x2 case and Figure 3.10 1x4 and 1x2 antenna constellations, respectively. We can notice that in the 1x4 case the coverage gain increases with UL load. The total coverage gain is obtained by taking both reduced noise raise and reduced Tx E_b/N_0 into account [3]. This means that e.g., having 30 simultaneous 64 kb/s user in the sector of interest the 2x2 MIMO approach can provide 1.3 dB coverage gain compared against 1x2 case whereas 1x4 case can provide as much as 6.6 dB (2.3 + 4.3 dB) better coverage. Figure 3.11 shows the corresponding result for Vehicular channel.

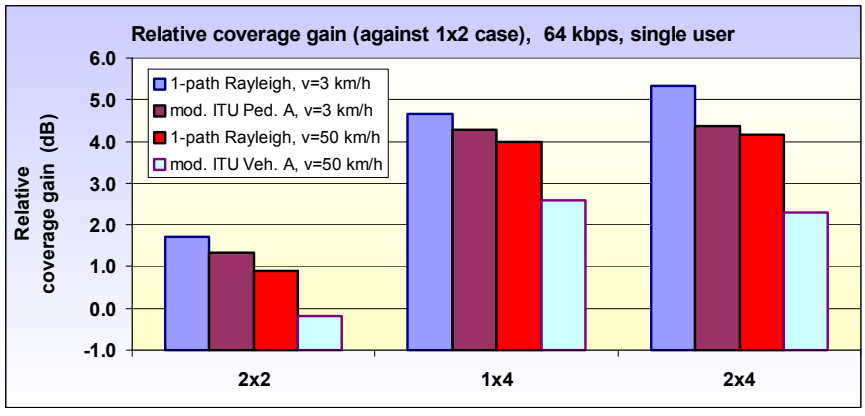

Figure 3.8. Relative coverage improvement of different antenna constellations vs. conventional 1 TX- and 2 RX-antenna case.

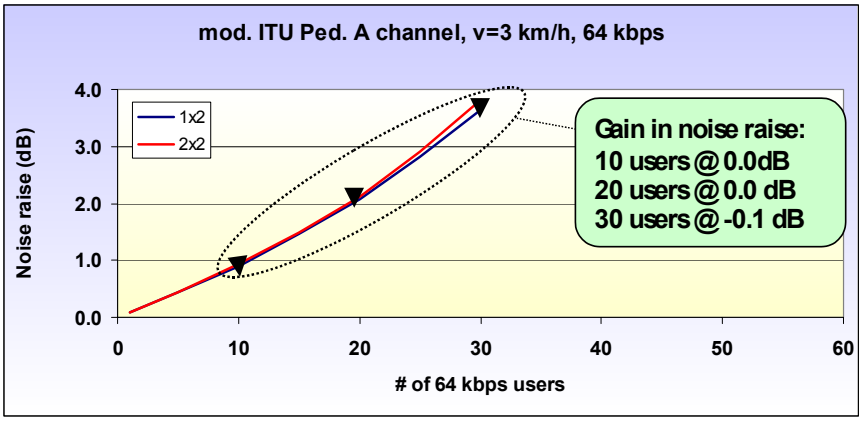

Figure 3.9. Noise rise of 2x2 MIMO vs. conventional 1 TX- and 2 RX-antenna case as a function of cell throughput.

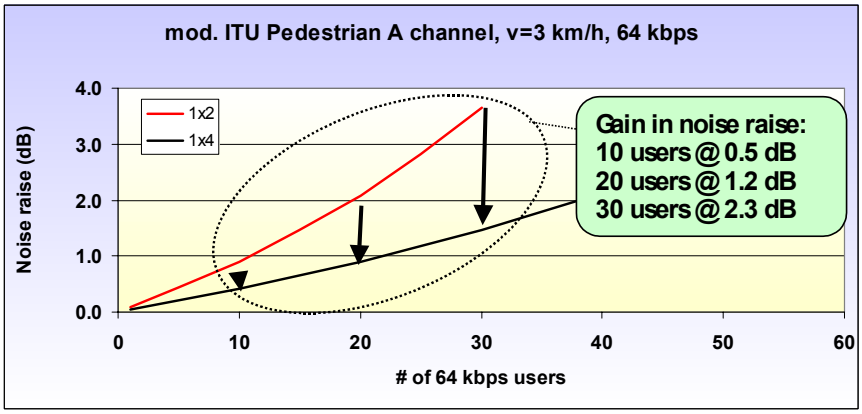

Figure 3.10. Noise rise of 1x4 antenna constellation vs. conventional 1 TX- and 2 RX-antenna case as a function of cell throughput, Ped A, 50 km/h.

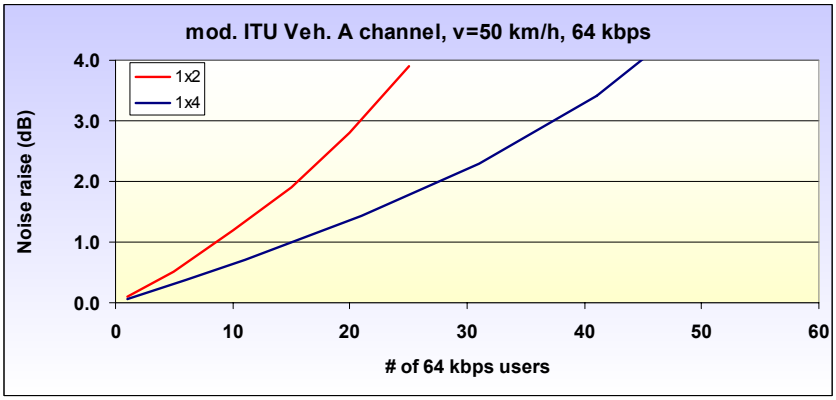

Figure 3.11. Noise rise of 1x4 antenna constellation vs. conventional 1 TX- and 2 RX-antenna case as a function of cell throughput, Veh A, 50 km/h.

Table 3.4 summarizes the coverage improvement for the Pedestrian A and Vehicular A channels as a function of the cell loading. It can be approximated that the coverage gains for pedestrian and vehicular environments at 50% loading level are approximately 6 dB and 4.5 dB, respectively.

As a conclusion from the coverage studies it can be stated that increasing the number of receive antennas is more feasible than employing the MIMO concept. The coverage improvement of 4 Rx antennas vs. 2 Rx antennas is significant. Those operators which do not have an existing base station infrastructure can exploit this gain effectively since fewer base station sites are needed for the initial network roll-out. Moreover, as the data services get more popular this gain can be also realized as improved coverage for medium or high data rates.

Table 3.4. Coverage gain for 4-antenna MRC.

Radio Channel	**Relative gain vs. 2-ant MRC [dB]**			
	1 user	10 users	20 users	30 users
Ped. A 3 km/h	4.3	4.8	5.5	6.6
Veh. A 50 km/h	2.9	3.5	4.4	6.2

3.4 HSUPA Performance with Advanced Receivers

MIMO techniques in WCDMA uplink increase the number of data streams in a cell, which inevitably leads to the conclusion that advanced receiver have to be applied in a form or another to control the interference. In fact, the modeling of multiple uncorrelated data streams from MIMO users corresponds the typical scenario of a base station receiver in which multiple users have to be extracted from the composite receive signals. Therefore, the receiver performance can be evaluated with similar multi-user simulations which were carried out in previous sections.

In this section, isolated cell capacity was studied with a single high data rate user as an intracell interferer. The data rates of 384 kbps, 768 kbps, and 2048 kbps were used for the interfering user. Inter-cell interference was modeled as Gaussian noise. The same channel and simulation models as in the previous sections were applied using 10% BLER as a target for each of the 64 kbps users. The performance of an adaptive antenna receiver and a 1-stage partial PIC (Parallel Interference Canceller) receiver was compared to that of a conventional Rake receiver.

3.4.1 Adaptive Antenna Receiver

Adaptive antenna receivers can be defined using different optimization criteria as a starting point. These criteria include e.g. mean-square error, maximum signal-to-

interference-and-noise ratio (SINR), and maximum likelihood measures. All these criteria lead to similar optimum combining solution which can be expressed as [4]

$$\mathbf{w}_{\text{opt}} = c\,\mathbf{R}_{nn}^{-1}\mathbf{r}^{*} \qquad (5)$$

in which $\mathbf{R}_{\text{nn}}$ is the spatial correlation matrix of the noise and interference, **r** is the signal vector of the desired signal, (*) denotes the complex conjugate operation, and c is a scalar. In practice, estimation of the $\mathbf{R}_{nn}$ matrix may be difficult and therefore often the mean-square error (Wiener) solution is used [5]:

$$\mathbf{w}_{\text{opt}} = a\,\mathbf{R}_{xx}^{-1}\mathbf{r}^{*} \qquad (6)$$

It is evident that the performance of the smart antenna algorithm depends strongly on the properties of the spatial correlation matrix $\mathbf{R}_{nn}$ (or $\mathbf{R}_{xx}$) and the quality of estimation processes. In WCDMA multiple access interference dominates the correlation matrix and Eqs. (5) and (6) give approximately the same performance. However, in WCDMA the ratio between the interference power density and the noise power density (I_0/N_0) is typically small due to power control. Therefore, advanced receivers have only a limited possibility to reduce interference. The estimation quality of the desired signal vector **r** plays also an important role. In practice, it corresponds to to the channel estimation of the desired signal.

The smart antenna algorithm updates the antenna weights as the radio channel and the interference structure varies with time. This adaptation can be achieved by different well-known algorithms such as the LMS, RLS, DMI (Direct Matrix Inversion), which was applied in this study. The algorithm is denoted as IRC (Interference Rejection Combining).

In the following three receiver algorithms applied in this study are briefly reviewed. The particular algorithms were chosen mainly due to their comparable complexity.

3.4.1.1 MRC

Maximal Ratio Combining (MRC) is a special case of Eq. (6). MRC is an optimal combining if the interference is spatially and temporally white. Then the correlation matrix $\mathbf{R}_{xx}$ is a diagonal matrix with signal powers of different antennas at the diagonal (fully uncorrelated $\mathbf{R}_{xx}$). Thus the weighting is proportional to signal-to-noise ratio (SNR) at different antennas. A conventional Rake receiver applies MRC.

3.4.1.2 IRC (Max SINR)

With colored interference optimal combiner output can be achieved using complex antenna weights from Eq.(5). The algorithm requires that the contribution of the desired signal is removed from the total correlation matrix $\mathbf{R}_{xx}$. If the despread symbol s of desired signal for multipath n and sample k is received at M antennas through

fading channel vector $\mathbf{h}_n$ with noise and interference $\mathbf{u}(k)$ the sample of received signal vector $\mathbf{x}(k)$ can be modeled as

$$\mathbf{x}_n(k) = \mathbf{h}_n s(k) + \mathbf{u}_n(k) \quad (7).$$

The estimates of $\mathbf{h}_n$ and $\mathbf{R}_{nn}$ can be obtained for P pilot symbols by applying Eqs. (6) and (7):

$$\tilde{\mathbf{h}}_n = \tilde{\mathbf{r}}_n = \Sigma\, s_p^*(p)\, \mathbf{x}_n(p) \quad (8)$$

$$\tilde{\mathbf{R}}_{nn} = \Sigma\, \{[\mathbf{x}_n(p) - \tilde{\mathbf{h}}_n s_p(p)]\, [\mathbf{x}_n(p) - \tilde{\mathbf{h}}_n s_p(p)]^h\} \quad (9)$$

where summation is performed over the pilot symbols.

3.4.2 Partial PIC

In this study a simple 1-stage partial Parallel Interference Canceller (PIC) was also applied for comparison. The general block diagram of the PIC receiver is illustrated in Figure 3.12. The receiver is designed for cancellation of only the largest data rate (dominant) interferer and it exploits only pilot symbols for channel estimation.

3.4.3 Performance Comparisons

Figure 3.13 shows the performance of advanced receivers in 1-path Rayleigh channel compared to a Rake receiver with two and four receive antennas. The structured interference was generated as a single 384 kbps user. In general, it can be observed that doubling the number of receive antennas gives a significant capacity improvement with all the three algorithms. It is also apparent that doubling the number of receive antennas gives significantly better improvement in WCDMA uplink performance than applying advanced algorithms for the 2-antenna signals. Actually, even the ideal cancellation does not improve the 2-antenna performance significantly. This can be easily explained by the fact that the 384 kbps interferer is rather weak and it forms a relative small portion of the total interference. Figure 3.14 and Figure 3.15 depict the cases of larger interference which is seen as increased gains from advanced receiver. In all these figures the notation “n64” denotes an ideal case in which the high data rate interferer has been completely cancelled. Notation “PIC_noE” corresponds also to an ideal situation in which the tentative decisions of the partial PIC receiver are all correct.

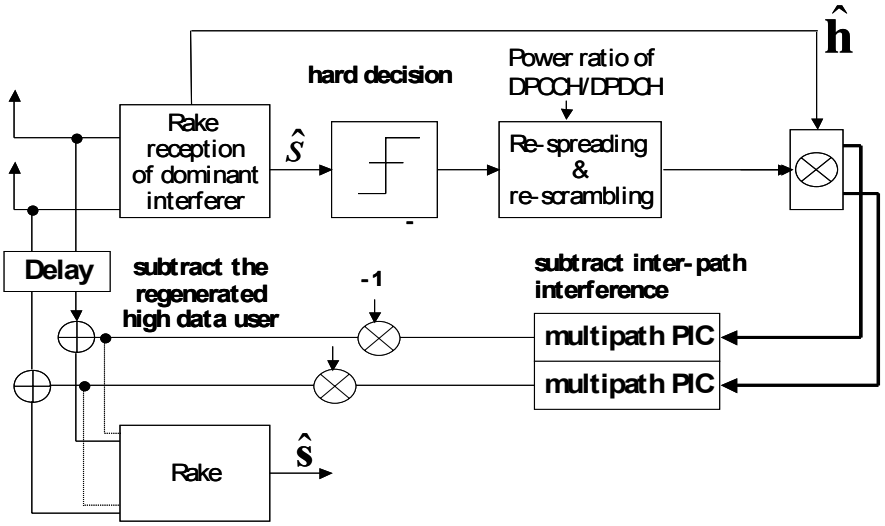

Figure 3.12. Block diagram of the 1-stage partial PIC receiver.

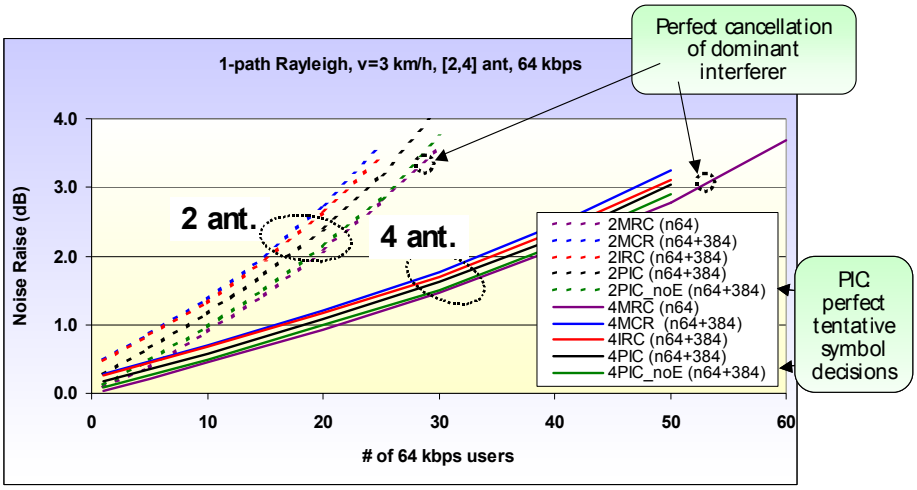

Figure 3.13. Noise rise as a function of cell loading with advanced receivers: 384 kbps interferer, 1-tap Rayleigh channel, UE velocity3 km/h.

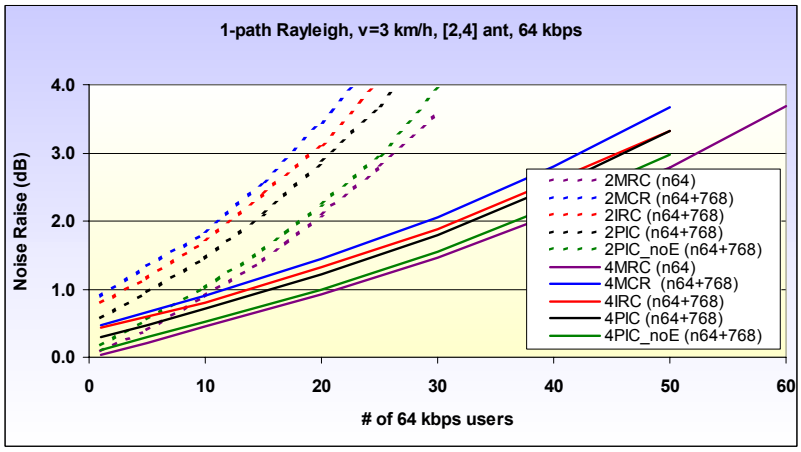

Figure 3.14. Noise rise as a function of cell loading with advanced receivers: 768 kbps interferer, 1-tap Rayleigh channel, UE velocity3 km/h.

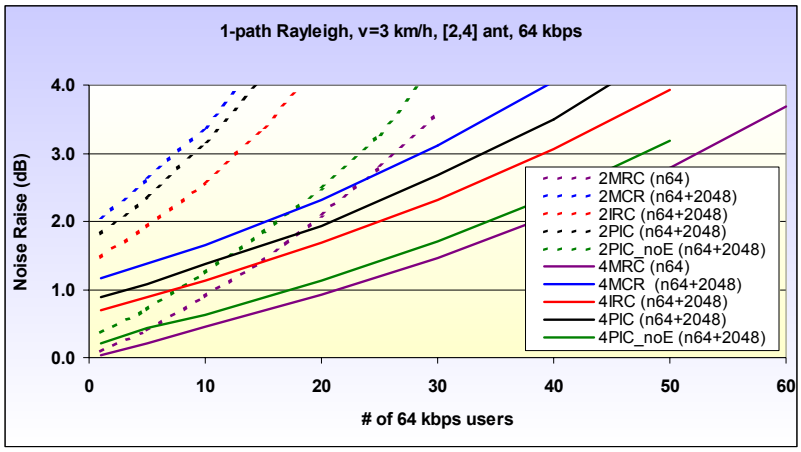

Figure 3.15. Noise rise as a function of cell loading with advanced receivers: 2048 kbps interferer, 1-tap Rayleigh channel, UE velocity3 km/h.

Figure 3.16, Figure 3.17 and Figure 3.18 plot the performance of advanced receivers in a multi-tap Vehicular A channel. The same behaviour is visible in the relative performance of different algorithms as in a single-tap Rayleigh channel. The relative capacity gain of the 4-antenna receivers compared to the 2-antenna receivers is smaller than in the 1-tap channel. This is partly due to increased channel estimation errors in multi-tap channels and partly due to the fact that the 2-antenna receivers exploit four strongest multi-paths of each antenna while the 4-antenna receivers exploit only two of them per antenna (all receivers employ eight Rake fingers). From the curves it is evident that the advanced algorithms applied in this study do not give significant capacity gain at a typical operating point of the WCDMA uplink when using realistic channel estimation algorithms. A good example is the IRC receiver which performs only marginally better than the MRC receiver in case of 384 kbps and 768 kbps interference. The IRC gives significant gain only in case of a single 2048 kbps interferer. The optimum combiner like the IRC receiver requires a large interference-to-noise ratio, I0/N0, for significant link level gain [6]. In the present scenario the total interference-to-noise ratio is 0 dB at cell loading of 50% and only part of the interference is caused by the high data rate user. Partial PIC does not have as good performance as the IRC. Only the idealistic PIC receiver with no hard decision errors (marked as “NoE”) performs considerably better than simple MRC.

As a conclusion from the studies with advanced receivers it can be stated that increasing the number of receive antennas to four and applying the Rake receiver is more feasible than employing simple advanced receivers with two receive antennas.

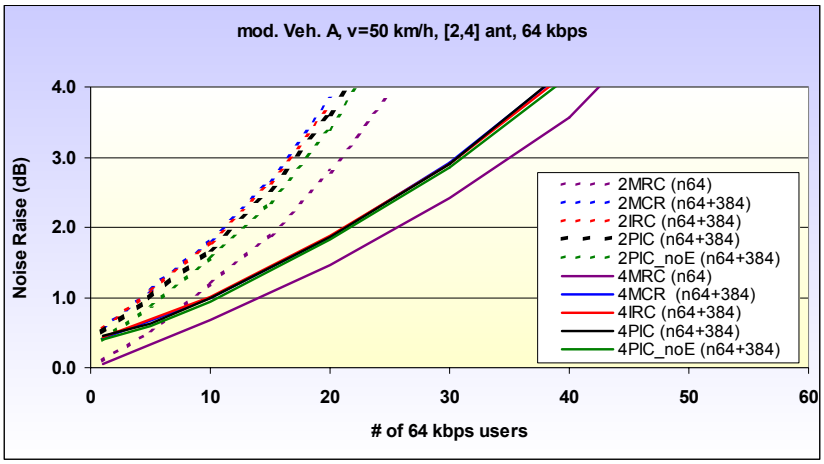

Figure 3.16. Noise rise as a function of cell loading with advanced receivers: 384 kbps interferer, Vehicular A channel, UE velocity 50 km/h.

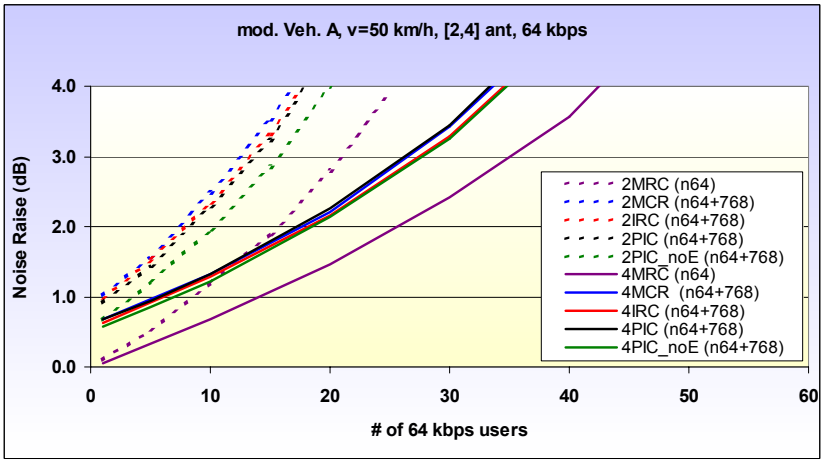

Figure 3.17. Noise rise as a function of cell loading with advanced receivers: 768 kbps interferer, Vehicular A channel, UE velocity 50 km/h.

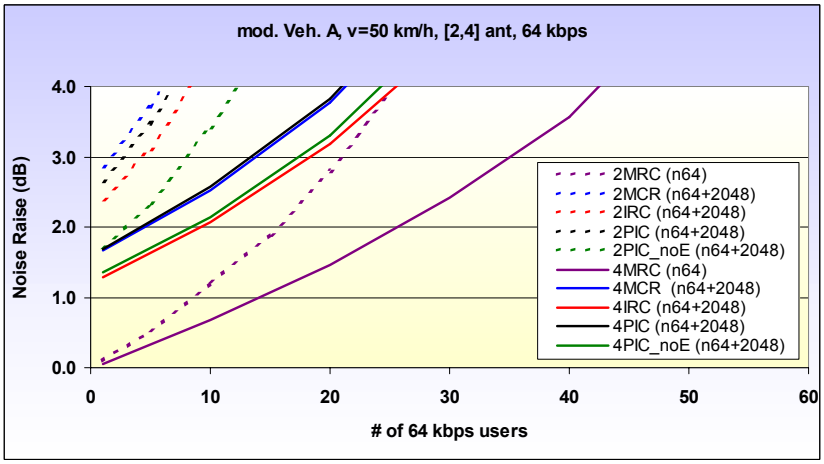

Figure 3.18. Noise rise as a function of cell loading with advanced receivers: 2048 kbps interferer, Vehicular A channel, UE velocity 50 km/h.

3.5 HSUPA Performance with ARQ and HARQ

In this section the performance of packet-mode transmission in WCDMA uplink is investigated in a similar manner as in the previous sections. The noise rise in an isolated cell is evaluated in single user simulations in which the noise rise is evaluated analytically as a function of cell throughput. In the following the term "Enhanced Dedicated Channel" (E-DCH) is used for the HSUPA channel. Table 3.5 shows the main simulation parameters used in the present study.

Table 3.5. Simulation parameters for HSUPA

Parameter	Default value
Antenna constellation	1x2, 2x2, 1x4, 2x4
E-DCH data rate	384 / 144 kbps
Channel coding	1/3 Turbo
HARQ scheme	Chase combining
Max no of re-transmissions	2
Re-transmission delay	20 ms
TTI length*	10 ms
Power control	ON
HARQ feedback channel	Error-free

* TTI= Transport Time Interval

Figure 3.19 illustrates single user throughput for 144 kbps service in Pedestrian A channel as the UE is moving at 3 km/h. Results for both ARQ and hybrid ARQ are presented. The plot on the top demonstrates that gain of HARQ against ARQ is largest as the BLER of the 1st transmission is large. More specifically, it can be evaluated that at the effective operating point of 100 kbps the HARQ operates at about 0.5 dB lower E_b/N_0 requirement than the ARQ. Moreover, the 4-antenna receiver operates at about 3 dB lower E_b/N_0 requirement than the 2-antenna receiver. The plot at the bottom shows that the second transmission is almost always correct for the HARQ even if the BLER is as high as 67%. Thus, one conclusion from the results is that with HARQ the maximum number of re-transmissions and the corresponding transmission power levels have to be carefully optimised.

Single user throughput for the 384 kbps service in Pedestrian A channel is plotted in Figure 3.20. In this case also the performance of 2x2 and 2x4 MIMO schemes is compared to the corresponding 1-antenna UE cases. It can be stated again that the 4-antenna receiver is superior to the 2-antenna receiver. For example, at 300 kbps throughput the 4-antenna receiver operates at about 3 dB smaller E_b/N_0 requirement. The hybrid ARQ gives improvement of about 1 dB over ARQ at the operating point of 200 kbps for both the 2-antenna and 4-antenna case. As in previous sections, the MIMO approach does not bring any performance gains. The reasons are the same as described in previous sections.

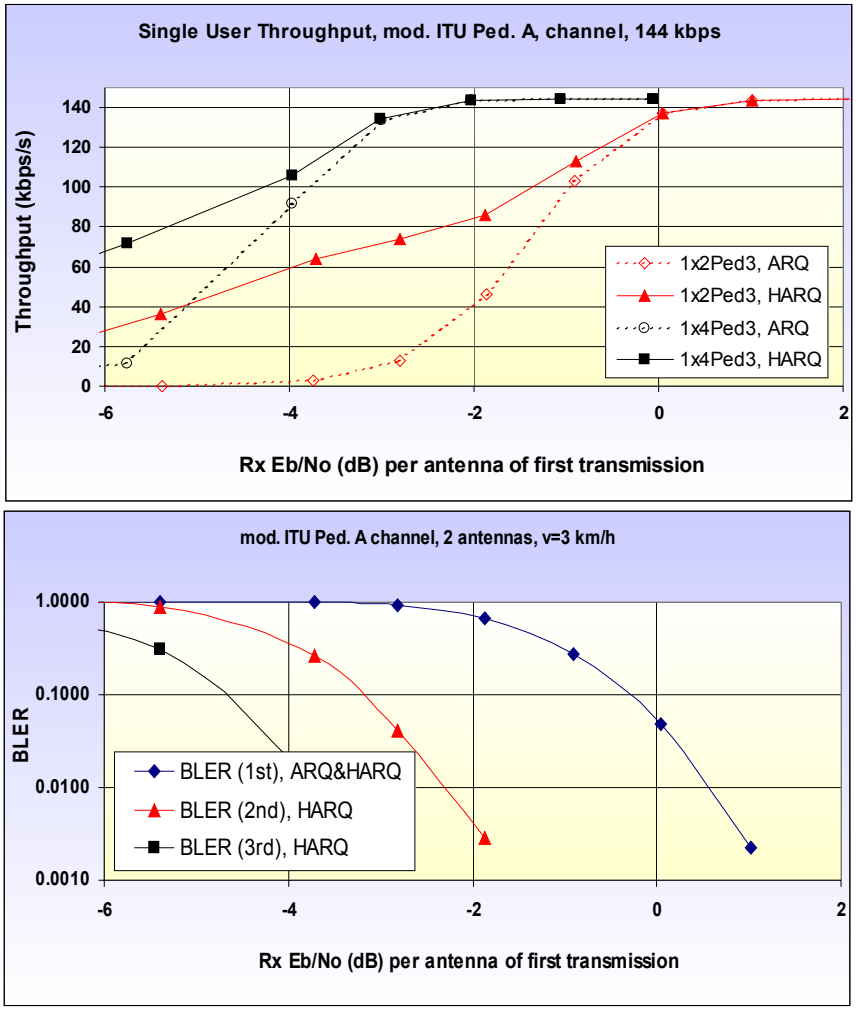

Figure 3.19. Single user throughput, 144 kbps, Pedestrian A, 3 km/h.

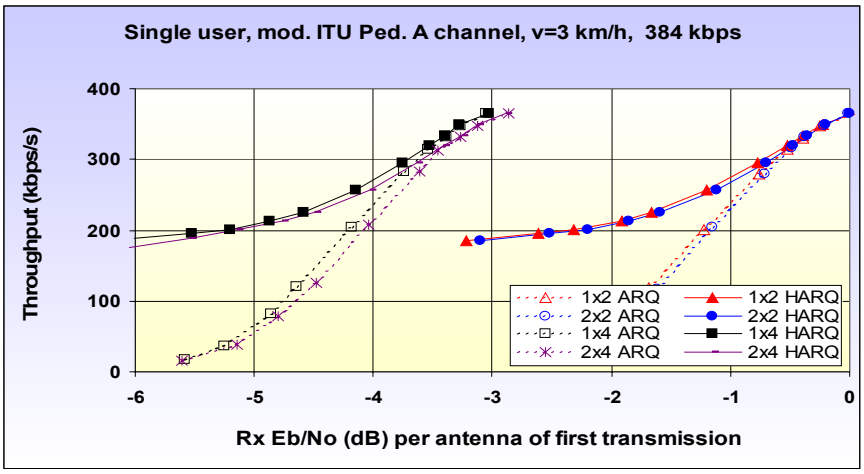

Figure 3.20. Single user throughput, 384 kbps, Pedestrian A, 3 km/h.

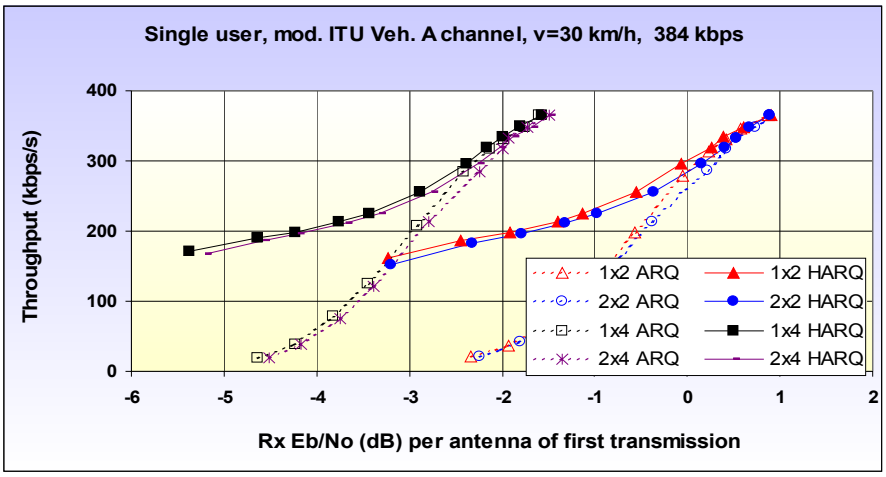

Figure 3.21. Single user throughput, 384 kbps, Vehicular A, 30 km/h.

Figure 3.21 shows the single user throughput for the 384 kbps service in Vehicular A channel with the UE speed of 30 km/h. In vehicular channel the E_b/N_0 requirement is approximately 1 dB larger than in pedestrian channel due to smaller SNR per tap and higher speed of the UE. These two factors impact the quality of the channel estimation. The 4-antenna receiver is only about 2-2.5 dB better than the 2-antenna receiver. This relative degradation in the performance is due to the fact that only eight Rake fingers were applied in all cases and the loss from channel estimation is larger with 4-antenna receiver in multi-tap channel.

The probability distribution of re-transmissions with ARQ and HARQ is presented in Figure 3.22. The block error rate of the first transmission was 80%. It is evident that with the current simulation assumptions the first re-transmission already gives an error-free data reception with HARQ and second re-transmission is needed very rarely. However, the re-transmission probability of ARQ is remarkably larger for the second re-transmission. Therefore it can be stated that the HARQ allows on average significantly shorter packet delays than the ARQ. In addition, the variance of the packet delays is much smaller for HARQ.

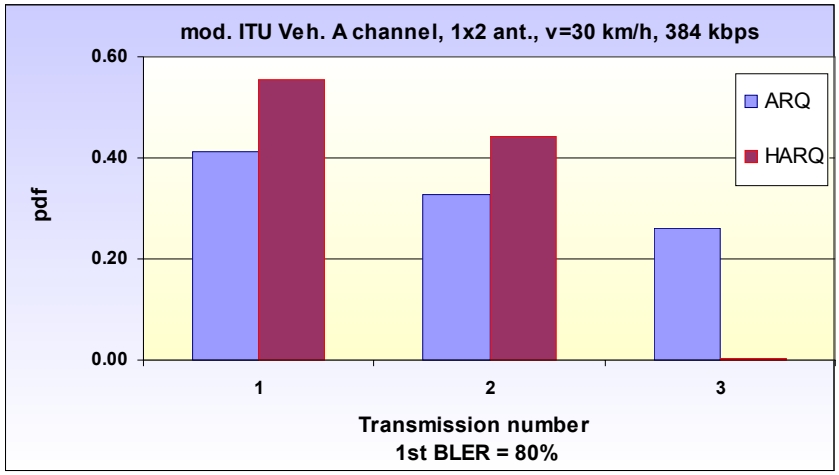

Figure 3.22. Probability of re-transmissions with ARQ and HARQ in Vehicular A channel, 384 kbps service, UE speed 30 km/h.

The different behaviour of ARQ and HARQ is further studied in Figure 3.23 and Figure 3.24, which illustrate the optimisation of the transmit power of the first transmission. This power optimisation corresponds to optimal BLER target setting. In case of ARQ the optimal BLER of the first transmission is about 10%, while the corresponding BLER target with HARQ is almost 100%. It must be noted that these simulations cover the isolated cell throughput without modelling of the inter-cell interference. However, even if inter-cell interference was taken into account it should not affect the optimal BLER target since minimum power of the first transmission is beneficial also from inter-cell interference point of view. Therefore, it can be expected that the results would have similar tendency also in multi-cell case with inter-cell interference.

Figure 3.25 and Figure 3.26 demonstrate the total throughput in an isolated cell with ARQ and HARQ assuming optimised power in 1st transmission. First observation is the same as in previous simulations: four receive antennas at Node B bring significant performance improvement compared to the 2-antenna receiver. This holds for all SIMO and MIMO cases. The throughput increase at 3 dB noise rise is approximately 90% for Pedestrian A channel and 75% for Vehicular A channel. Second observation is that the uplink capacity performance of ARQ and HARQ is roughly the same. Only in Vehicular A channel HARQ gives small gain which is probably related to the power control mechanism at 30 km/h. Moreover, this gain is achieved at the cost of reduced average bit rate. Similar performance of ARQ and HARQ is due to the fact that the gain from HARQ in cell level is seen in reduced transmit power of the UE. The power reduction improves performance in the network level, which cannot be seen at the cell level.

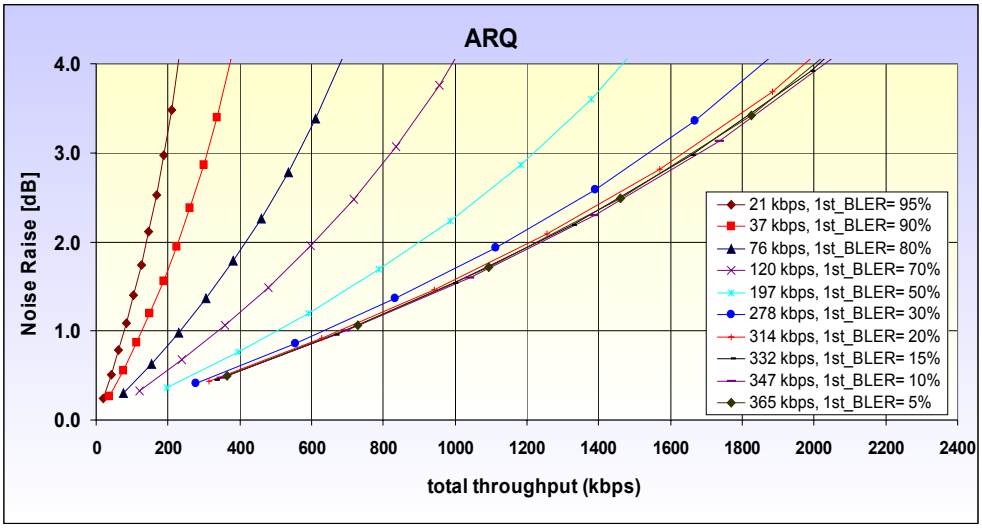

Figure 3.23. Noise rise as a function of throughput with ARQ and different BLER of 1st transmission, Vehicular A channel, 1Tx/2Rx, UE speed 30 km/h.

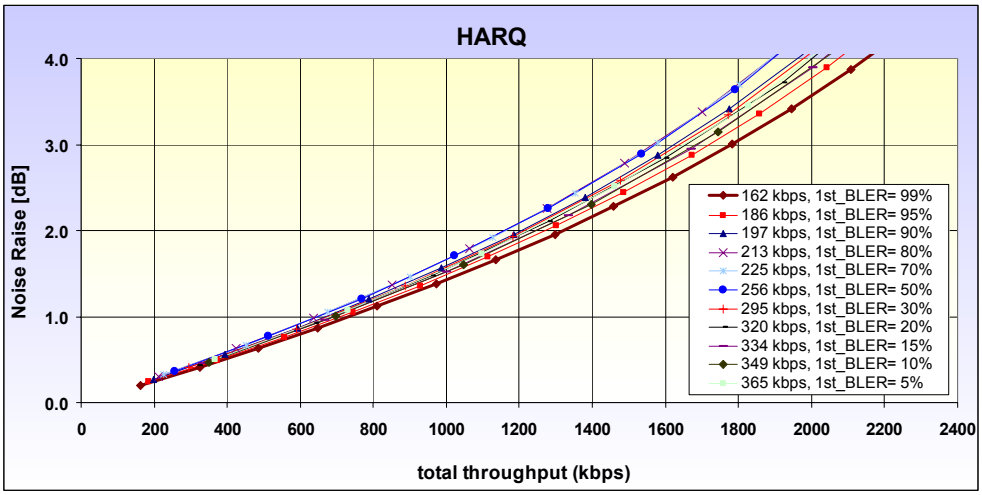

Figure 3.24. Noise rise as a function of throughput with HARQ and different BLER of 1st transmission, Vehicular A channel, 1Tx/2Rx, UE speed 30 km/h.

Third observation is again that the MIMO approach does not perform better that the corresponding SIMO approach. As stated earlier, there are two main reasons for the similar performance of SIMO and MIMO in WCDMA uplink. First one is the characteristics of the WCDMA uplink and the second one is that the Rake receiver was applied in both cases.

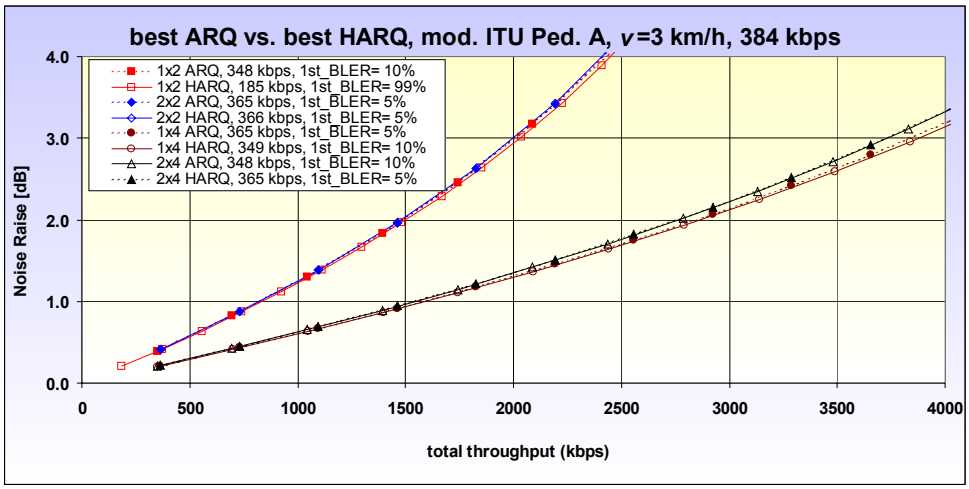

Figure 3.25. Noise rise as a function of throughput with ARQ and HARQ and different SIMO and MIMO schemes, Pedestrian A channel, UE speed 3 km/h. The power of 1st transmission is optimised.

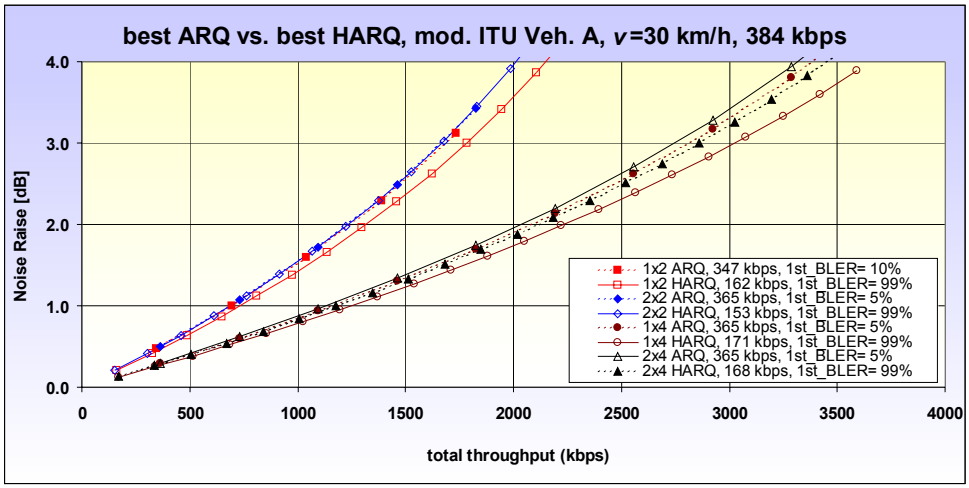

Figure 3.26. Noise rise as a function of throughput with ARQ and HARQ and different SIMO and MIMO schemes, Vehicular A channel, UE speed 30 km/h. The power of 1st transmission is optimised.

As a conclusion from the HSUPA studies with ARQ and HARQ it can be noted that the HARQ scheme has the potential to bring significant performance improvement in cell and system throughput assuming that all the parameters are optimised for that purpose.

3.6 Conclusions from HSUPA Performance Evaluation

HSUPA performance in WCDMA uplink was studied with SIMO and MIMO approaches using different antenna constellations. Both uplink coverage and capacity results indicate that doubling the number of receive antennas from two to four brings significant improvement. However, the MIMO approach does not perform better than the SIMO scheme. Moreover, simple advanced receiver techniques such as interference rejection (optimum) combining and 1-stage partial PIC do not give significant gains compared to the Rake receiver performance. HSUPA studies with ARQ and HARQ showed that the HARQ scheme has the potential to bring significant performance improvement in cell and system throughput.

4 SYSTEM-LEVEL PERFORMANCE OF MIMO TECHNIQUES

The system simulations have been carried out using a dynamic UTRAN system simulator developed by Vodafone Group R&D. The simulator has a time step of 1 slot and encompasses both release '99 and release 5 (HSDPA) functionality. Details of the implemented functionality can be found in the earlier deliverable [1].

The link level results in Chapter 2 are used in the system simulator following the definition in [1] and with the metrics described in Section 2.6.

4.1 Simulation Procedure

The following general procedure is followed for the dynamic system simulation:

- Drop K HSDPA users per sector within the geographic area of the system. Users are assigned to node B based on received CPICH power.

FOR n = 1 to N frames

- Update the traffic data arrivals at the Node B according to the traffic model
- Compute the channel response for the serving cells as well as all interfering cells. The channel response is updated once per slot.
- The channel metric is fed back to the node B on the uplink.
- The Node B selects the user to be served and its data rate according to the scheduling algorithm (including H-ARQ), power available for HSPDA users and the state of the users traffic queues.
- For the served users and its service data rate, a PER is determined as function of the channel state at the time of data transmission. The transmitted frame is in error if a random variable (uniformly distributed between 0 and 1) is less than the FER.
- ACK/NACK is set for the served user

END

4.2 Simulation Configuration

4.2.1 Simulation Layout

- 19 sites, 3 sectors
- Site-to-site spacing: 1.5km
- Users are uniformly distributed in the centre site, all other sites transmit at constant full power.
- Results recorded for central site only

4.2.2 Simulation Parameters

Table 4.1. Simulation parameters

Parameter	Value
Simulation length	30 seconds
Pathloss	128.1 + 37.6 log10(d)
Carrier frequency	2GHz
Lognormal fading Correlation between sector Site-to-site correlation Standard deviation Correlation distance	 1.0 0 10dB 50m
Fast fading	Ped A (3km/h), Veh A (30km/h)
Serving cell selection	CPICH Ec/N0
HSDPA scheduler	Round Robin, max C/I
HSDPA resource Maximum power Codes	 80% node B power 10
Node B power	43dBm
Control channels CPICH SCH Others	 33dBm 30dBm 33dBm

4.2.3 Antenna Pattern

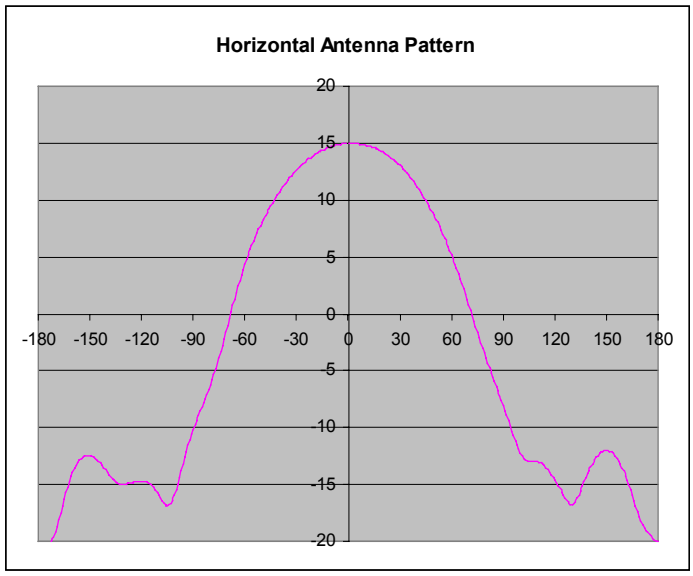

Figure 4.1. Horizontal antenna pattern.

4.2.4 Users

The modelled users will have no mobility but fast fading and log-normal characteristics will be updated according to the speeds in Table 4.1. The service is web-browsing modelled by an open-loop process with parameters in Table 4.2 below. Associated DCHs are modelled explicitly.

Table 4.2. Packet traffic model parameters

Parameter	Random Variable	Parameters
Packet Calls Size	Pareto with cutoff	A=1.1, k=4.5 Kbytes, m=2 Mbytes, μ=25 Kbytes
Time Between Packet Calls	Geometric	μ = 3 seconds
Packet Size	Segmented based on MTU size	1500 octets
Packets per Packet Call	Deterministic	based on Packet Call Size and Packet MTU
Packet Inter-arrival Time	Geometric	μ = MTU size / link peak rate (e.g. [1500 octets * 8] /2 Mbps = 6 ms)

4.3 Results

The results are first presented for the Pedestrian A channel simulations and then for the Vehicular A channel. The performance metrics are described in [1] but repeated here for easy reference. Throughput measures 1 and 2 taken from [7].

1) Throughput per cell

- Total number of successful bits for a given sector (cell)

$$ServiceSector(s) = \frac{1}{T_{\text{sec}onds}} \sum_{t=1}^{T_{\text{sec}onds}} \#\text{ good bits for t}^{\text{th}}\text{ second interval for sector s}$$

2) Cdf of packet call throughput

The packet call throughput is given by

$$PktCall(c,k,d) = \frac{\#\text{ bits in pkt call c}}{t_{end\_c} - t_{arrival\_c}}$$

where: c = the c^{th} packet call from a group of C packet calls
k = the k^{th} user from a group of K users
d = the d^{th} drop from a group of D drops

3) Cdf of user throughput

The user packet call throughput in figure 4.4 is the total of good bits received by the user divided by the simulation time.

4) Cdf of delay per packet call

The delay for each packet call will be recorded in the simulation and then plotted as a cumulative density function, both per user and per cell. The delay is considered as the time of arrival of the first packet at the node B to the time of arrival of the last packet at the user.

The aggregate cell throughput for the algorithms studied for the Pedestrian A (3km/h) channel is given in table 4.3 below. Note that the link-level results showed that LDC(3,2) and VBLAST(4,4) combinations did not effectively operate in this slow-fading channel.

Table 4.4 – Aggregate Cell Throughput, Ped A

Technique	Antenna Configuration	Cell Throughput (Mb/s), RR Scheduler	Cell Throughput (Mb/s), C/I Scheduler
SISO (Baseline)	1,1	1.57	2.41
Dual Rake	1,2	1.93	2.91
STTD	2,1	2.13	2.43
STTD + Dual Rake	2,2	2.41	-
Equaliser	1,1	1.94	2.61
Dual Equaliser	1,2	2.23	-
VBLAST + OSIC	2,2	2.08	2.49
TSTC, Alamouti	2,1	2.00	2.03

As expected and well-known the C/I scheduler improves the performance of the system in all cases. STTD shows good performance improvement for the round robin scheduler. This arises because the RR scheduler will schedule users in bad fades which are reduced by STTD. Dual Rake is comparable to or better than the equaliser due to the low multipath environment for the equaliser to work with. VBLAST with the OSIC receiver does not provide significantly better gains than the other techniques in terms of cell throughput. The performance of the Turbo Space-Time Coding with Linear Dispersion (Alamouti) is encouraging with the limited MCS from only 1 coding rate available. On the other hand ideal channel estimation is assumed in this case.

Figures 4.2 and 4.3 show the packet call throughput and packet delay. Only part of the cdf of the packet call delay is shown as the cdfs converge for lower delay values.

Figure 4.2

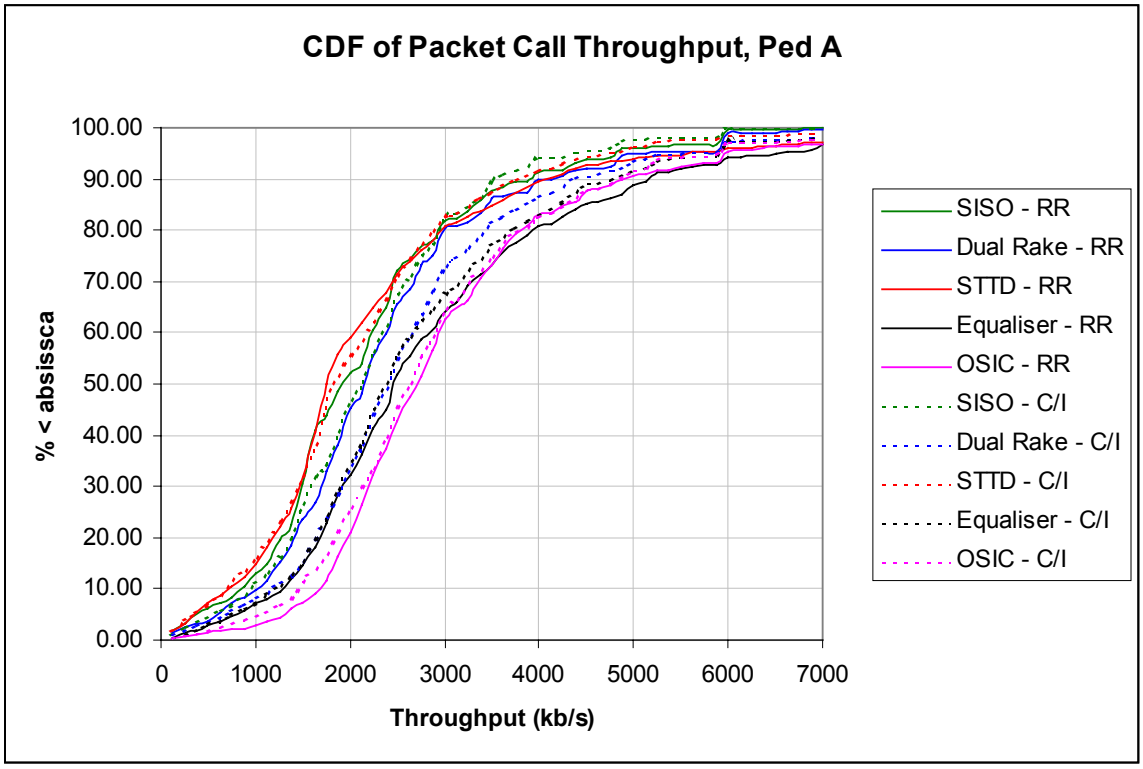

Figure 4.3

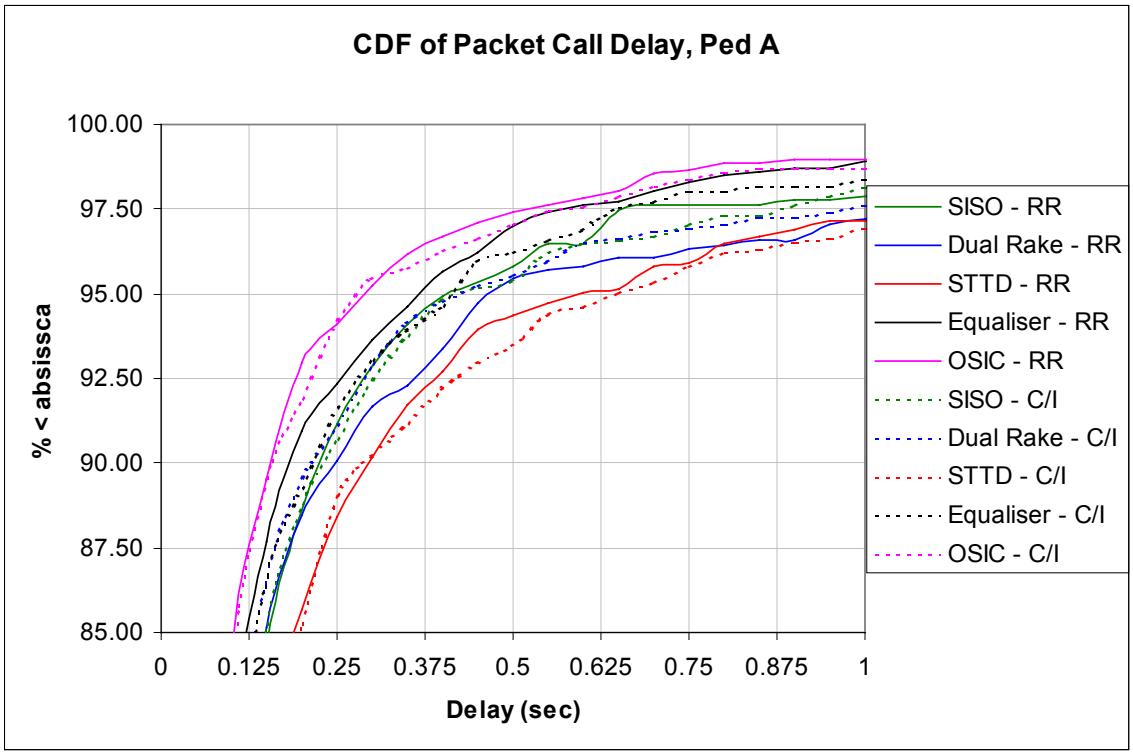

From figure 4.2 we can see that STTD provides a lower throughput than the baseline case but that all the other techniques (involving enhanced receiver architecture)

improve the throughput. The impact of the different schedulers is variable depending on the specific interaction of the multiple antenna techniques and the scheduler.

The plot of delay in figure 4.3 shows that for the round robin scheduler the equaliser and VBLAST+OSIC reduce the delay while dual Rake receiver and STTD increase the delay. However for the C/I scheduler there is less variation in performance with only noticeable differences for the VBLAST+OSIC and STTD from the baseline.

There appears to be a mis-match between the packet call performance where VBLAST is generally the best performer and the aggregate cell throughput results. The user throughput is given in figure 4.4 below, which shows that VBLAST does not over time provide better performance to the user. This may be due to the fact that in 'bad' locations and hence using the lowest MCS VBLAST is often unable to deliver packets even with the help of Chase Combining. This may be resolved by added lower coding rates into the MCS or switching to a non-layered technique in those situations.

Figure 4.4

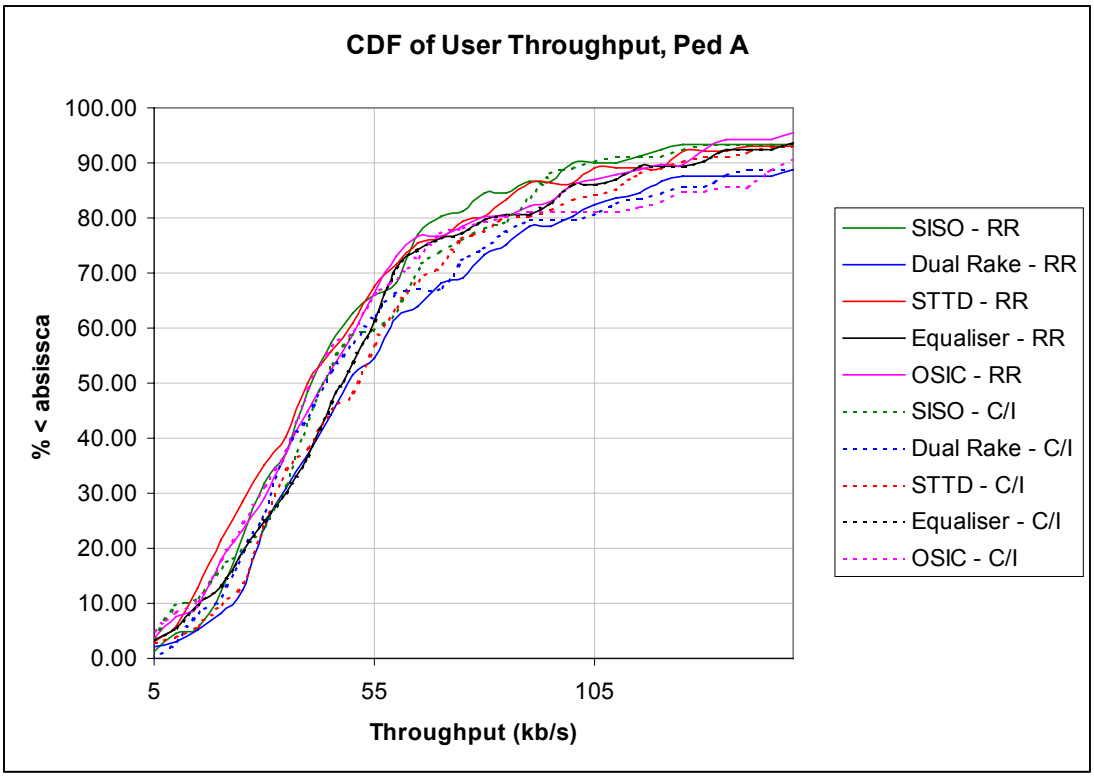

Results are now presented for the Vehicular (50km/h) simulations. VBLAST(2,2) was shown not operate in this scenario due to problems with channel estimation. However the Linear Dispersion Codes – Alamouti (2,1) and also the (3,2) arrangement were simulated. The aggregate cell throughputs are given in table 4.5. Now it can be seen there is little benefit from STTD for the round robin scheduler and the equaliser now provides a better performance than the dual Rake. Again the results for the Turbo Space-Time with LDC are promising, although the C/I scheduler result is underperforming. This is likely to be because the system had a different value of BLER operating point.

Table 4.5

Technique	Antenna Configuration	Cell Throughput (Mb/s), RR Scheduler	Cell Throughput (Mb/s), C/I Scheduler
SISO (Baseline)	1,1	1.47	1.57
Dual Rake	1,2	1.54	2.06
STTD	2,1	1.50	-
STTD + Dual Rake	2,2	1.54	-
Equaliser	1,1	1.69	-
Dual Equaliser	1,2	1.94	2.19
TSTC, Alamouti	2,1	1.83	1.87
TSTC, LDC	3,2	2.12	1.95

Figure 4.5

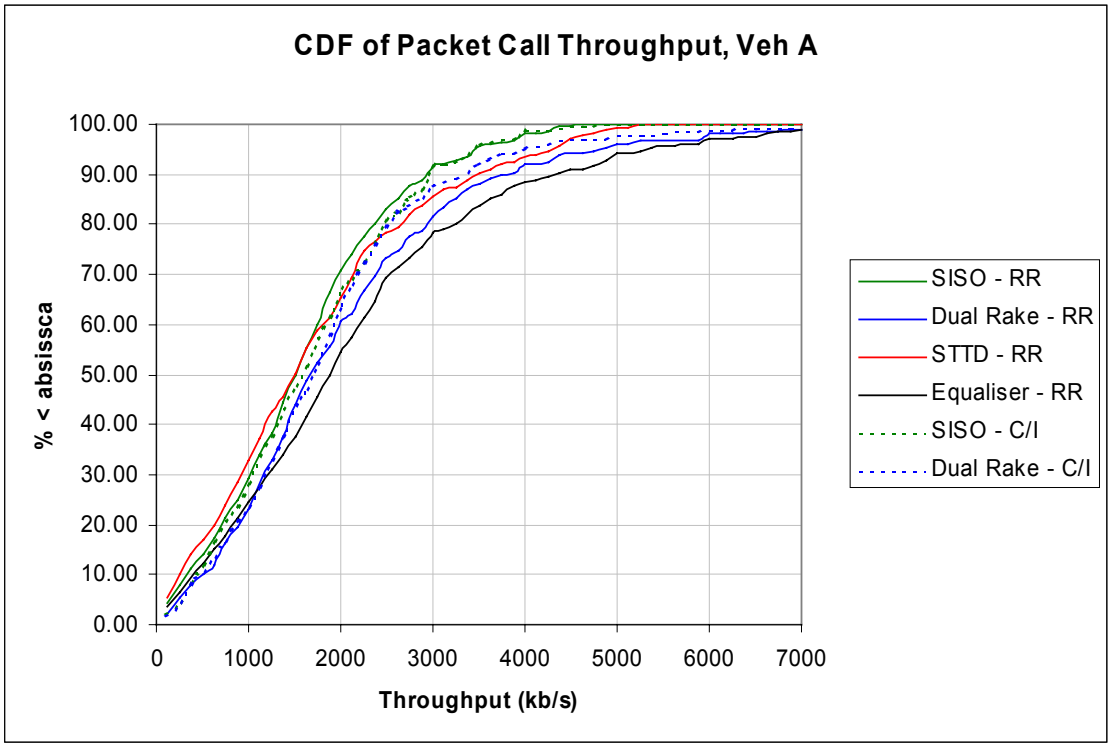

Figures 4.5 and 4.6 show the packet call performance in the vehicular A channel. These results show improvement from the advanced receivers (dual rake and equaliser) and degradation from STTD.

Figure 4.6

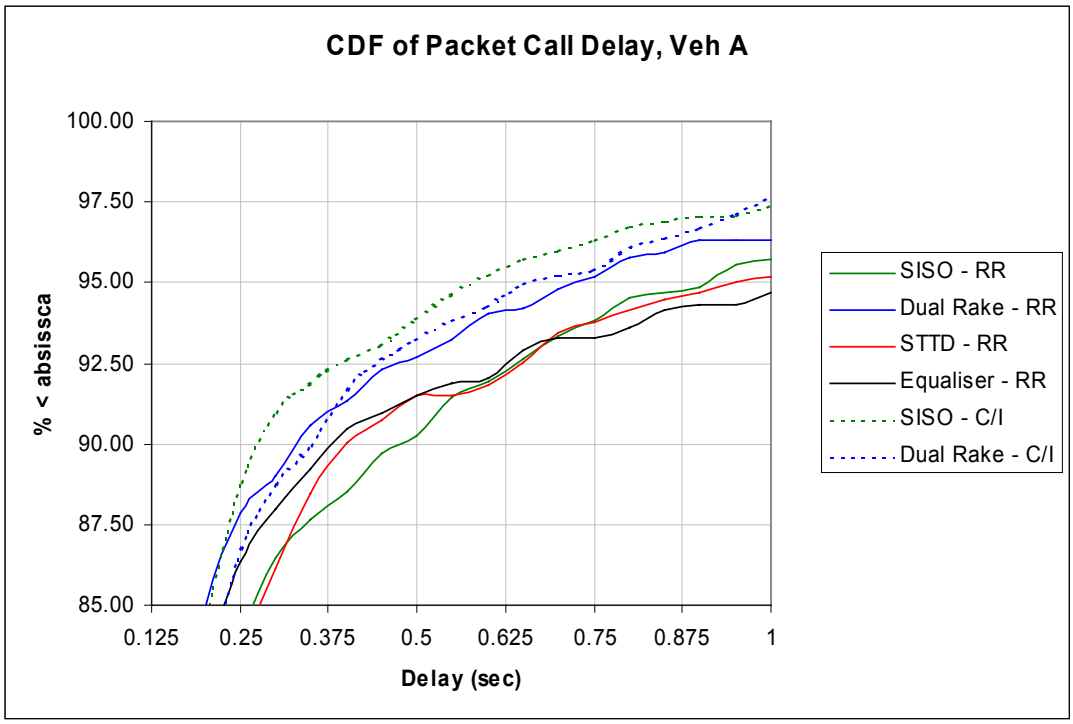

4.4 Conclusions and Further Work

From these dynamic radio system simulations the following conclusions can be drawn:

- VBLAST does not provide significant gain in cell throughput in Ped A channel.
- STTD provides improved cell throughput in Ped A channel for the round robin scheduler only.
- Advanced receivers provide good performance advantage over the baseline case in all scenarios.
- Turbo Space-Time Coding with Linear Dispersion codes appear promising.

Further work could focus on the following areas:

- Simulations with different number of users to find sensitivity to cell load
- Simulations with different schedulers such as proportional fair, which would more closely represent a real implementation.
- Simulations of the Linear Dispersion Codes with real channel estimation and expanded MCS set to investigate further their potential.

4.5 Simplified Statistical System Simulation Approach

In the following, we present a simple, alternative HSDPA system simulation approach which is based on the distribution of average geometry factor G [4]. The simulator assumes

- round-robin scheduling
- hybrid-ARQ with Chase combining
- long retransmission delay (uncorrelated channel between transmissions).

Although very simplified, the simulator can be applied for obtaining initial estimate of system level performance of different HSDPA methods.

Figure 4.2 illustrates the system simulation technique. Input data to the simulator includes G distribution which defines the environment (either macro or micro environment). In addition, E_b/N_0 distribution has been recorded in link simulator as a function of G. In this way, a fading channel need not to be simulated at system level at all. Packet error rate (PER) is also determined by link-level simulations. PER is given as a function of E_b/N_0 and average G factor. The latter parameter is included since performance of advance receivers, especially linear equalizers, depends on this factor. Since intercell interference is modeled as additive white Gaussian noise in the link simulator, G factor holds rather accurate information about how structured (colored) the signal is. Since a linear equalizer (internally) whitens the signal, its performance gain depends strongly on the geometry factor.

HSDPA users have randomly selected *long-term average* G factors obeying the chosen G distribution. This models their geographic location in the cell. During each TTI, a new E_b/N_0 is randomized for the user to be served by the Node B. In case of a packet retransmission, Chase-combined E_b/N_0 is computed. Given average G and E_b/N_0, PER can be obtained and is then used for emulating possibly erroneous packet decoding. For each new packet, the best modulation and coding scheme (MCS) so that

$$(1 - \text{PER}) \times (\text{packet payload})$$

is maximized. The bit payload of correctly received packets determines the average system (cell or sector) throughput.

Figure 4.3 shows the simulated system throughput in ITU Pedestrian A channel when five HSDPA code channels are in use. It is clearly seen that channel equalization is not required in this channel. (The small loss due to dual-antenna equalization when compared to dual-antenna RAKE is because of intentional mismatch in the equalizer filter in order to guarantee stability of the used algorithm.) Most of the performance gain is due to the diversity and SNR gain due to the second receive antenna. Throughput in micro cell environment is clearly better than in macro environment. This is because intercell interference power is lower in micro cells thanks to better cell isolation.

Channel equalization becomes more important when channel has significant delay spread. Figure 4.4 depicts the throughput in ITU Vehicular A channel with different

receiver algorithms. Gain due to equalization is the greatest in micro cells because signal-to-noise ratio is there much higher than in macro cells. Throughput increase is as large as 63% when a dual-antenna equalizer is used instead of single-antenna RAKE.

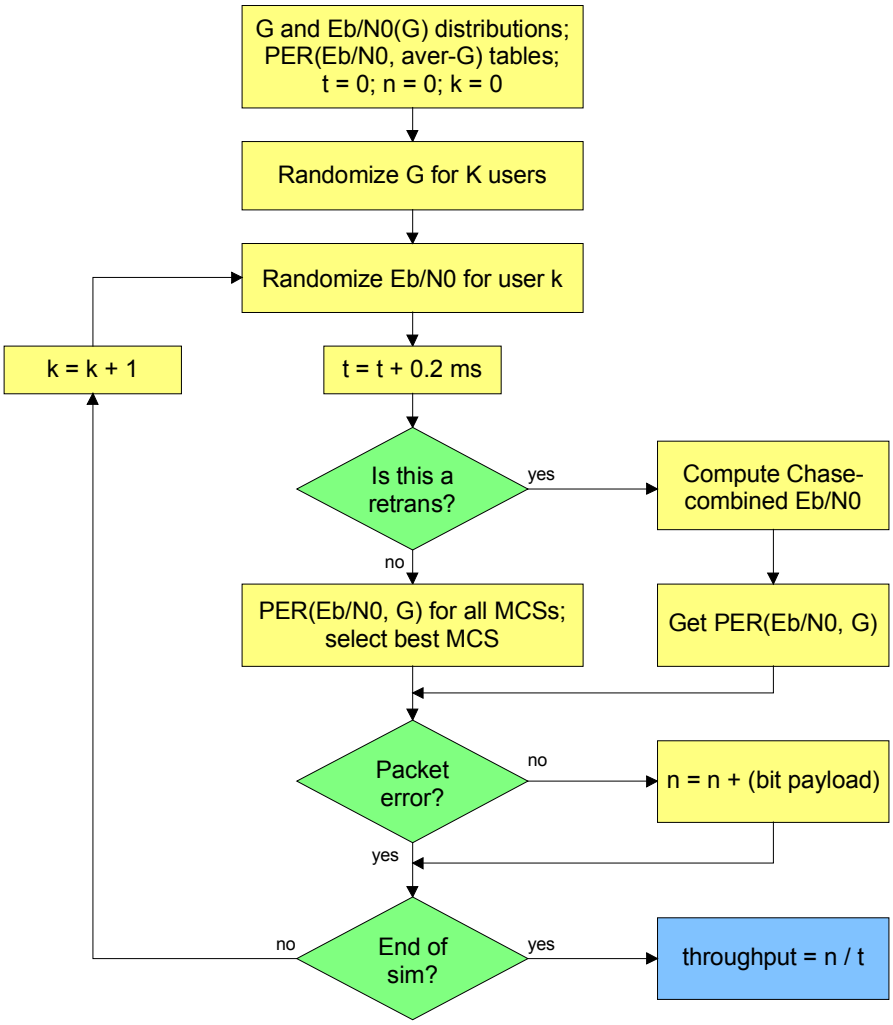

Figure 4.2. The principle of the simplified statistical system simulation method.

It is interesting to study what is the probability of using different MCSs with different receiver algorithms. Figure 4.5 and Figure 4.6 illustrate MCS usage in the pedestrian channel in macro and micro cell environments, respectively. It can be seen that the system throughput increase is due to the higher probability of using more bandwidth efficient MCSs utilizing 16-QAM modulation. Figure 4.7 and Figure 4.8 show the MCS usage in the vehicular channel. Clearly, a single-antenna RAKE can support 16-QAM modulation only very rarely while a dual-antenna space-time equalizer uses 16-QAM modulation almost 80% of time. The shown high usage probabilities are the source of the throughput increase illustrated in Figure 4.4.

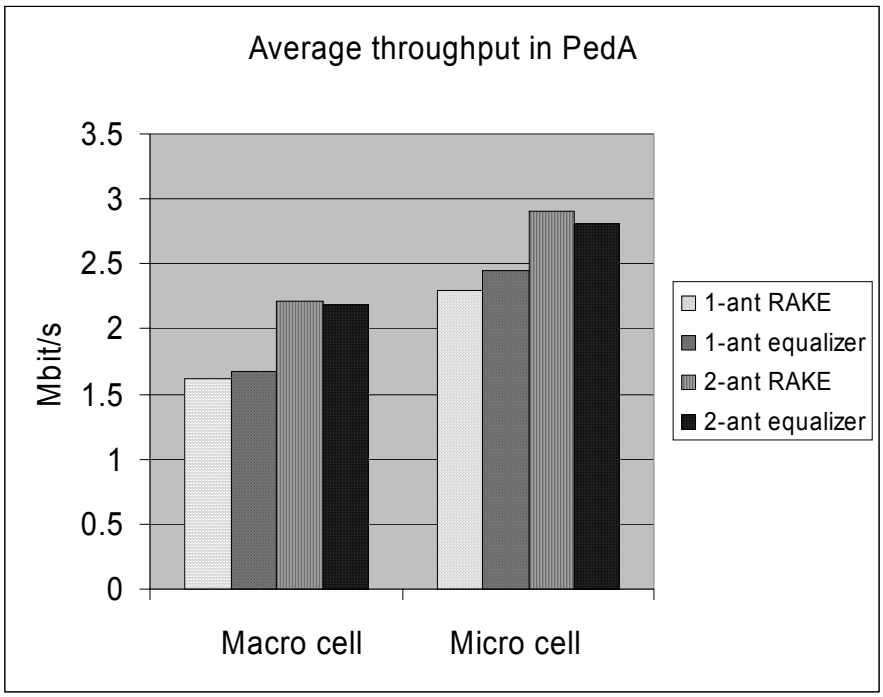

Figure 4.3. System throughput with single-antenna transmission and different receiver algorithms in Pedestrian A channel (5 active HSDPA code channels with 80% power allocation).

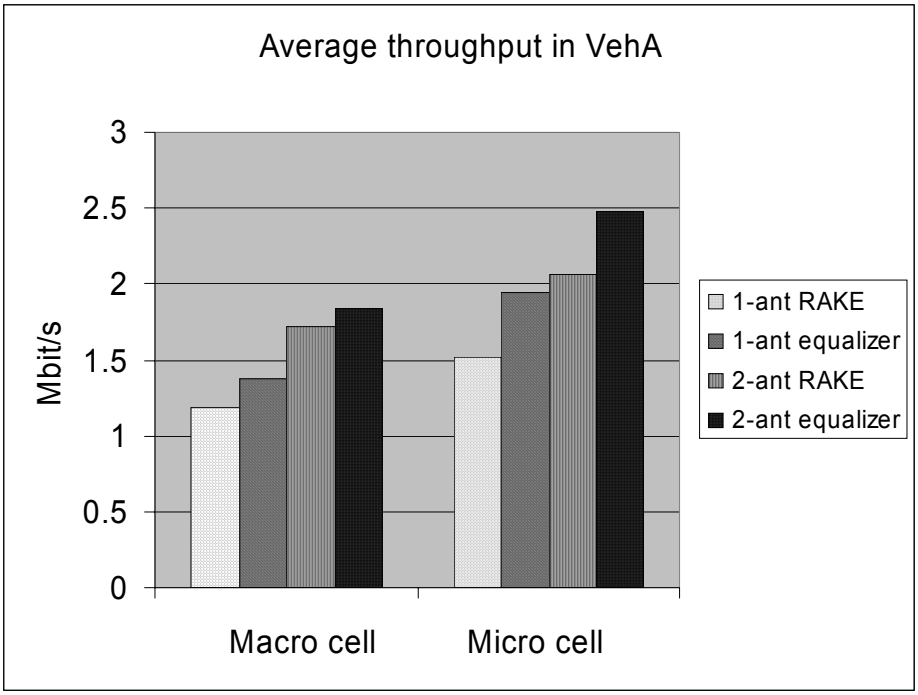

Figure 4.4. System throughput with single-antenna transmission and different receiver algorithms in Vehicular A channel (5 active HSDPA code channels with 80% power allocation).

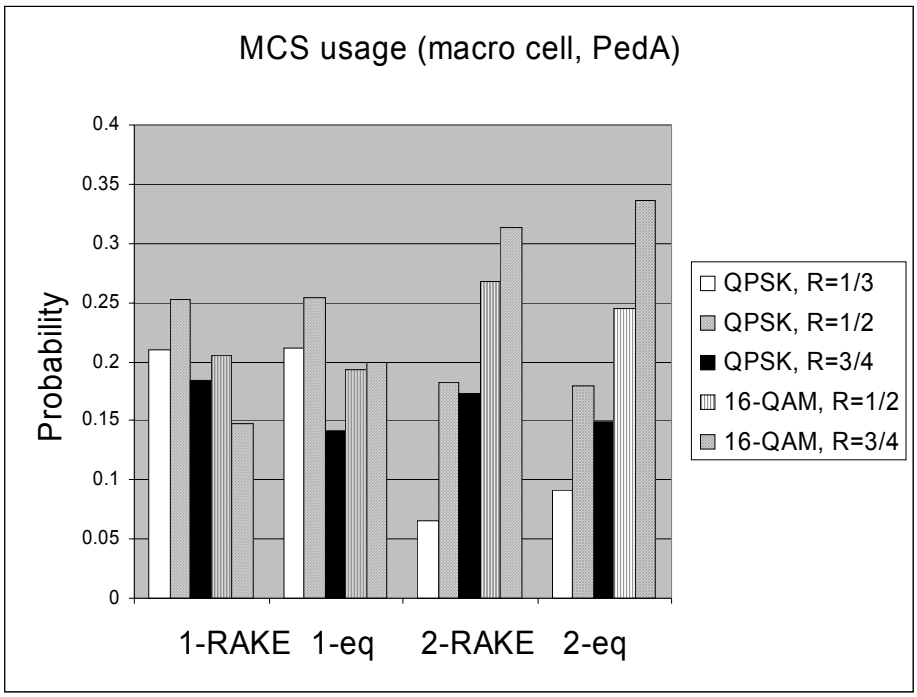

Figure 4.5. Probability of using different modulation and coding schemes in macro cell and Pedestrian A channel.

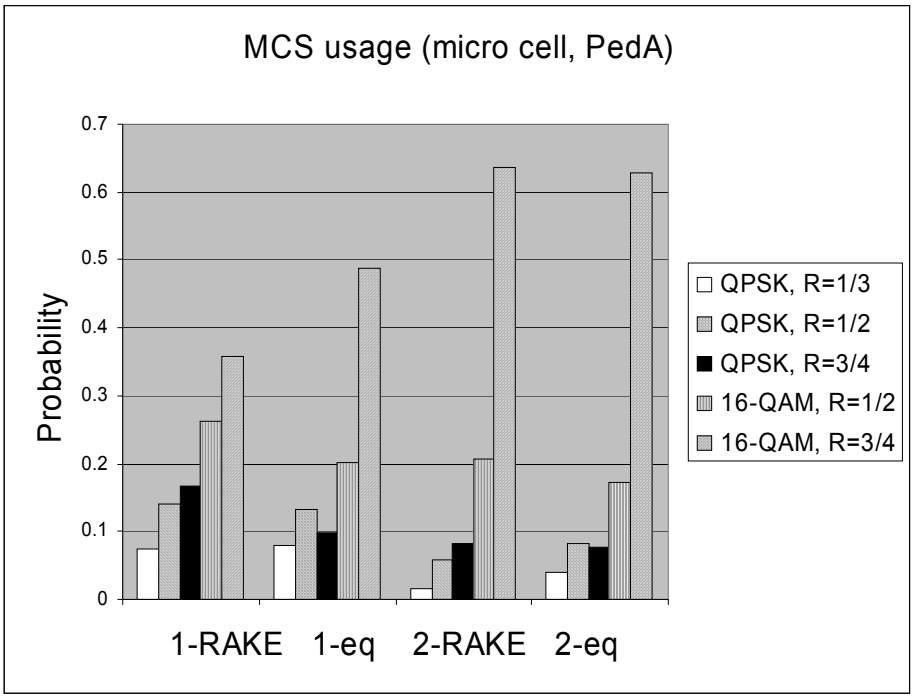

Figure 4.6. Probability of using different modulation and coding schemes in micro cell and Pedestrian A channel.

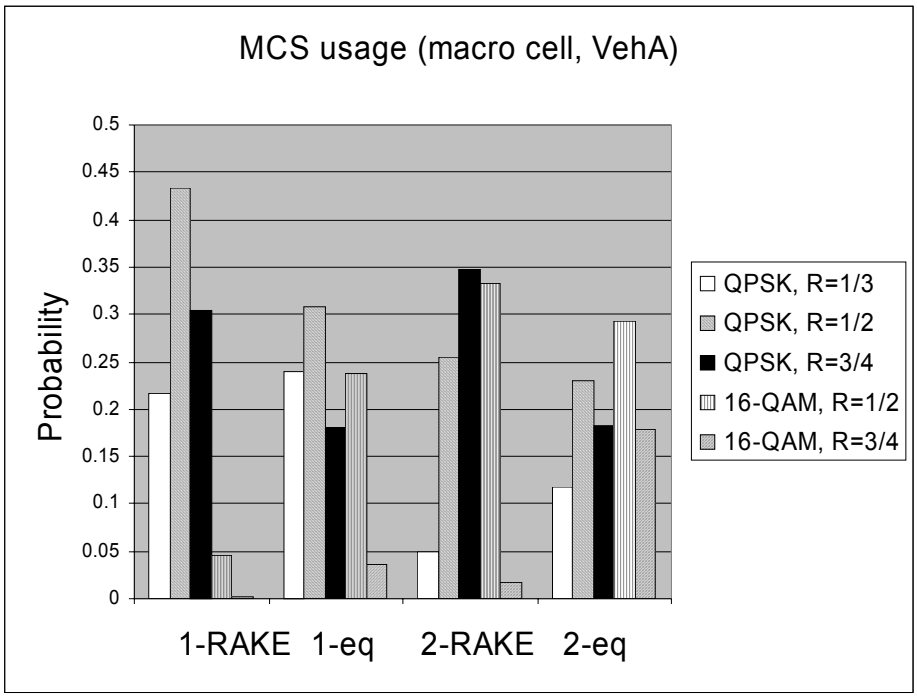

Figure 4.7. Probability of using different modulation and coding schemes in macro cell and Vehicular A channel.

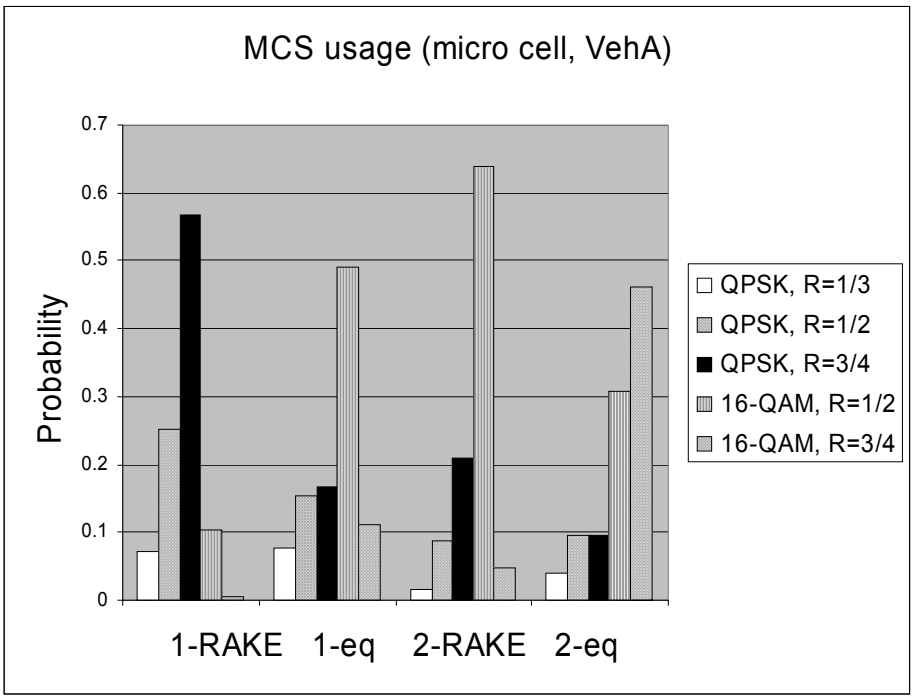

Figure 4.8. Probability of using different modulation and coding schemes in micro cell and Vehicular A channel.

5 REFERENCES

[1] IST-2000-30148 I-METRA, Deliverable 3.1, "*Design, Analysis and Selection of Suitable Algorithms*", available at http://www.ist-imetra.org.

[2] IST-2000-30148 I-METRA, Deliverable 3.2, "*Implementation of Relevant Algorithms*", available at http://www.ist-imetra.org.

[3] METRA Project Deliverable D5.1, "*Architectural Design and Cost Impact*", available at http://www.ist-imetra.org.

[4] J. R. Fonollosa, M. Heikkilä, X. Mestre, A. Pagès, A. Pollard, L. Schumacher, A. Wiesel and J. Ylitalo, "Adaptive Modulation Schemes for MIMO HSDPA," *IST Mobile & Wireless Telecommunications Summit 2002*, Thessaloniki, Greece, June 2002.

[5] B. Hassibi and Bertrand M. Hochwald. "High rate codes that are linear in space and time", Submitted to IEEE Trans. Info. Theory, August 2000. Revised April 2001.

[6] S. M. Alamouti, "A Simple Transmitter Diversity Scheme for Wireless Communications", *IEEE J. Sel. Area Comm*., pp. 1451-1458, Oct. 1998.

[7] Motorola, "Voice and HSDPA Data Peformance Results", 3GPP TSG_R WG1 Document TSGR1#20(01)-0545, 21st-25th May, 2001, Busan, Korea.

6 APPENDIX A. LINK LEVEL RESULTS FOR THE SCHEME COMBINING LINEAR DISPERSION CODES WITH TURBO SPACE TIME DECODING.

Pedestrian A 3Km/h for Alamouti 2x1

Case 1

EbNo	1	1.5	2	2.5	3	3.5	7
FER	0.6100	0.2200	0.0260	0.0040	0.0015	0.0002	0
Throughput	0.0924	0.1849	0.2308	0.2361	0.2366	0.2370	0.2370

Case 2

EbNo	3.5000	4.0000	4.5000	5.0000	5.5000	6.0000	7.0000
FER	0.6800	0.1800	0.0130	0.0042	0.0008	0	0
Throughput	0.1526	0.3911	0.4708	0.4750	0.4766	0.4770	0.4770

Case 4

EbNo	1.0000	1.5000	2.0000	2.5000	3.0000	7.0000	
FER	0.9600	0.2333	0.0050	0.0010	0.0004	0	
Throughput	0.0479	0.9177	1.1910	1.1958	1.1965	1.1970	

Case 5

EbNo	3.5000	4.0000	4.5000	5.0000	5.5000	7.0000	
FER	0.9600	0.2500	0.0045	0.0010	0.0008	0	
Throughput	0.0959	1.7978	2.3862	2.3946	2.3951	2.3970	

Case 7

EbNo	0.00	0.5	1	1.5	2	4.5	5
FER	0.4700	0.1100	0.0141	0.0027	0.0006	0	0
Throughput	0.6344	1.0653	1.1801	1.1938	1.1963	1.1970	1.1970

EbNo	5.5	6
FER	0	0
Throughput	1.1970	1.1970

Case 10

EbNo	1.0000	1.5000	2.0000	2.5000	6.0000	7.0000	
FER	0.9867	0.2600	0.0027	0.0004	0	0	
Throughput	0.0320	1.7738	2.3906	2.3961	2.3970	2.3970	

Case 11

EbNo	3.5000	4.0000	4.5000	5.0000	5.5000	7.0000	
FER	0.9800	0.3350	0.0376	0.0047	0.0014	0	
Throughput	0.0959	3.1880	4.6137	4.7716	4.7873	4.7940	

Vehicular A 50Km/h for Alamouti 2x1

Case 1

EbNo	1.0000	1.5000	2.0000	2.5000	3.0000	3.5000	7.0000
FER	0.8200	0.3550	0.0617	0.0057	0.0012	0	0
Throughput	0.0427	0.1529	0.2224	0.2357	0.2367	0.2370	0.2370

Case 2

EbNo	3.5000	4.0000	4.5000	5.0000	5.5000	6.0000	7.0000
FER	0.7400	0.3100	0.0315	0.0043	0.0012	0	0
Throughput	0.1240	0.3291	0.4620	0.4749	0.4764	0.4770	0.4770

Case 4

EbNo	1.0000	1.5000	2.0000	2.5000	3.0000	7.0000	
FER	0.9800	0.5800	0.0261	0.0014	0	0	
Throughput	0.0239	0.5027	1.1658	1.1953	1.1970	1.1970	

Case 5

EbNo	3.5000	4.0000	4.5000	5.0000	5.5000	7.0000	
FER	1.0000	0.8800	0.0780	0.0018	0.0006	0	
Throughput	0	0.2876	2.2100	2.3927	2.3956	2.3970	

Case 7

EbNo	0.00	0.5	1	1.5	2	4.5	5	5.5	6
FER	0.9167	0.5447	0.184	0.044	0.0153	0.0055	0.0016	0	0
Throughput	0.0998	0.5449	0.9763	1.1443	1.1787	1.1904	1.1951	1.1952	1.1970

Case 10

EbNo	1.5000	2.0000	2.5000	3.0000	6.0000	7.0000	
FER	0.8800	0.1300	0.0085	0.0008	0	0	
Throughput	0.2876	2.0854	2.3765	2.3951	2.3970	2.3970	

Case 11

EbNo	4.5000	5.0000	5.5000	6.0000	6.5000	7.0000	
FER	0.7200	0.2500	0.0698	0.0053	0.0010	0	
Throughput	1.3423	3.5955	4.4595	4.7688	4.7892	4.7940	

Vehicular A 120Km/h for Alamouti 2x1

Case 1

EbNo	1.0000	1.5000	2.0000	2.5000	3.0000	3.5000	7.0000
FER	0.8367	0.4400	0.0700	0.0083	0.0029	0.0004	0
Throughput	0.0387	0.1327	0.2204	0.2350	0.2363	0.2369	0.2370

Case 2

EbNo	3.5000	4.0000	4.5000	5.0000	5.5000	6.0000	7.0000
FER	0.8600	0.3800	0.0550	0.0064	0.0016	0.0008	0
Throughput	0.0668	0.2957	0.4508	0.4739	0.4762	0.4766	0.4770

Case 4

EbNo	1.0000	1.5000	2.0000	2.5000	3.0000	7.0000	
FER	1.0000	0.6504	0.0410	0.0015	0.0006	0	
Throughput	0	0.4185	1.1479	1.1952	1.1963	1.1970	

Case 5

EbNo	3.5000	4.0000	4.5000	5.0000	5.5000	7.0000	
FER	1.0000	0.8400	0.0960	0.0022	0.0010	0	
Throughput	0	0.3835	2.1669	2.3916	2.3946	2.3970	

Case 10

EbNo	1.7500	2.0000	2.2500	2.5000	2.7500	3.0000	7.0000
FER	0.6700	0.2667	0.0520	0.0087	0.0018	0.0002	0
Throughput	0.7910	1.7578	2.2724	2.3762	2.3927	2.3965	2.3970

Case 11

EbNo	4.5000	5.0000	5.5000	6.0000	6.5000	7.0000	
FER	0.7600	0.3900	0.0566	0.0077	0.0018	0.0004	
Throughput	1.1506	2.9243	4.5227	4.7571	4.7854	4.7921	

Pedestrian A 3Km/h for LDC 3x2

Case 14

EbNo	4.5	5	5.5	6	6.5	7	7.5
FER	0.1625	0.0978	0.0870	0.0520	0.0280	0.0178	0.0129
Throughput	0.3995	0.4303	0.4355	0.4522	0.4636	0.4685	0.4708

EbNo	8	8.5	9	9.5
FER	0.0087	0.0060	0.0026	0.0009
Throughput	0.4729	0.4741	0.4758	0.4766

Case 17

EbNo	3.5000	4.0000	4.5000	5.0000	5.5000	6.0000	6.5000
FER	0.3804	0.2397	0.1400	0.1250	0.1047	0.0380	0.0240
Throughput	1.4851	1.8224	2.0614	2.0974	2.1461	2.3058	2.3394

EbNo	7.0000	7.5000	8.0000	8.5000	9.0000
FER	0.0175	0.0073	0.0032	0.0021	0.0006
Throughput	2.3551	2.3794	2.3893	2.3920	2.3956

Case 22

EbNo	4.0000	4.5000	5.0000	5.5000	6.0000	6.5000	7.0000	7.5000
FER	0.2234	0.2185	0.1350	0.1040	0.0647	0.0295	0.0225	0.0095
Throughput	3.7230	3.7463	4.1468	4.2956	4.4836	4.6524	4.6861	4.7484

EbNo	8.0000	8.5000	9.0000	9.5000
FER	0.0044	0.0025	0.0013	0.0004
Throughput	4.7729	4.7818	4.7879	4.7920

Vehicular A 50Km/h for LDC 3x2

Case 14

EbNo	-1.5000	-1.0000	-0.5000	0	0.5000	9.5000	
FER	0.5600	0.0960	0.0148	0.0008	0.0002	0	
Throughput	0.2099	0.4312	0.4699	0.4766	0.4769	0.4770	

Case 15

EbNo	0.5000	1.0000	1.5000	2.0000	2.5000	3.0000	3.5000
FER	0.9286	0.8000	0.3090	0.0982	0.0258	0.0090	0.0028
Throughput	0.0684	0.1914	0.6613	0.8630	0.9323	0.9484	0.9543

Case 16

EbNo	4.0000	9.5000
FER	0.0006	0
Throughput	0.9564	0.9570

Case 17

EbNo	-1.5000	-1.0000	-0.5000	0	0.5000	9.5000	
FER	0.9400	0.2440	0.0334	0.0043	0.0006	0	
Throughput	0.1438	1.8121	2.3170	2.3866	2.3956	2.3970	

Case 18

EbNo	1.5000	2.0000	2.5000	3.0000	3.5000	4.0000	4.5000	9.5000
FER	0.9400	0.4300	0.1790	0.0651	0.0158	0.0056	0.0012	0
Throughput	0.2876	2.7326	3.9357	4.4817	4.7181	4.7671	4.7882	4.7940

Case 22

EbNo	-1.000	-0.500	0	0.5000	1.000	1.500	9.500
FER	0.9136	0.405	0.0960	0.0144	0.0008	0.0004	0
Throughput	0.4143	2.8524	4.3338	4.7249	4.7902	4.7921	4.7940

Case 23

EbNo	2.5000	3.0000	3.5000	4.0000	4.5000	5.0000	5.5000
FER	0.8333	0.5480	0.2890	0.1231	0.0444	0.0206	0.0072
Throughput	1.5980	4.3338	6.8171	8.4079	9.1628	9.3901	9.5190

EbNo	6.0000	6.5000	9.5000
FER	0.0020	0.0008	0
Throughput	9.5688	9.5803	9.5880

Pedestrian A 3Km/h for V-BLAST 4x4

Case 26

EbNo	4.5	5	5.5	6	6.5		
FER	0.72	0.61	0.49	0.455	0.3650		
Throughput	0.268	0.3732	0.4881	0.5216	0.6077		

Case 27

EbNo	17.5	18	18.5	19	19.5	20	
FER	0.26	0.27	0.2160	0.1680	0.1370	0.1084	
Throughput	1.4186	1.3994	1.5029	1.5949	1.6544	1.7091	

Vehicular A 50Km/h for V-BLAST 4x4

Case 26

EbNo	-4	-3.5	-3	-2.5	-2	-1.5	2
FER	0.66	0.23	0.0311	0.0037	0.0013	0.0002	0
Throughput	0.3254	0.7369	0.9273	0.9534	0.9557	0.9568	0.9570

Case 27

EbNo	-1	-0.5	0	0.5	1	2	
FER	0.6	0.1478	0.0545	0.01	0.0012	0	
Throughput	0.7668	1.6336	1.8125	1.8978	1.9148	1.9170	

Case 29

EbNo	-3	-2.5	-2	-1.5	3.5		
FER	0.6080	0.0193	0.0031	0.0003	0		
Throughput	1.8792	4.7013	4.7791	4.7928	4.7940		

Case 30

EbNo	0	0.5	1	1.5	2	2.5	3.5
FER	0.43	0.166	0.0467	0.0089	0.0034	0.0007	0
Throughput	5.4652	7.9964	9.1406	9.5027	9.5555	9.5814	9.5880

Case 33

EbNo	-3	-2.5	-2	-1.5	-1	-0.5	5
FER	0.7533	0.2467	0.052	0.0068	0.0009	0	0
Throughput	2.365	7.223	9.0894	9.5229	9.5798	9.5880	9.5880

Case 34

EbNo	0.5	1	1.5	2	2.5	3	3.5	5
FER	0.93	0.69	0.3567	0.1555	0.0507	0.0137	0.0033	0
Throughput	1.3423	5.9446	12.3366	16.1940	18.2035	18.9131	19.1121	19.1760